Dissertation
submitted to the
Combined Faculties for the Natural Sciences and for Mathematics
of the Ruperto-Carola University of Heidelberg, Germany
for the degree of
Doctor of Natural Sciences

presented by
Diplom-Biochemist Johanna Dzieran
born in: Kiel, Germany
Oral-examination: July 2013

Systematic analysis of TGF-β/Smad signaling and (loss of) cytostatic outcome in human hepatocellular carcinoma cell lines

Referees:

Prof. Dr. Steven Dooley, University of Heidelberg, Germany

Prof. Dr. Stefan Wölfl, University of Heidelberg, Germany

Für meine Eltern
und Großeltern

TABLE OF CONTENT

SUMMARY

Primary liver cancer, of which hepatocellular carcinomas (HCCs) accounts for 90 %, is the fifth most common and third deadliest cancer worldwide. As HCCs are strongly heterogenic and with symptoms occurring late, the development of efficient treatment strategies is until now challenging. Transforming growth factor beta (TGF-β) is a multifactorial cytokine and a driver of chronic liver disease progression, which eventually ends in HCC. TGF-β, which acts as a tumor suppressor during cancer development, may switch to tumor-supporting characteristics during cancer progression. The ambiguous nature of TGF-β, together with the strong heterogeneity of HCC, leads to a highly complex situation in regard to TGF-β signaling during hepatocarcinogenesis. As TGF-β signaling is frequently altered in HCC, it is an interesting target to develop new therapeutic strategies. However, this requires deep knowledge about the time point and underlying mechanisms of the switch in TGF-β signaling.

This question was addressed by a systematic in-depth analysis of cytostatic effects of TGF-β and mechanisms of resistance in ten commonly used liver cancer cell lines. TGF-β induced cell death or growth arrest in one group of cell lines (PLC/PRF/5, Hep3B, HuH7 and HepG2) in a Smad3 dependent manner. These cells commonly expressed relatively low basal levels of TGF-β1 and its inhibitor Smad7, but elevated levels of TβRII (TGF-β receptor II). Furthermore, they exhibited a high inducibility of Smad3 and TβRI expression, Smad3 transcriptional activity and target gene expression, as exemplified for Bim, PAI-1 and Smad7. Interestingly, all cell lines have previously been described to express an early TGF-β-response gene signature, which was also identified in HCC patients and correlates with a better prognosis. In contrast, the second group (HLE, HLF, FLC-4 and to some extent HuH6 cells) was resistant against cytostatic effects of TGF-β and further characterized by high Smad7 and TGF-β1, low TβRII expression and low TGF-β induced Smad3 transcriptional activity. In addition, all but HuH6 cells had a highly motile phenotype. HCC-M and HCC-T cells shared characteristics of both groups, showing, e.g., resistance against TGF-β induced cytostasis but low TGF-β1, Smad7 and TβRII levels. Finally, analysis of patient samples showed an overexpression of Smad7 in 59 % of HCCs with a significant correlation to tumor size in a HBV related subgroup from China.

In conclusion, HCC cell lines can be allocated into two main groups regarding the cytostatic TGF-β response, which is accompanied by distinct differences in basal and TGF-β induced expression patterns of TGF-β signaling components and target genes. Smad7 upregulation seems to be an important mechanism in transformed hepatocytes to establish insensitivity against TGF-β induced cytostasis, and once this is accomplished, a more malignant phenotype may develop.

ZUSAMMENFASSUNG

Primärer Leberkrebs, wovon 90 % hepatozelluläre Karzinome (HCCs) sind, ist weltweit der fünfthäufigste und dritttödlichste Tumor. Eine hohe Heterogenität und spät auftauchende Symptome erschweren die Entwicklung effizienter Therapien gegen HCCs. Transforming growth factor beta (TGF-β) ist ein multifaktorielles Zytokin und ein wichtiger Regulator chronischer Lebererkrankungen, die in HCC resultieren können. TGF-β, ein Tumorsuppressor in der Krebsentstehung, kann tumorfördernde Eigenschaften während der Krebsprogression annehmen. Diese duale Rolle und die hohe Heterogenität des HCCs erzeugen eine hohe Komplexität bezüglich des TGF-β-Signalweges während der Hepatokarzinogenese. Da die TGF-β-Kaskade in HCCs häufig modifiziert ist, bietet sie einen guten Ansatzpunkt für dringend benötigte neue Therapiestrategien. Dies setzt aber ein detailliertes zeitliches und mechanistisches Verständnis des Funktionalitätswechsels von TGF-β voraus.

Vor diesem Hintergrund wurde eine systematische Analyse der zytostatischen TGF-β-Wirkung sowie möglicher Resistenzmechanismen in zehn häufig verwendeten Leberkrebszelllinien durchgeführt. TGF-β induzierte über Smad3 Zelltod oder Proliferationsinhibition in einer Gruppe von Zelllinien mit niedriger Expression von TGF-β1 und dessen Inhibitor Smad7, aber erhöhten TGF-β Rezeptor II (TβRII)-mRNA-Mengen (PLC/PRF/5, Hep3B, HuH7, HepG2). TGF-β-Behandlung führte zu einer starken Induktion der Smad3 und TβRI-Expression, der Smad3-Transkriptionsaktivität sowie der Expression der Zielgene Bim, PAI-1 und Smad7. Diese Zelllinien wurden bereits zuvor einer Gruppe zugeordnet, die korrelierend mit einer besseren Prognose für Patienten sogenannte frühe TGF-β-Zielgene exprimiert. Die zweite Gruppe (HLE-, HLF-, FLC-4- und zum Teil HuH6-Zellen) war resistent gegen TGF-β induzierte Zytostase und zeigte hohe Smad7- und TGF-β1-, aber niedrige TβRII-Expression und eine abgeschwächte TGF-β-induzierte Smad3-Transkriptionsaktivität. Zudem besaßen außer HuH6 alle Zelllinien dieser Gruppe eine hohe Migrationsfähigkeit. HCC-M- und HCC-T-Zellen zeigten Charakteristika beider Gruppen: Trotz Resistenz gegen zytostatische TGF-β-Effekte waren die TGF-β1-, Smad7-, aber auch TβRII-mRNA-Niveaus niedrig. Eine abschließende Analyse von Patientenproben zeigte in 59 % aller HCCs eine Smad7-Überexpression, die in HBV-assoziierten Proben aus China mit der Tumorgröße korrelierte.

Zusammenfassend zeigt die vorliegende Arbeit, dass HCC-Zelllinien bezüglich der zytostatischen TGF-β-Antwort zwei Hauptgruppen zugeordnet werden können, die klare Unterschiede in basalen und TGF-β-induzierten Expressionsmustern von TGF-β-Signalkomponenten und Zielgenen aufweisen. Die Daten weisen darauf hin, dass Smad7-Überexpression ein wichtiger Mechanismus zur Entwicklung einer Resistenz gegen zytostatische TGF-β-Effekte in transformierten Hepatozyten zu sein scheint. Eine so etablierte Resistenz könnte zur Entwicklung eines bösartigeren Phänotyps führen.

ABBREVIATIONS

° C	Degree Celsius
ALK	Activin receptor-like kinase (e.g. ALK5)
AMH	Anti-Müllerian hormone
AP	Alkaline phosphatase
AP-1	Activator protein-1
APS	Ammonium persulfate
ARE	Activin responsive element
ATP	Adenosine triphosphate
Bcl-2	B-cell lymphoma 2
Bcl-XL	B-cell lymphoma-extra large
Bim	Bcl-2 interacting mediator of cell death
BMP	Bone morphogenetic protein
BSA	Bovine serum albumin
CBP	CREB (cAMP responsive element binding protein)-binding protein
CCC	Cholangiocarcinoma
Cdc	Cell division cycle (e.g. Cdc42)
CDK	Cycline dependent kinases
cDNA	Complementary DNA
CI5	Cancer Incidence in Five Continents
cm	Centimeter
CREB	cAMP responsive element binding protein
DAXX	Death-associated protein 6
ddH2O	Double distilled water
DEPC	Diethyl pyrocarbonate
DMEM	Dulbecco’s modified eagle medium
DMSO	Dimethyl sulfoxide
DNA	Deoxyribonucleic acid
dNTP	Deoxyribonucleotide
e.g.	"exempli gratia" (for example)
EGF	Epidermal growth factor
ELF	Embryonic liver beta-fodrin
EMT	Epithelial-to-mesenchymal transition
ERK	Extracellular signal-regulated kinase
FAST-1	Forkhead activin signal transducer 1
FBS	Fetal bovine serum
FGF	Fibroblast growth factor
FoxO	Forkhead box O
GADD34-PP1c	Growth-arrest and DNA-damage-inducing protein 34-protein phosphatase 1c
GAPDH	Glyceraldehyde-3-phosphate dehydrogenase
GDF	Growth and differentiation factor
h	Hour
HBsAG	Hepatitis B surface antigen

HBSS	Hank's buffered salt solution
HBV	Hepatitis B virus
HCC	Hepatocellular carcinoma
HCl	Hydrochloric acid
HCV	Hepatitis C Virus
HDAC1	Histone deacetylase 1
HER2	Human epidermal growth factor receptor 2
hiFBS	Heat inactivated FBS
HRP	Horseradish peroxidase
hTERT	Human telomerase reverse transcriptase
IARC	International Agency for Research on Cancer
iCCC	Intrahepatic cholangiocarcinoma
IL-x	Interleukin (e.g. IL-1)
INF-γ	Interferon gamma
I-Smad	Inhibitory Smad
Jab1	Jun activation domain-binding protein 1
JNK	c-Jun N-terminal kinase
LAP	Latency associated protein
LDH	Lactate dehydrogenase
LTBP	Latent TGF-β binding protein
Luc	Luciferase
mA	Milliampere
MAPK	Mitogen activated protein kinase
MEK	Mitogen-activated protein kinase (MAPK) kinase (also called MKK)
mg	Milligram
$MgCl_2$	Magnesium chloride
MH	Mad homology domain, e.g. MH1 and MH2
min	Minute
MKK	Mitogen-activated protein kinase (MAPK) kinase (also called MEK)
mL	Milliliter
mM	Millimolar
mRNA	Messenger RNA
MTT	3-(4,5-Dimethylthiazol-2-yl)-2,5- diphenyltetrazolium bromide
mV	Millivolt
N	Normal
NaOH	Sodium hydroxide
NEDD4-2	Neural precursor cell expressed, developmentally down-regulated 4-2
NFkB	Nuclear factor of kappa light polypeptide gene enhancer in B-cells
ng	Nanogram
nM	Nanomolar
nm	Nanometer
NOX4	NADPH (Nicotinamide adenine dinucleotide phosphate) oxidase 4
p	p-value (significance level)
PAI-1	Plasminogen activator inhibitor-1
PARP	Poly(ADP-ribose)-polymerase 1
PCR	Polymerase chain reaction

PDGF	Platelet-derived growth factor
PET	Polyethylene terephthalate
pg	Picogram
PI3K	Phosphatidylinositide 3-kinases
PLC	PLC/PRF/5 (HCC cell line)
PP1	Protein phosphatase 1
PPM1A	Protein phosphatase methyltransferase 1 A
r	Pearson coefficient
RhoA	Ras homolog family member A
RNA	Ribonucleic acid
rpm	Rotations per minute
rRNA	Ribosomal RNA
R-Smad	Receptor Smad
s	Second
SBE	Smad binding element
SDS	Sodium dodecyl sulfate
SDS-PAGE	Sodium dodecyl sulfate-polyacrylamide gel electrophoresis
SE	Standard error
ShcA	Src homology domain containing transforming protein
siRNA	Small interfering RNA
Smad	Human homolog of Drosphila gene Mad (Mothers against decapentaplegic) and C.elegans genes Sma
Smurf1/2	Smad specific E3 ubiquitin protein ligase 1/2
Sp-1	Stimulating protein 1
STAT1	Signal transducer and activator of transcription 1
STRAP	Serine/threonine kinase receptor-associated protein
SXS	Serine-X-serine (amino acid sequence in R-Smads)
TAK-1	TGF-β-associated kinase-1
TGFBR1	TGF-β receptor I
TGF-β	Transforming growth factor β
TIMP-1	Tissue inhibitor of metalloproteinase 1
TNF-α	Tumor necrosis factor alpha
TRAF6	TNF receptor associated factor 6
TRAIL	TNF-related apoptosis inducing ligand
Tris base	Tris(hydroxymethyl)aminomethane
Tris-HCl	Tris base hydrochloride buffer
Tiul1	TGIF (TGF-β induced factor homeobox) interacting ubiquitin ligase 1
TβRI	TGF-β receptor I
TβRII	TGF-β receptor II
UV	Ultraviolet
V	Volt
xg	Earth's gravitational force
YB-1	Y box binding protein 1
ZO-1	Zonula occludens 1
µL	Microliter
µM	Micromolar

1 INTRODUCTION

1.1 TGF-β and signaling components

1.1.1 TGF-β and its receptors

Transforming growth factor beta (TGF-β) is a multifunctional and pro-fibrogenic cytokine, which belongs to the eponymous TGF-β cytokine family. In humans, it comprises at least 33 members belonging to two different subgroups: TGF-β isoforms 1-3, the activins and Nodal belong to the TGF-β subfamily, whereas the bone morphogenetic protein (BMP) subfamily consists of BMPs, growth and differentiation factors (GDFs) as well as anti-Müllerian hormone (AMH) [1, 2]. Members of the TGF-β family are involved in a wide range of cellular processes, such as growth arrest, apoptosis, differentiation, matrix remodeling and migration and thereby carry out important functions during, e.g., embryogenesis, tissue homeostasis, the control of the immune system and angiogenesis, as well as during development and progression of diverse diseases.

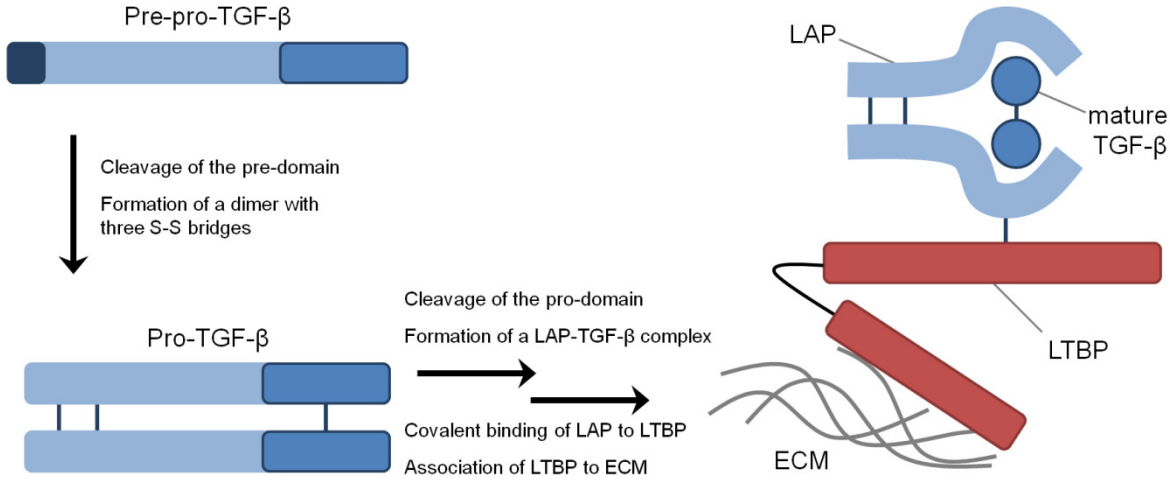

Figure 1.1 Production and secretion of latent TGF-β (based on [3]). See text for details.

TGF-β1 is synthesized as a 391 amino acid pre-pro-peptide consisting of a signal sequence, a pro-region and an N-terminal 112 amino acid sequence encoding the TGF-β monomer [4, 5] (Figure 1.1). After cleavage of the signal sequence, a homodimeric pro-peptide is formed, with three disulfide bridges connecting both chains. Once the dimeric pro-region is cut off, it remains tightly associated to the mature TGF-β dimer, giving it the name latency associated protein (LAP). Additionally, each LAP protein is covalently bound to the latent TGF-β binding protein (LTBP) [6-8], which is involved in the association of TGF-β-LAP with extracellular matrix (ECM) [9]. In this complex, TGF-β is inactive and not able to exert its biological functions. Various proteases (e.g., plasmin [10]), but also non-proteolytical proteins

(e.g., thrombospondin 1 [11] and integrins [12, 13]) and environmental factors such as a mild acidic pH [14] are able to activate TGF-β.

Activated TGF-β signals through cell surface transmembrane serine/threonine kinase receptors. It induces the formation of a heterotetrameric type I (TGF-β receptor 1, TβRI) and type II (TGF-β receptor 2, TβRII) receptor complex (Figure 1.2): Mature TGF-β dimers bind to constitutively active TβRII, which results in a recruitment of two TβRI molecules between two type II receptors [15-17]. TβRI and TβRII are structurally similar proteins containing an extracellular ligand binding domain, a transmembrane region and a C-terminal intracellular domain with a serine/threonine kinase. TβRII phosphorylates TβRI at a glycine-serine-rich sequence, just N-terminal of the kinase domain, leading to activation and subsequent autophosphorylation of TβRI. Activated type I receptors are then able to transmit the signal to soluble TGF-β signaling components within the cells, to so called receptor (R)-Smads (see chapter 1.1.2, reviewed in [18, 19]).

Despite a high number of different members in the TGF-β superfamily, their signal is mediated by only five type II and seven type I receptors. Each cytokine binds to a specific combination of type I and II receptors, allowing for a diverse and specific signal conversion (outlined in [18]). The main signaling mediators for TGF-β were identified to be TβRII, TβRI (activin receptor-like kinase 5, ALK5), R-Smads 2 and 3 [18, 20]. However, binding of TGF-β by other type I receptors was found in endothelial (ALK1) [21, 22] and epithelial (ALK2 or ALK3) cells [23], both in an ALK5 dependent manner and leading to the activation of R-Smads 1 and 5 instead of Smad2 and 3 (see chapter 1.1.2) [23, 24].

1.1.2 Canonical TGF-β signaling

The intracellular canonical signaling of the TGF-β superfamily is mediated and controlled by the so-called "mothers against decapentaplegic" or Smad proteins. The Smad family consists of eight members of whom five are receptor (R)-Smads (Smad1, 2, 3, 5 and 8), one is a universal signaling partner (Smad4) and two, Smad6 and Smad7, are inhibitors of some signaling branches (reviewed in [25]). R-Smads and common (co)-Smad4 are structurally subdivided in a conserved N-terminal Mad-homolgy (MH) 1 and a C-terminal MH2 domain with a flexible linker region in between (Figure 1.3) [25-27].

Upon ligand binding, heterotetrameric receptor complexes transfer the cytokine signal into the cell through phosphorylation of a specific R-Smad subset (chapter 1.1.1). TGF-β mainly activates Smad2 and Smad3 through phosphorylation of two serine residues within a highly conserved C-terminal serine-X-serine (SXS) motif [28]. All the different activated R-Smads

associate to the same protein, common mediator (co)-Smad4. Two R-Smads bind one Smad4 protein to form a heterotrimeric transcription factor [29]. These complexes then translocate into the nucleus to modify expression of a broad spectrum of genes (Figure 1.2).

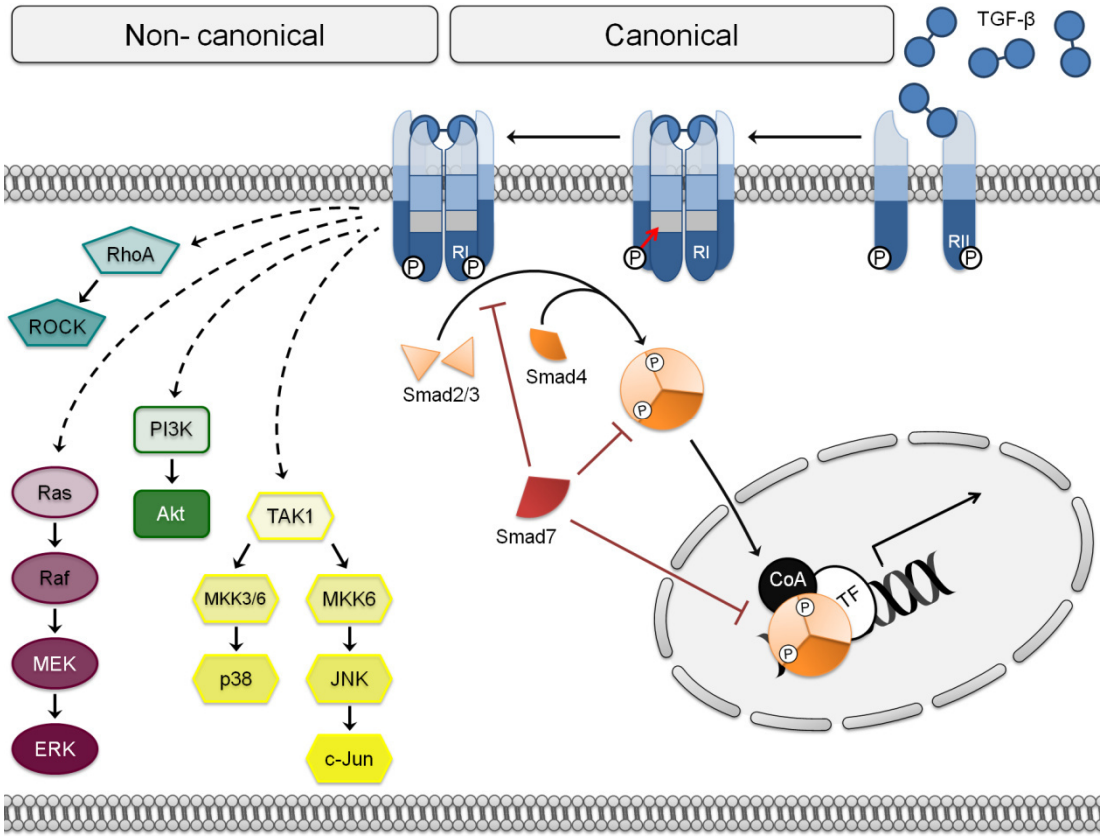

Figure 1.2 **Canonical and non-canonical TGF-β signaling** (modified from [30] and other publications mentioned in this thesis). CoA = Co-activator, TF = transcription factor. For further details see chapter 1.1.

Smad3/Smad4 recognize a specific palindromic DNA sequence (5'-GTCTAGAC-3') called Smad binding element (SBE). Here, a conserved β-hairpin structure within the Smad3 MH1 domain binds a 5'-GTCT-3 or the reverse 5'-CAGA-3 sequence. In contrast to Smad3, Smad2 is unable to directly interact with DNA, caused by an interfering amino acid sequence next to the crucial β-hairpin [27, 31, 32]. Smad2/Smad4 therefore exert its transcriptional activity by additional associations with DNA binding proteins, e.g., FAST-1 (Forkhead activin signal transducer 1, FoxH1) leading to activation of an activin response element (ARE) [33]. The Smad binding element (SBE) by itself is a very short nucleotide sequence for a protein recognition side and the binding of Smad3 happens with low affinity [32]. In promoters, a SBE is usually in close proximity to recognition sites of Smad-interacting factors, which are able to increase the Smad-DNA binding efficiency. Therefore, R-Smad proteins interact with various transcription factors of different classes (e.g., zinc finger proteins, forkhead and nuclear receptor family proteins): FoxO (Forkhead box O), for example, cooperates with Smad2/3 to regulate p21Cip1 expression [34] or Sp-1 (stimulating protein 1) associates with

Smad2 and/or Smad3 to activate various TGF-β target genes (e.g., $p15^{Ink4B}$, [35],$p21^{Cip1}$ [36], Smad7 [37], PAI-1 (plasminogen activator inhibitor-1) [21, 22] or Collagen Col1A [38]) and many others (reviewed in [18, 39]). However, R-Smads may also inhibit gene expression. Smad3, for instance, cooperates with the transcription factor E2F4/5 and the co-repressor p107 in order to exert repressive effects of TGF-β on the proto-oncogene c-Myc [40]. Here, Smad3 recognizes, as opposed to the classical mechanism, a repressive binding element (5'-TTGGCGGGAA-3') [41].

Additionally, Smad proteins are known to interact with a broad range of cofactors (reviewed in [18]), which modulate the intensity of the target gene expression. While co-activators such as CBP/p300 (CREB binding protein) increase the activity of the Smad transcription factor complex [42, 43], it is reduced by co-repressors such as c-Myc [44] and YB-1 (Y box binding protein 1, a mediator of inflammatory interferon-gamma (INF-γ) signaling) [38].

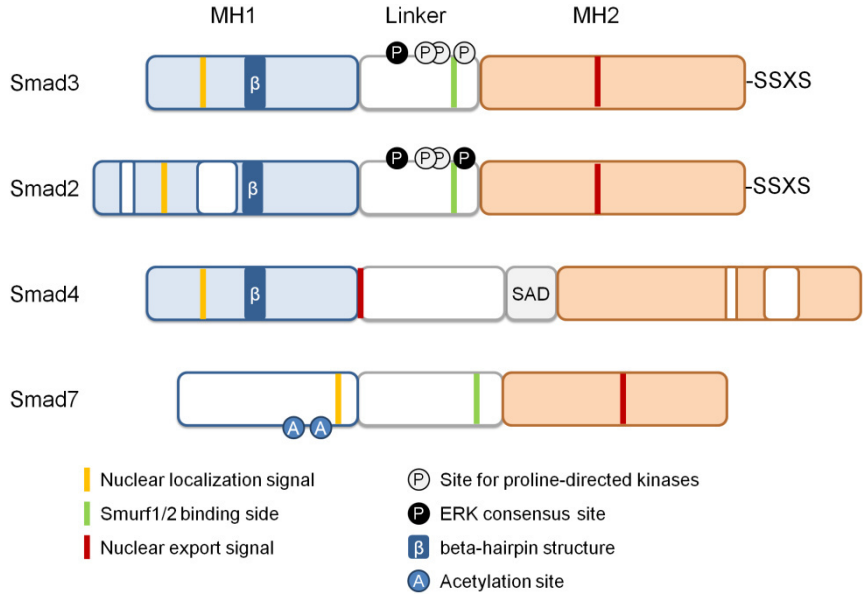

Figure 1.3 **Structure of receptor, common mediator and inhibitory Smad proteins** (based on reviews [25, 45] and publications in the text). The figure shows a simplified Smad structure, mainly with motifs discussed in this thesis. See chapter 1.1.2, 1.1.3 and 1.1.4.2 for further details.

A third subgroup of the Smad family members is formed by Smad6 and Smad7; two potent inhibitors of TGF-β superfamily signaling [46-48]. Inhibitory (I)-Smads share a conserved MH2 domain with the R-Smads (Figure 1.3). However, they lack the C-terminal serine-X-serine motif, which is fundamental for R-Smad signaling. Additionally, N-termini of I-Smads are shorter and less conserved than the ones of other Smads [47, 49, 50]. I-Smad expression is upregulated in a negative feedback mechanism by different members of the TGF-β cytokine superfamily [48, 51-53]. While Smad7 is a more general inhibitor, interfering with TGF-β and BMP subfamily signaling, Smad6 mainly antagonizes the latter [46-49, 54, 55]. Smad7 will be extensively discussed in chapter 1.1.4. Next to I-Smads, other proteins

are also able to terminate TGF-β signaling, e.g., TGF-β target genes Ski and SnoN. They inhibit the association of the Smad-DNA binding complex with the co-activator p300 [56, 57]. Many other mechanisms exist to regulate duration and intensity of TGF-β signaling. For example, phosphatase PPM1A dephosphorylates Smad2/3 and thereby shortens the nuclear stopover of Smad complexes [58].

In conclusion, canonical TGF-β superfamily signaling represents a relatively straightforward signaling cascade whose different effects are mediated by seven type I and five type II receptors and are specifically converted by five receptor Smad molecules. TGF-β signaling itself is mainly exploited by TβRI, TβRII and Smad2/3. However, a broad variety of different collaborating factors ensures a cell type and context specific target gene expression and thereby creates a more complex picture. TGF-β's ability to additionally exert Smad independent functions and cross-talk with a number of other signaling pathways further increases this intricacy (next chapter).

1.1.3 Non canonical TGF-β signaling and cross-talk with other pathways

TGF-β exerts its functions not only via the classical canonical signaling pathway, but also modulates a broad spectrum of different pathways in a Smad independent and often cell type and context dependent manner (Figure 1.2, left). For example, TGF-β activates the mitogen activated protein kinase (MAPK) pathway, which transmits either survival signals via Ras and ERK (extracellular signal-regulated kinase) or, activating p38 or JNK (c-Jun N-terminal kinase), stress signals. TGF-β may induce the interaction of TβRI with adaptor protein ShcA (src homology domain containing transforming protein) leading to activation of Ras and ultimately MAP kinase ERK [59]. ERK activation by TGF-β was found in epithelial cells and fibroblasts [59-61], for example, and was shown to participate in induction of EMT (epithelial to mesenchymal transition) [62, 63]. Similarly, TGF-β may induce stress mediated MAPK signaling via activation of JNK or p38 [64-67]. One possible mechanism suggests the involvement of TRAF6/TAK-1 (TNF receptor associated factor 6/TGF-β-associated kinase-1) and links TGF-β induced apoptosis and EMT to p38 and JNK mediated signaling [67, 68]. Another non-canonical pathway utilized by TGF-β is phosphatidylinositide 3-kinases (PI3K)/Akt signaling, which can be involved in TGF-β mediated survival signaling or EMT in epithelial cells [69-71] and induction of proliferation in mesenchymal cells [72]. Intriguingly, TGF-β may also block Akt activity, which, for example, may happen during TGF-β induced apoptosis [73, 74]. Finally, RhoA (Ras homolog family member A) and Cdc42 (Cell division cycle 42) of the Rho family of GTPases, offer another possibility for TGF-β to affect R-Smad independent signaling pathways. They are involved in the regulation of intracellular actin

dynamics and stress fiber formation, and their activation by TGF-β is linked to EMT (RhoA) and alterations of the actin cytoskeleton (Cdc42) [75-77]. Smad7 can be an important scaffold protein which mediates some non-canonical TGF-β signaling by recruiting non-Smad proteins to the TGF-β receptor complex (chapter 1.1.4.3).

While TGF-β regulates several independent signaling cascades, canonical TGF-β signaling, in turn, can also be modified by cross-talking signaling pathways. A common motif is the phosphorylation of linker regions of the R-Smads (Figure 1.3). Unlike the C- and N-terminal domains, the connecting region is less conserved between the different Smad proteins, offering an additional and more specific regulation level. Linker regions are modified at ERK consensus sites and serine/proline motifs, which are recognized by proline-directed kinases [78]. Cycline dependent kinases (CDK) 2 or 4 mediate linker phosphorylation of Smad2 and 3 and thereby decrease TGF-β induced p15 expression and growth arrest [79]. Cam kinase II (Ca2+-calmodulin-dependent protein kinase II) preferentially phosphorylates linker regions of Smad2 and inhibits its nuclear translocation [80]. Finally, IL-1β (interleukin 1-beta) induces JNK mediated linker phosphorylation of Smad3. Interestingly, TGF-β itself is able to use this signaling branch and an increasing ratio of linker/C-terminal phosphorylation is observed during liver disease progression [81, 82]. Additionally, other mechanisms exist to regulate R-Smads, e.g., Akt, which hinders activated Smad3 to enter the nucleus (see chapter 1.4.2).

1.1.4 Smad7 – inhibitor of canonical TGF-β signaling and cross-talk mediator

TGF-β is a key regulator of various cellular processes and is involved in many (patho-) physiological processes. Logically, it is tightly regulated by different mechanisms, often with Smad7 as a key player. Coherently, Smad7 activity, as a potent inhibitor of canonical TGF-β signaling, is also carefully controlled. Additionally, Smad7 is an important cross-talk mediator.

1.1.4.1 Inhibition of canonical TGF-β signaling by Smad7

Smad7, as an effective inhibitor of canonical TGF-β signaling, exerts its inhibitory functions via various mechanisms (outlined in [2]):

a) Binding of TGF-β receptor 1 (TβRI)
   Due to the conserved MH2 domain (chapter 1.1.2), Smad7 is able to compete with R-Smads for the binding sites of TβRI. It forms a stable complex with the type I receptor leading to decreased activation of R-Smads and canonical TGF-β signaling [46, 48, 83, 84].

b) Smad7 as an adapter protein to promote TGF-β receptor 1 degradation
E3 ubiquitin ligases Smurf1/2 (Smad specific E3 ubiquitin protein ligase), Tiul1 and NEDD4-2 recruit nuclear Smad7 to the active TGF-β receptor complex to initialize lysosomal or proteasomal degradation of TβRI and, except for Tiul1, Smad7 itself [85-89].

c) Induction of TGF-β receptor 1 dephosphorylation
Next to induction of type I receptor degradation, Smad7 is also able to regulate it reversibly by mediating dephosphorylation of the activated TβRI and ALK1 by GADD34-PP1c (growth-arrest and DNA-damage-inducing protein 34-protein phosphatase 1c) and PP1α, respectively [90, 91].

d) Interactions with proteins assisting Smad7 with regulation of TβRI
Proteins, such as STRAP (serine/threonine kinase receptor-associated protein) [92], SIK (salt-inducible kinase) [93] and many more (reviewed in [2]) were shown to interact with Smad7 in order to modify TβRI activity.

e) Blocking DNA binding sites
Smad7 is present in the nucleus and cytoplasm. It can interfere with TGF-β signaling by competing with Smad transcription factor complexes for the corresponding DNA binding sites [94]. Additionally, Smad7 interacts with acetyltransferase p300 [95] as well as histone deacetylase 1 (HDAC1) [96] and is thereby possibly able to regulate TGF-β target gene transcription by epigenetic modifications.

f) Binding of Smad4 and inducing its degradation
Smurfs directly interact with R- and I-Smads via specific motifs within the Smad linker region. Smad4 does not possess this motif (Figure 1.3). However, Smad7 is able to interact with Smad4 and thereby facilitate Smurf1 mediated degradation of Smad4. Similar collaborative effects were observed for Smurf2, Tiul1 and NEDD4-2 [97].

1.1.4.2 Regulation of Smad7

Smad7 is an important regulator of TGF-β signaling. Because of that, it is tightly controlled by different factors and mechanisms (summarized in [2]):

a) Negative feedback loop
Smad7 is directly induced by canonical TGF-β signaling because of a Smad binding element within the Smad7 promoter [37, 98-100]. Optimal induction of the inhibitor's expression is reached when the R-Smad/Smad4 complex cooperates with other

transcription factors, e.g., AP-1 (activator protein-1) or Sp-1 [37, 98, 101] and co-activators such as CBP/p300 [43, 100]. Many of those factors are regulated by other pathways underlining the role of Smad7 as cross-talk mediator (see chapter 1.1.4.3).

b) Regulation of Smad7 stability by induction of proteasomal degradation
Smad7 is able to recruit Smurf1/2 for degradation of TβRI and reduction of TGF-β signaling. This leads to the decomposition of the inhibitor itself (see above). Additionally, Jab1 and Arkadia mediate nuclear export, ubiquitination and degradation of Smad7, resulting in enhanced TGF-β signaling [102, 103].

c) Regulation of Smad7 stability by acetylation
p300 acetylates Smad7 at two lysine residues (Figure 1.3) and thereby inhibits Smurf-mediated degradation of the inhibitor (see above) [95]. HDAC1 [96], on the other hand, can reverse this effect by deacetylation of Smad7.

d) Induction of Smad7 expression by TGF-β antagonizing pathways
Because Smad7 is a potent inhibitor of canonical TGF-β signaling, its expression is induced by many antagonizing pathways (discussed in chapter 1.1.4.3).

1.1.4.3 Smad7 and its importance as cross-talk mediator

On the one hand, TGF-β signaling is involved in the regulation of many different processes and therefore needs delicate fine tuning, which includes interaction with other signaling pathways. On the other hand, TGF-β is involved in the regulation of other signaling cascades. Smad7 plays an important role as mediator of those interacting pathways (cross-talk).

TGF-β is a pro-fibrogenic and anti-inflammatory cytokine and therefore exerts inhibitory effects on several opposing proteins (summarized in [104]), e.g., tumor necrosis factor alpha (TNF-α) or IL-1 [105]. Vice versa, it is not surprising that pro-inflammatory cytokines (illustrated in Figure 1.4, left), such as IFN-γ [100, 106, 107], IL-1β and TNF-α directly induce Smad7 expression to suppress TGF-β effects [108]. Next to inflammatory pathways, Smad7 is induced by other factors, e.g., epidermal growth factor (EGF) [51] and HER2 (human EGF receptor 2) [109] or by UV irradiation [110].

Smad7 was shown to be involved in the regulation of several proteins belonging to other pathways (Figure 1.4, right). TGF-β dependent activation of the TβRI-TβRII complex may as well result in a recruitment and activation of TRAF6, which in turn leads to activation of TAK-1, MAPK kinases (MKKs) and ultimately MAP-kinases JNK or p38 [67, 111]. Smad7 is

crucial for TGF-β induced cell death via p38 in the prostate cancer cell line PC-3U. Here, it likely acts as a scaffold protein during the formation of a receptor-TRAF6-TAK1-MKK complex [68]. Further evidence for the importance of Smad7 as a mediator of TGF-β induced cell death (chapter 1.2) was collected on several cell lines of various origins [112-114]. However, in other cells, e.g., gastric epithelial [115] and HCC (Hep3B) [116] cell lines,

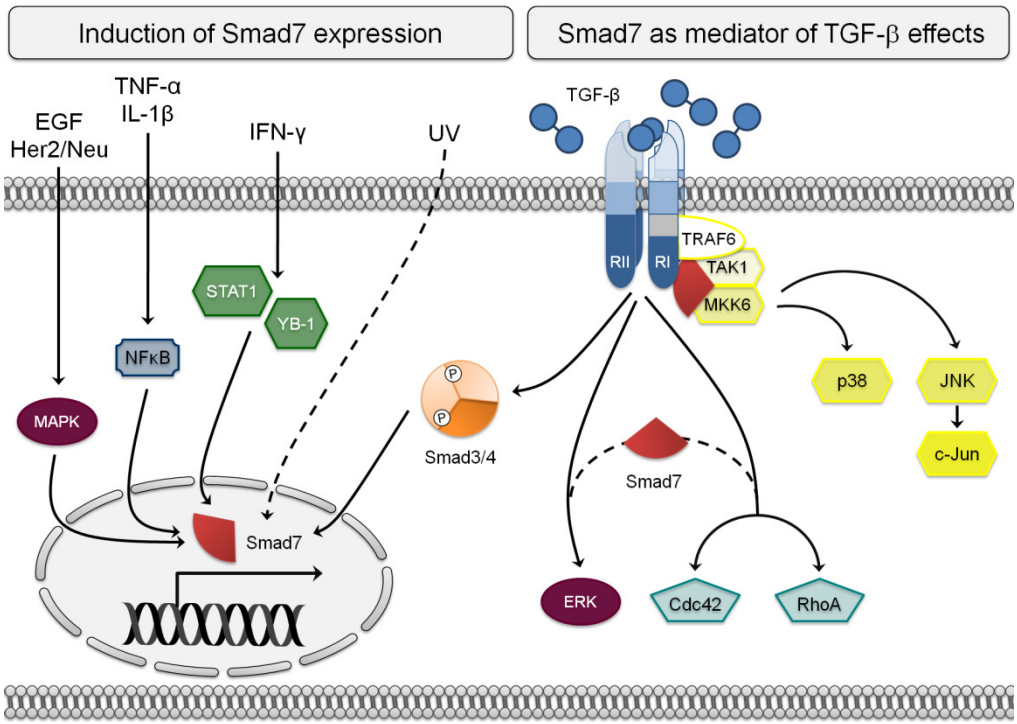

Figure 1.4 **Smad7 as cross-talk mediator.** (Left) Smad7 links various signaling pathways to the TGF-β cascade. (Right) Smad7 mediates effects of TGF-β on other signaling pathways. (adapted from [2]).

Smad7 was able to promote inhibitory effects on apoptosis. Smad7 is involved in TGF-β mediated activation of ERK or JNK in a bronchial and kidney epithelial cell line, respectively [114, 117]. The high complexity as well as cell type and status dependency is mirrored by the fact that contrary effects are found in other situations: TGF-β induced erythrocyte differentiation, for example, is inhibited by Smad7 overexpression *in vitro*, accompanied by a blockage of ERK1/2, JNK1/2 and p38 activity [118]. In another setting, Smad7 was shown to be necessary for TGF-β induced Cdc42 and RhoA GTPases mediated rearrangement of actin filaments in prostate carcinoma cells [76]. Finally, Smad7 may participate in the well known interaction of TGF-β and Wnt signaling. TGF-β is able to decrease but also enhance the latter one. β-catenin is an important component of adherens junctions but also an intracellular signaling transducer of Wnt leading to e.g., induction of EMT. Similar to TGF-β, Smad7 was shown to inhibit, but also to induce β-catenin activity [119-122].

In conclusion, Smad7 expression is induced by several factors with opposing functions to TGF-β to inhibit TGF-β signaling. Further, Smad7 itself is involved in the regulation of several

Smad independent signaling pathways by TGF-β. In both situations, ambiguous effects can be sometimes observed and the final outcome is likely cell and context dependent.

1.2 Effects of TGF-β on cytostasis and epithelial-to-mesenchymal transition (EMT)

TGF-β is a well recognized mediator of programmed cell death (apoptosis) in various cell types, including B- and T-cells, lymphocytes, endothelial and epithelial cells (reviewed in [123]), and hepatocytes [71, 124]. Since then, different possibly involved pathways (Smad dependent and independent) were identified, but the situational and mechanistic understanding still needs improvement in some areas.

For some cell systems, a non-canonical, but Smad7 dependent mechanism was identified for TGF-β induced apoptosis (chapter 1.1.4.3). In non-transformed murine hepatocytes (AML-12 cell line), TGF-β exerts its proapoptotic functionality via recruitment of DAXX (Death-associated protein 6) to TβRII and subsequent activation of JNK [125]. In primary human hepatocytes and some, but not all, liver (cancer) cell lines, TGF-β enhances TRAIL (TNF-related apoptosis inducing ligand) expression in a Smad4 and AP-1 dependent manner. Herzer et al demonstrated that TGF-β induced cell death is at least partly TRAIL dependent in those cell lines which are responsive to the death ligand [126, 127]. Furthermore, Smad dependent initiation of apoptosis in primary murine hepatocytes is mediated by Smad3 and not Smad2 in dependency of p38 [128, 129]. In fetal rat hepatocytes, ROS production by NADPH oxidase 4 (NOX4) was identified as a key mediator of TGF-β induced apoptosis, involving Bcl-XL reduction, increased caspase 3 activity and the release of mitochondrial cytochrome C into the cytosol [130, 131].

In the past, induction of apoptosis has been considered as the main task of TGF-β. However, this is not true for all circumstances and the response of hepatocytes is more likely context dependent: In healthy liver TGF-β and activin seem to fulfill anti-proliferative tasks and thereby keep hepatocytes in a quiescent state [132]. In general, TGF-β is a well known inhibitor of cell division in endothelial, hematopoietic and, especially, epithelial cells (reviewed in [133]). The mechanism is cell type specific but it often leads to inactivation of cyclin dependent kinases (CDKs), key components of the cell cycle, or to downregulation of pro-proliferative c-Myc. CDK activity is tightly controlled by different mechanisms; by CDK inhibitors of the INK4 or Cip/Kip protein family, among others. TGF-β exerts its anti-proliferative tasks by upregulation of some of those inhibitors, e.g., p15INK4b [35, 134] and p21CIP1 [36, 135], or by interference with CDK4 expression [136]. Moreover, TGF-β inhibits

c-Myc expression (see chapter 1.1.2) and thereby overrides the repression of p15 and p21 transcription [137, 138].

Another important effect of TGF-β on hepatocytes is the induction of epithelial to mesenchymal transition (EMT). EMT is a process during which an epithelial cell detaches from the epithelial cell assembly and adopts a mesenchymal like and more motile phenotype. TGF-β induced EMT comes along with several changes in TGF-β target gene expressions [139]: While epithelial markers such as E-cadherin or zonula occludens 1 (ZO-1) are repressed, an increase in typical mesenchymal markers, such as vimentin, can be observed. Additionally, TGF-β induces expression of profibrogenic genes, e.g., TIMP-1 (Tissue inhibitor of metalloproteinase 1), collagens and PAI-1, which suggests that hepatocytes contribute to changes in extracellular matrix composition during fibrogenesis [139, 140].

1.3 Hepatocellular carcinoma

In 2008, an estimated 12.7 million new cancer cases and 7.6 million cancer related deaths were counted worldwide. With about 750 000 cases and 694 000 deceased, primary liver cancer is the sixth most common and third deadliest cancer and has with 93 % one of the highest mortality rates of all. For men, it is even among the top 5 of the most common and the second most lethal cancer worldwide with 2.4 times more incidences than women (Figure 1.5). Almost 84 % of all incidences occur in developing countries, while, except for Southern Europe, liver cancer is not as common in well developed areas. In Europe, for example, it was ranked number 13 of the most frequent tumor types but was responsible for the 7th highest cancer related mortality rate (Globocan 2008 database of the International Agency for Research on Cancer, IARC [141]). Nevertheless, liver cancer caused increasing interest towards the end of the last millennium because, between 1970 and 1990, age standardized incidence rates were constantly rising in many European countries (CI5plus database of the IARC [142]). Hepatocellular carcinoma (HCC) derives from transformed hepatocytes and represents, with about 85-90 %, the majority of all primary liver cancers. Other tumors belonging to this group are, for example, hepatoblastomas and intrahepatic bile duct carcinoma (intrahepatic cholangiocarcinoma, iCCC) [143].

The liver is a highly regenerative organ, which is therefore able to fulfill its most important tasks even under difficult circumstances. Due to this, liver cancer can often silently develop over a long period of time, reaching big tumor sizes without symptoms. This results in a late diagnosis and is the main reason for the high lethality of HCC [144]. Even in well developed countries, in 2003 only a minority of 30-40 % of HCC patients was diagnosed at an early

stage, and thus suitable for the most promising treatment options such as tumor resection, radiofrequency ablation and liver transplantation [145]. In 2005, early diagnosed HCCs treated with those therapies reached five year survival rates above 50 % in some studies, while treatment following the first occurrence of symptoms resulted in very poor prognosis with survival rates below 10 % (reviewed in [146]). Sorafenib (a comparably new treatment option for HCC) was hailed as a success when survival rates increased by 3 months. This provides a good example of how limited treatment options are to date [147, 148]. Therefore, new therapeutic strategies and tools for diagnosis are urgently needed.

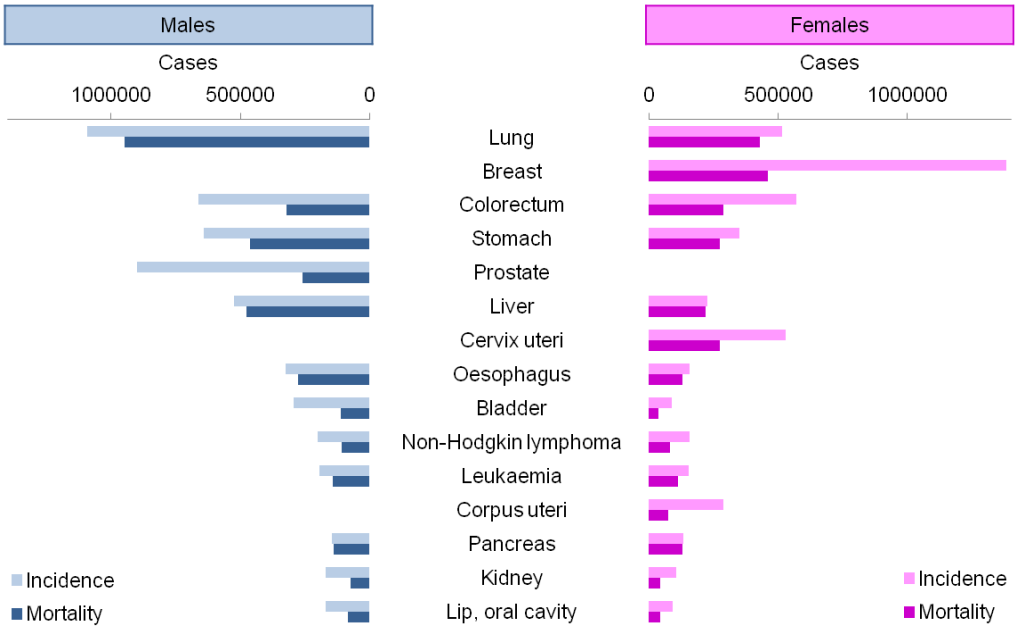

Figure 1.5 **Estimates of new cancer incidences and mortality worldwide in 2008** (according to Globocan 2008 v2.0, Cancer Incidence and Mortality Worldwide [141]). Numbers of new cases and deaths of the 15 most common cancers are shown for males (blue) and females (pink).

Development of HCC is thought to be a complex, multi-factorial and multistep process, which is the underlying reason for its complex molecular pathogenesis. A broad variety of well defined factors, dependent on gender, geographic area and race could be associated to occurrence of HCC. Up to 80 % of all HCCs arise in cirrhotic liver caused by different liver diseases [145]. Estimated age-standardized incidence rates per 100 000 inhabitants varied from 1.6 for females from Northern Europe or South Central Asia to 35.5 for males in Eastern Asia (Globocan 2008 database [141]). In China, Hepatitis B virus (HBV) is the main cause of HCC, while hepatitis C virus (HCV) and alcohol abuse related HCC are the dominant etiologies in Western countries, including Germany. Aflatoxin B1, a mycotoxin produced by mold fungus, causes liver inflammation, which if chronic may lead to fibrosis, advance to cirrhosis and ultimately end in HCC. Aflatoxin B was identified as a common etiology of HCC in Africa where fungus contaminated food is consumed regularly. Other risk factors are, e.g., diabetes, smoking and obesity (reviewed in [144, 145]). The different etiologies suggest that

the incident rate of HCC can be significantly reduced by different approaches, such as vaccination against HBV or avoidance of contaminated food. Until then, diagnosis and therapy strategies urgently need to be improved.

1.4 TGF-β and cancer

TGF-β is evolutionarily considered a rather young cytokine, only occurring during the appearance of vertebrates in order to support the development of increasingly complex organisms. It is involved in the regulation of complex epithelial and neural networks, the immune system, wound healing and many more processes [149]. Overtaking such important functions, it is not astonishing that malfunctioning TGF-β signaling results in a broad variety of different diseases, such as cancer, among others.

1.4.1 The TGF-β paradox

TGF-β, with its pro-apoptotic and anti-proliferative nature, was first identified as a tumor suppressor, which was confirmed *in vivo* in a heterozygous TGF-β knockdown mouse model: In these animals, chemically induced tumorigenesis in liver and lung is enhanced suggesting an inhibitory function of TGF-β during tumor initiation [150]. The majority of all cancers are of epithelial origin (carcinomas) [151, 152], and the growth limiting and apoptosis inducing effect of TGF-β on epithelial cells is well documented. Paradoxically, TGF-β is highly present in several cancers, e.g., T cell leukemia, colorectal cancer and renal and breast carcinoma [153-157]. Elevated amounts of the cytokine were also detected in human HCC and malignant hepatocytes were identified as one source for the overexpression [158, 159]. Increased TGF-β levels can often be correlated to increased tumor aggressiveness and poorer prognosis [156, 157], indicating that TGF-β may as well act as an oncogene. Indeed, TGF-β was not only found to exert anti-tumorigenic functions, but, in certain contexts, also to promote tumor growth and progression (see chapter 1.4.2). This ambiguous behavior of TGF-β and its signaling components is described as “the TGF-β paradox”. The dual role of TGF-β signaling during carcinogenesis was nicely demonstrated in a chemically induced murine skin cancer multistage-model. TGF-β overexpression decreases the total number of benign skin papillomas. However, this relatively low tumor number shows an explicit enhancement of malignant transformation compared to wild type animals [160]. TGF-β signaling is tightly controlled by several factors. Smad7 is a potent inhibitor of the canonical TGF-β signaling cascade and is therefore defined as a potential tumor promoter in healthy tissue. Similar to the ambiguous effects of TGF-β in cancerogenesis, its inhibitors, e.g.,

Smad7 (discussed in chapter 1.4.3), Ski and SnoN [161] may also overtake tumor promoting and suppressing tasks. Hence, the functional outcome is probably dependent on the context and the stage of disease.

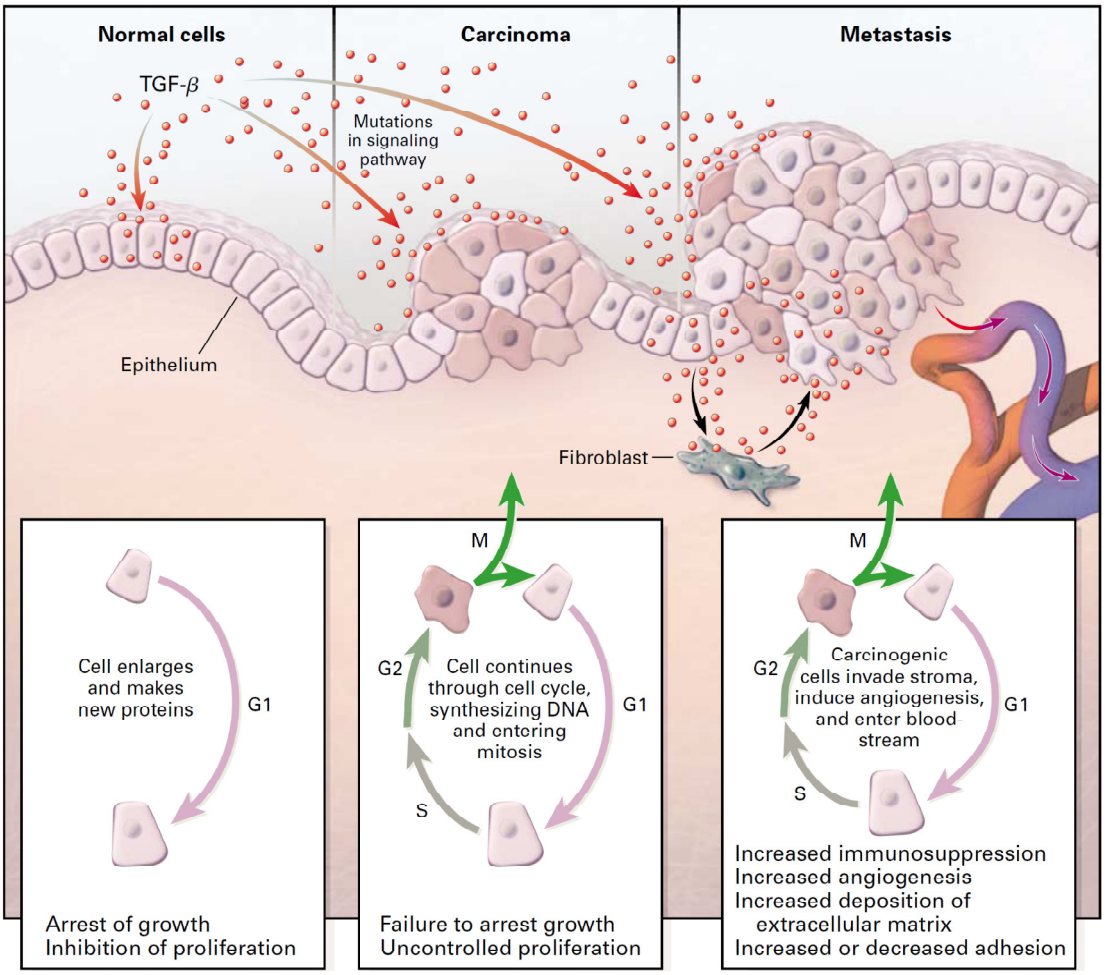

Figure 1.6 The ambiguous functions of TGF-β signalling during tumorigenesis (taken from [162])

Many findings indicate that neoplastic cells may convert TGF-β from a tumor suppressor to a tumor promoter (reviewed in [149, 163, 164]). However, this switch from anti- to protumorigenic behavior is not a mandatory step. During cancerogenesis, two different scenarios are imaginable, which were discussed in detail by Joan Massague [149]:

a) TGF-β acts as a tumor suppressor as it is a strict regulator of, e.g., tissue homeostasis, as well as apoptosis, proliferation, differentiation, survival and adhesion. In a functional TGF-β signaling cascade, this cytokine is therefore able to inhibit development of tumors or their progression to more malignant stages. Cancer cells can circumvent those effects by virtually inhibiting the whole TGF-β signaling cascade. This is accomplished by inactivation of main signaling components such as TGF-β receptors.

b) In a second scenario, not core but downstream components are inactivated. Dependent on the affected protein, this could lead to a specific aberration of the cytostatic TGF-β branch, while other TGF-β signaling tasks are still functional. In doing so, cancer cells can still benefit from the pro-oncogenic nature of TGF-β.

Thus, inactivation of TGF-β signaling at the very start may inhibit tumor suppressive effects. However, inhibitory aberrations in specific downstream components may not only block growth inhibitory effects of TGF-β but also allow tumor cells the use of other TGF-β functions to promote tumor growth or malignant transformation. The dual role of TGF-β underlines the importance to fully understand TGF-β signaling in a time and context deciphered manner in order to develop adjusted therapy strategies. Further, the double edged behavior of TGF-β is the basis for its possible involvement in almost all fundamental steps during tumorigenesis, the so-called hallmarks of cancer, which will be discussed in the following chapter.

1.4.2 TGF-β signaling and the hallmarks of cancer

The complex and necessary steps of cancer formation and progression are described as hallmarks of cancers (outlined in [165, 166]). TGF-β may play important roles in all of them (Figure 1.7; summarized in [167]):

Resistance to growth limiting factors and evasion of apoptosis
Under normal circumstances, inhibition of proliferation and induction of programmed cell death are important features to keep tissue homeostasis and healthy cells, e.g., without damaged DNA. Among others, TGF-β is an important regulator of tissue homeostasis. Cancer cells are usually resistant against such signals. Thus, many tumors develop strategies to inhibit TGF-β signaling as a whole or exclusively the cytostatic TGF-β branch.

To avoid cytostatic effects of TGF-β, aberrations in TGF-β receptors and common-mediator Smad4 were found in different tumors (reviewed in [163]). Mutational inactivation of TβRII or a decrease of TβRI and TβRII expression was found in various cancers (reviewed [149]). Carriers of a common hypomorphic TβRI allele (TGFBR1*6A) have a 20-40 % higher risk to suffer from breast, ovarian or colorectal cancer [168]. Mutations in receptor Smads are detected rather seldom. However, Smad2 is mutated in a subset of colorectal cancers [169] whereas Smad3 expression is lost in gastric cancers and T cell lymphoblastic leukemia [149]. In contrast to R-Smads, Smad4 is a well recognized tumor suppressor, which is underrepresented in a few cancers, e.g., pancreatic carcinomas (55 %) [170] and sporadic colorectal tumors [169]. In some tumors, underlying mechanisms of TGF-β resistance are

well defined (aberrations in Smad4 and TβRII). Nevertheless, there are still a broad number of cases, for which the mechanism is not yet understood. Different findings suggest, as a beneficial event, an upregulation of inhibitors Smad7 (chapter 1.4.3), Ski or SnoN [57, 171] or the inhibition of TGF-β signaling by pro-tumorigenic factors, e.g., c-Myc [172], mutated p53 [136] or Ras [78].

Depletion of Smad4 occurs in about 10 % and downregulation of TβRII in a subset of 25 % of HCCs [173, 174]. However, mutations in TGF-β signaling components, such as Smad4 and Smad2, are rather scarce in HCC when compared to other cancers. Nevertheless, aberrant TGF-β signaling is frequently observed in HCC [175], suggesting other mechanisms underlying the observed dysregulation. For example, induction of the PI3K/Akt pathway, an important mediator of proliferation and survival, inhibits TGF-β mediated apoptosis in the HCC cell line Hep3B [176]. Independent of its kinase activity, Akt binds Smad3 and prevents its activation by TGF-β. However, this complex formation is inhibited by TGF-β itself, so that the balance between Akt and Smad3 decides over the cell fate [177, 178]. In line with this, Akt is frequently overexpressed and hyperactive in HCC [179, 180]. Smad7 is overexpressed in a limited number of HCCs [159, 181] and is able to protect HCC cell line Hep3B against cytostatic effects of TGF-β [116]. Finally, ELF (embryonic liver beta-fodrin) and PRAJA (PJA1) provide another possible mechanism to establish resistance against cytostatic effects of TGF-β. ELF interacts with Smad3, but not Smad2, and guides it into the nucleus. PRAJA, an E3 ligase, marks ELF and Smad3 but not Smad4 for its proteasomal degradation [182, 183]. Aberrant levels of those two components may therefore build up the cytostatic resistance. In fact, ELF is underrepresented in HCC [184].

Proliferation despite missing exogenous growth factors

Tumors develop an independency of exogenous growth signals by autonomous production of mitogenic proteins or by constitutive activation of corresponding signal cascades. TGF-β was named after its ability to induce proliferation as well as transformation of mesenchymal cells [185]. However, in epithelial, endothelial and hematopoietic cells, its antiproliferative effects are well known (chapter 1.2). Similar to mesenchymal cells, TGF-β was found to induce proliferation in some cancer cell lines of epithelial origin, e.g., prostate cancer [186] and HCC cell lines HCC-M and HCC-T [187] suggesting that tumors of epithelial origin may even invert cytostatic TGF-β effects. One underlying reason might be the capability of TGF-β to elevate the production of mitogenic growth factors (e.g., PDGF [188] and FGF [189]) and some of their receptors, e.g., PDGF receptor [188]. Next to a direct impact on various growth factors, TGF-β is known to activate Smad independent pathways (chapter 1.1.3 and 1.1.4), e.g., the mitogenic branch of Ras-Raf-MAPK pathway, a mediator of different growth factors, e.g., EGF and FGF [190].

Capability of invasion and migration

Tumor aggressiveness is increased by migration, invasion and metastasizing to surrounding tissue and, more importantly, to more distant sites. To acquire those abilities, several events have to take place in a cell and TGF-β may be involved: TGF-β loosens (epithelial) cell-cell contacts by initiating EMT (chapter 1.2). Coherently, blockage of TGF-β leads to an increase of epithelial marker E-cadherin and inhibition of migration and invasion in highly invasive HCC cell lines [191]. Additionally, TGF-β induces expression of α3β1-integrin and thereby transforms HCC cell line HepG2 to a migrative and invasive cell line under certain circumstances. Integrins are transmembrane receptors which are involved in processes such as adhesion, migration, invasion, proliferation and survival [192]. TGF-β may enhance levels of extracellular matrix proteins, e.g., collagen. Further, it inhibits the expression of matrix degrading enzymes such as collagenase, while it induces the expression of their inhibitors, PAI-1 and TIMP-1, amongst others [139, 162]. During tumorigenesis, this feature may change and, suddenly, TGF-β even enhances levels of matrix-degrading proteins, e.g., protease uPA (urokinase-type plasminogen activator) [193]. Hence, TGF-β possibly increases tumorigenicity by dissolving cell-cell-contacts and enhancing proteolytic activity and thereby facilitates enhanced cell motility.

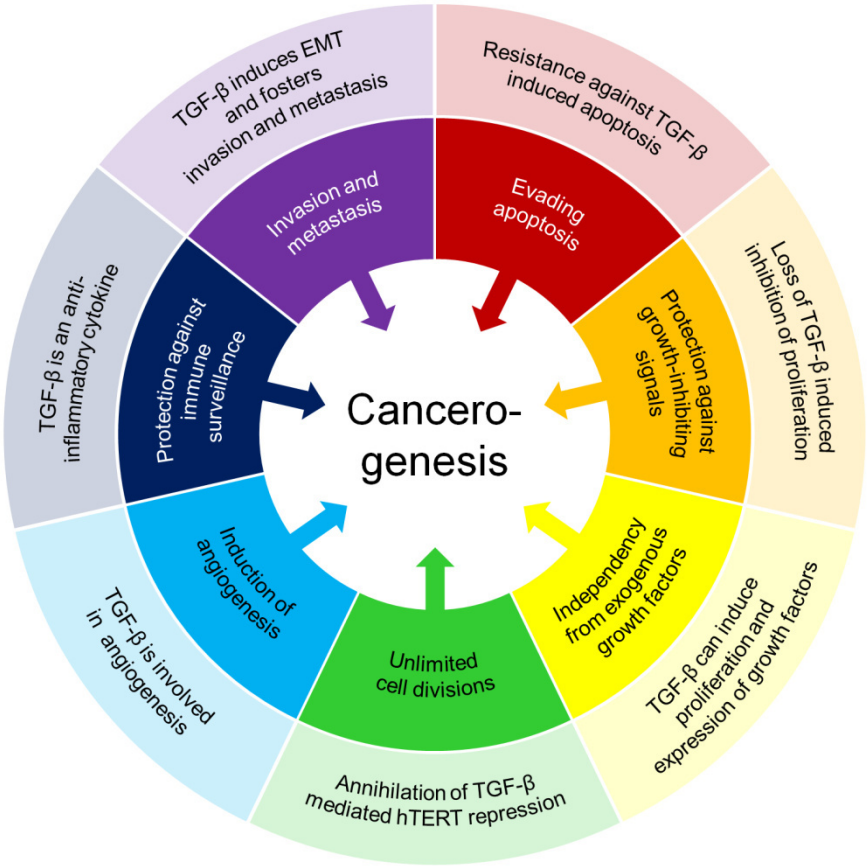

Figure 1.7 Hallmarks of cancer and involvement of TGF-β in it (inspired by [165-167].

Induction of angiogenesis and creation of access to blood supply

To increase sizes of solid tumors, an access to the blood system is needed to grant supply of nutrients and oxygen. TGF-β is involved in the regulation of angiogenesis, the formation of new blood vessels, and was shown to be pro-angiogenic *in vivo*. Knockdown of TGF-β signaling components, such as TGF-β [194] or TβRI [195] leads to defective vessel formation in mouse models. In human, the relevance of TGF-β for angiogenesis was demonstrated by the correlation of TGF-β receptor endoglin mutations with hereditary hemorrhagic telangiectasia, a genetic disease which is based on aberrant blood vessel formation [196]. Accordingly, TGF-β has been linked to tumor vascularity in HCC [197].

Circumvention of limited cell divisions

Mature somatic cells usually exhibit, based on inactive telomerase and therefore telomere shortening during each mitotic cycle, a limited life span. Reaching immortality by resetting this "mitotic clock" is a crucial step during the conversion of a normal cell to a neoplastic one. One approach of normal cells to inhibit telomerase activity is to contain expression of human telomerase reverse transcriptase (hTERT), the catalytic and rate limiting subunit of human telomerase. In cancers, including HCC, telomerase activity and hTERT expression is usually increased [198-200] to maintain protective chromosome ends despite enhanced cell division. TGF-β is a potent inhibitor of hTERT expression [201]. Hence, TGF-β may exert its tumor suppressive effects by restricting hTERT expression and activity. Cancer cells could benefit from interference with those mechanisms.

Evasion of attack by the immune system

The expression of tumor-specific antigens on the cell surface would normally lead to the recognition and destruction of tumor cells by the immune system. Most cancer cells evade this attack through various mechanisms. Regarding the immune response, TGF-β mainly exerts anti-inflammatory functions (outlined in [104]). Its importance as key regulator of immune and inflammatory processes was demonstrated in a TGF-β1 knockout mouse [202]. In line with this, TGF-β levels are elevated in various cancers [154-156, 203] including HCC [158, 159], possibly also to overcome immune surveillance. Interestingly, elevated TGF-β levels are often observed in T cell leukemia, which is frequently accompanied by disturbed cellular immunity [153]. These findings indicate that increased TGF-β levels within neoplastic areas eventually contribute to building up protection against the immune system. Noteworthy, there is accumulating evidence of a pro-tumorigenic cancer-associated inflammation.

"Genome instability"

There are different intracellular processes which control genomic integrity and repair possible defects. Aberrations in one of those processes, sooner or later, lead to an enrichment of

genomic mutations. Tumor cells usually show defects in some of those genome monitoring processes. Radiation induced apoptosis and p53 activity (an important protein for the regulation of cell cycle, DNA repair and apoptosis) are reduced in heterozygous TGF-β knockout mice [204]. However, p53 mutation is a frequent motif in tumors. On the contrary, TGF-β inhibits DNA repair in epithelial cells through downregulation of Rad51, a component of a DNA repair complex. This suggests that TGF-β is able to inhibit DNA repair and might therefore promote genomic instability [205]. An increased mutation rate accelerates the formation of a phenotype with advantages over healthy cells. Hence, this genomic instability is a basic requirement to facilitate the above described hallmarks of cancer.

1.4.3 The role of Smad7 during cancerogenesis

In line with the ambiguous functions of TGF-β during tumorigenesis and different outcomes in different cancers, Smad7 shows similar double edged behavior in various cancers.

Smad7 as a tumor suppressor

Smad7, accompanied by INF-γ induction, promotes colitis but protects against colitis associated colorectal cancer in a Smad7 overexpressing mouse model [206]. Similarly, Smad7 was observed to block invasion of murine mammary carcinoma cell line JygMC to liver or lung *in vivo,* accompanied by an increase of β-Catenin and E-Cadherin expression [120]. In human patients with esophageal squamous cell carcinoma, low Smad7 expression correlated with metastasis and a poorer prognosis [207].

Smad7 as an oncogene

Smad7 may exert pro-tumorigenic functions in a broad range of different cancers: Colorectal cancer patients with a Smad7 deletion have a better prognosis [208], which is in line with enhanced metastasis of Smad7 overexpressing human colorectal cancer cell lines in mouse [209]. However, another publication showed an opposite but not significant result in patients [156]. Further, elevated Smad7 can be associated with poorer prognosis for patients with endometrial or gastric cancer [210, 211]. Chen et al. demonstrated that Smad7 protein levels increase with ascending malignant transformation of oral epithelium [212]. Similarly, Smad7 seems to correlate with a more aggressive phenotype in invasive breast cancers [213, 214]. In thyroid tumors, Smad7 staining intensifies during tumor formation and even more during malignant transformation [215]. Furthermore, Smad7 overexpression in mouse airway Clara cells protects against asthma but promotes chemically induced lung cancer [216].

Smad7 with possible dual roles during cancerogenesis

In some cancers, the role of Smad7 is still not fully clarified. In pancreatic cancer, for example, Smad7 was identified as a tumor suppressor, as undetectable Smad7 protein levels correlated with metastasis and poorer prognosis [217]. In contradiction, Kleeff et al found that Smad7 mRNA (messenger RNA) is elevated in human pancreatic cancer tissue samples. Smad7 protects pancreatic cancer cells against TGF-β induced growth arrest without blocking PAI-1 induction *in vitro* and enhances tumor growth *in vivo* [218]. Smad7 levels are elevated in human skin areas exposed to sun light [219] suggesting a possible oncogenic role of Smad7 of neoplastic skin diseases. Additionally, Smad7 in combination with oncogene Ras, but not alone, induces malignant transformation of keratinocytes *in vitro* and *in vivo* [220]. On the other hand, it has to be noted that DiVito et al show a tumor suppressive effect of Smad7 in a melanoma cell line *in vitro* and *in vivo* [122]. In HCC, Smad7 staining was more present in neoplastic tissue when compared to adjacent areas [159, 181]. However, the inhibitor was found to inhibit β-catenin activation and nuclear translocation as well as HCC promotion in a mouse model [121].

1.5 Aims of this study

HCC is the third most common cause for cancer related deaths with limited treatment options. Because TGF-β signaling is frequently aberrant in HCC, it is an attractive and intensively studied, but so far seldom used, therapeutic target. The mechanistic elucidation of TGF-β signaling in HCC is still insufficient because of its ambiguous nature. Yet, to develop a deep understanding of TGF-β signaling in a context, stage and time dependent manner is indispensable. This alone will prevent from targeting a wrong TGF-β signaling component at the wrong moment and will facilitate the design of individual adjusted therapy strategies.

This study thus aimed to characterize TGF-β signaling in ten commonly used liver cancer cell lines, and to identify possible correlations to the cytostatic behavior. TGF-β induces growth arrest and apoptosis in hepatocytes, which is often disrupted in HCC. Hence, effects of TGF-β on proliferation and cell death were analyzed to identify resistant and responsive cell lines. Basal and TGF-β induced expression of TGF-β signaling components were evaluated to detect possible underlying reasons for different cytostatic responses. TGF-β signaling can be disrupted at different levels. Therefore, TGF-β induced R-Smad phosphorylation and the resulting transcriptional activity and target gene expression were analyzed to elucidate the position of signaling disruption. Furthermore, knockdown experiments aimed to work out the impact of Smad2 and 3 on observed cytostatic effects of TGF-β. Finally, a possible

involvement of different described protective mechanisms (inhibitory Smad7, Akt and other survival factors, PRAJA/ELF) against TGF-β induced cell death was examined.

Smad7 may interfere with TGF-β mediated cytostasis and is frequently overexpressed in cancer. Hence, the Smad7 expression levels in human HCC were of interest.

This study offers an in-depth analysis of canonical TGF-β signaling in HCC and hepatoblastoma cell lines and associates different phenotypes with resistance or responsiveness towards cytostatic effects of TGF-β.

2 MATERIALS AND METHODS

2.1 Materials

2.1.1 Instruments

Agarose gel electrophoresis system PerfectBlueTM Mini & Midi System	Peqlab Biotechnology (Erlangen, Germany)
Blotting module, XCell II Blot	Invitrogen GmbH (Darmstadt, Germany)
Cell culture incubator, HERAcell	Kendro Laboratory (Hanau, Germany)
Centrifuges	
Biofuge Primo R	Heraeus Holding (Solingen, Germany)
Biofuge Fresco	Heraeus Holding (Solingen, Germany)
Electrophoresis module, Mini-Protean	Bio-Rad Laboratories (Munich, Germany)
Gel casting system for immunoblot, Mini-Protean	Bio-Rad Laboratories (Munich, Germany)
Laminar flow hood, HA 2472 GS	Heraeus Holding (Solingen, Germany)
Luminescent image analyzer, FUSION SL™ Advance	Peqlab Biotechnology (Erlangen, Germany)
Microplate reader Infinite® M200	Tecan Group Ltd. (Männedorf, Switzerland)
NanoQuant plate	Tecan Group Ltd. (Männedorf, Switzerland)
PCR thermocycler, DNA engine Dyad®	Bio-Rad Laboratories (München, Germany)
Shaker, Duomax 1030	Heidolph (Schwabach, Germany)
Real time PCR cylcer AbiPrism 7000	Applied Biosystems (Foster City, CA, USA)
Ultra-Turrax T25	IKA®-Werke (Staufen, Germany)
UV transilluminator	INTAS (Göttingen, Germany)

2.1.2 Chemicals

Acrylamide/Bis Solution, 37.5:1 (30 % w/v)	Serva (Heidelberg, Germany)
Ammonium persulfate (APS)	Sigma Aldrich (St. Louis, Missouri, USA)
Bromphenol blue, sodium salt	Applichem (Darmstadt, Germany)
Chloroform	Sigma Aldrich (St. Louis, Missouri, USA)
p-Coumaric acid	Sigma Aldrich (St. Louis, Missouri, USA)
Deoxycholic acid, sodium salt	Serva (Heidelberg, Germany)
Diethyl pyrocarbonate (DEPC), 99 %	Sigma Aldrich (St. Louis, Missouri, USA)

3-(4,5-Dimethylthiazol-2-yl)-2,5-diphenyltetrazolium bromide	Sigma Aldrich (St. Louis, Missouri, USA)
Dimethyl sulfoxide, suitable for hybridoma	Sigma Aldrich (St. Louis, Missouri, USA)
Dimethyl sulfoxide (DMSO), 99.5 %	Sigma Aldrich (St. Louis, Missouri, USA)
Dimethyl sulfoxide, suitable for hybridoma	Sigma Aldrich (St. Louis, Missouri, USA)
EDTA, disodium salt	Carl Roth (Karlsruhe, Germany)
Ethanol, 99 %	Merck (Darmstadt, Germany)
Ethidium bromide	Sigma Aldrich (St. Louis, Missouri, USA)
Ficoll solution	Sigma Aldrich (St. Louis, Missouri, USA)
Formaldehyd	Sigma Aldrich (St. Louis, Missouri, USA)
Formamid	Merck Group (Darmstadt, Germany)
Glacial acetic acid	Merck Group (Darmstadt, Germany)
Glycerol	Sigma Aldrich (St. Louis, Missouri, USA)
Glycine	Merck (Darmstadt, Germany)
Hydrochloric acid (HCl), 1 N	Merck (Darmstadt, Germany)
Hydrogen peroxide solution, 30 %	Merck (Darmstadt, Germany)
Isopropanol	Merck (Darmstadt, Germany)
Luminol	Sigma Aldrich (St. Louis, Missouri, USA)
Magnesium chloride solution, 1 M, for molecular biology	Sigma Aldrich (St. Louis, Missouri, USA)
β-Mercaptoethanol	Merck (Darmstadt, Germany)
MOPS, buffer grade	Applichem (Darmstadt, Germany)
4-Nitrophenyl phosphate disodium salt hexahydrate	Sigma Aldrich (St. Louis, Missouri, USA)
Nonident P40	Roche (Mannheim, Germany)
SDS (sodium dodecyl sulfate), ultra pure	Carl Roth (Karlsruhe, Germany)
Sodium acetate trihydrate	Merck Group (Darmstadt, Germany)
Sodium hydroxide (NaOH), 1 N	Merck Group (Darmstadt, Germany)
Sodium chloride (NaCl)	Carl Roth (Karlsruhe, Germany)
TEMED (N,N,N',N'-Tetramethylethylene-diamine)	Sigma Aldrich (St. Louis, Missouri, USA)
Trypan blue solution	Sigma Aldrich (St. Louis, Missouri, USA)
Universal-Agarose "Seakem LE"	Lonza Group (Cologne, Germany)
Tris(hydroxymethyl)aminomethane (Tris base)	Sigma Aldrich (St. Louis, Missouri, USA)

2.1.3 Cell culture

2.1.3.1 Cell lines

For the cell culture experiments, ten different liver cancer cell lines and the reporter cell line MFB-F11 were used.

HCC-M — HCC-M cells were established and first described in 1983 [221]. This cell line of epithelial phenotype was isolated from a hepatocellular carcinoma (Edmondson type III) of a Hepatitis B surface antigen (HBsAG)-positive Japanese male. Injected in nude mice, tumors of this type of hepatocellular carcinoma developed at the sites of inoculation. HBV particles or HBsAg could not be detected in the cell culture.

HCC-T — This human hepatoma cell line was isolated from a male Japanese HCC patient (Edmondson type II) with cirrhosis and Hepatitis C virus infection (HCV) [222]. HCC-T cells show epithelial like morphology and features of malignant cells such as tumor development in nude mice.

HepG2 — Epithelial HepG2 cells derive from a well differentiated HCC of a 15 year old male Caucasian from Argentina [223].

Hep3B — This cell line was isolated from a well differentiated HCC from an 8 year old back male from the U.S.A. This cell line, when injected into nude mice, forms tumors of hepatocelluar character [223, 224].

HuH6 — HuH6 cells are epithelial like cells deriving from a hepatoblastoma of a Japanese infant [225].

HuH7 — This cell line was established from a well differentiated and serologically negative HCC, removed from a 57-year old Japanese male [226].

PLC/PRF/5 — PLC/PRF/5 or Alexander is a well differentiated HCC cell line obtained from an HCC of a 24 year old male patient from Mozambique with cirrhosis and HBV infection. It produces HBsAG and forms tumors in nude mice [224, 227].

FLC-4 — This cell line is a mutant of the HCC cell line JHH-4, which was established from a 51-year old Japanese male with HCC of Edmondson's type III. FLC-4 cells are well differentiated and secrete liver-specific proteins [228]. They show similar morphological and biological properties to its parental cell line JHH-4, which was established from a hepatocellular carcinoma of the Edmondson type III, and which forms tumors in nude mice [229].

HLE and HLF — HLE and HLF are two poorly differentiated cell lines, obtained from a HCC of a 68-year-old patient. While HLE cells show epithelial-like morphology, HLF cells are rather similar to fibroblasts. Nevertheless, it is supposed that the latter also originates from hepatoma cells. Unlike HLF, HLE cells produce α-fetoprotein. HLF, but not HLE cells form tumors upon transplantation into the cheek pouch of adult hamsters treated with cortisone acetate [230].

MFB-F11 — MFB-F11 is a murine fibroblast cell line from TGF-β-/- mice and expresses an introduced alkaline phosphatase under the control of Smad binding elements (SBE). Hence, it is used as reporter cell line for TGF-β1-3 quantification [231].

Cell lines were kindly provided by: Prof. Tetsu Watanabe and Prof. Yutaka Inagaki, Tokai University School of Medicine Basic Clinical Sciences and Public Health, Kanagawa, Japan (HCC-M and HCC-T); the SFB/TTR77 funded by the Deutsche Forschungsgemeinschaft (HepG2, Hep3B, PLC/PRF/5, HLE and HLF purchased from ATCC (American Type Culture Collection) and HuH7 purchased from JCRB (Japanese Collection of Research Bioresources Cell Bank)) and Prof. Michael Kern, Institute of Pathology, Cologne, Germany (FLC-4 and HuH6).

2.1.3.2 Cell culture reagents and additives

Dulbecco's Modified Eagle Medium (DMEM) with high glucose , without L-glutamine	Lonza Group Ltd. (Cologne, Germany)
Dulbecco's Modified Eagle Medium (DMEM) with high glucose , without L-glutamine, without phenol red	Lonza Group Ltd. (Cologne, Germany)
L-glutamine, 200 mM	PAA Laboratories (Cölbe, Germany)
Fetal bovine serum (FBS)	Invitrogen (Darmstadt, Germany)
Hank's Buffered Salt Solution (HBSS)	PAA Laboratories (Cölbe, Germany)
10x Trypsin-EDTA	PAA Laboratories (Cölbe, Germany)
Human recombinant TGF-β1	Peprotech (Hamburg, Germany)
Hygromycin B	Sigma Aldrich (St. Louis, Missouri, USA)

2.1.3.3 Materials for RNA interference, transfection and adenoviral infection technology

Reagents for transfection and siRNA knockdown

Lipofectamine® 2000 Transfection Reagent	Invitrogen (Darmstadt, Germany)
Lipofectamine® RNAiMax	Invitrogen (Darmstadt, Germany)
Opti-MEM® reduced serum medium	Invitrogen (Darmstadt, Germany)

siRNA oligonucleotides

Target gene	Company	Order No
negative control	Qiagen	1027281
Smad2		SI02757496
Smad3		SI00082495

Table 2.1 siRNAs used in this study. All siRNAs were obtained from Qiagen (Hilden, Germany)

Plasmids

β-galactosidase control vector, pCR3lacZ	Invitrogen (Darmstadt, Germany)
Smad7 promoter deletion mutant, p(-625 SacI)-Smad7 prom-Luc	described in [37]
pARE-Luc and Fast-1	gift from Prof. C.-H. Heldin (Ludwig Institute for Cancer Research, Uppsala University, Uppsala, Sweden) [232]

Adenoviruses

Ad$(CAGA)_9$-MLP-Luc	described in [31]
β-galactosidase control adenovirus	gift from Prof. C.-H. Heldin (Ludwig Institute for Cancer Research, Uppsala University, Uppsala, Sweden), described in [233]

Reagents for reporter assays

Passive lysis buffer	Promega (Mannheim, Germany)
β-galactosidase assay	Promega (Mannheim, Germany)
Luciferase substrate	Promega (Mannheim, Germany)

2.1.3.4 Reagents for MTT, LDH and ATP and alkaline phosphatase assays

MTT solution

5 mg/mL MTT powder (3-(4,5-Dimethylthiazol-2-yl)-2,5- diphenyltetrazolium bromide)
Dissolved in DMEM starvation medium, sterile filtered and stored at -20 °C

MTT solvent

4 mL 10 % SDS in double distilled water (ddH_2O)

4 mL DMSO

2 mL Acetic acid solution (1.2 mL glacial acetic acid in 100 mL ddH_2O)

Freshly prepared

AP buffer

3.75 g Glycine (50 mM)

12.11 g Tris base (100 mM)

1 mL Magnesium chloride ($MgCl_2$) solution, 1 M (1 mM)

Adjusted to pH 10.5 with NaOH and filled up with ddH_2O to 1 L

AP substrate solution

2 mg 4-Nitrophenyl phosphate disodium salt hexahydrate

1 mL AP-Puffer (see above)

Freshly prepared

Cytotoxicity Detection Kit	Roche (Mannheim, Germany)
Bovine serum albumin, Fraction V (BSA)	Merck (Darmstadt, Germany)
CellTiter-Glo Luminescent Cell Viability Assay	Promega (Mannheim, Germany)

2.1.4 Materials for DNA and RNA work

2.1.4.1 Kits, buffers and reagents for RNA isolation, reverse transcription, PCR and gel electrophoresis

Taq DNA polymerase, FastStart, dNTP Pack	Roche Diagnostics (Mannheim, Germany)
Omnitect Reverse Transcription Kit	Qiagen (Hilden, Germany)
RNeasy Mini Kit	Qiagen, Hilden, Germany
TRIzol® Reagent	Invitrogen (Darmstadt, Germany)
DNA ladder, 100 bp plus	AppliChem (Darmstadt, Germany)

50x TAE buffer

242 g Tris base

57.1 mL Glacial acetic acid

18.6 g EDTA, sodium salt

Adjusted with ddH_2O to 1 L

DNA loading buffer

35 mL Glycerol

2 mL 50x TAE buffer

Filled up with ddH_2O to 100 mL, addition of a spatula tip of bromphenol blue

DEPC-water

1 mL Diethyl pyrocarbonate (DEPC)

Adjusted with ddH_2O to 1 L; incubated at room temperature over night; autoclaved for 20 min.

20x MOPS (RNA running buffer)

400 mM MOPS

100 mM Sodium acetate trihydrate

20 mM EDTA, disodium salt

In DEPC-water, pH 7.0

RNA loading buffer

50 % Formamide

22 mM Formaldehyde

5 % 20x MOPS buffer

10 % Ficoll solution

In DEPC water; addition of 6 µL/mL ethidium bromide and 1 spatula tip of bromphenol blue

2.1.4.2 Human gene expression assays and primers for TaqMan and SYBR Green real time PCR

Gene	Assay name	Assay ID (Applied Biosystems)
Smad2	Smad2	Hs00998181_gH
Smad3	Smad3	Hs00969205_g1
Smad7	Smad7	Hs00178696_m1
TGF-β receptor 1	TGFBR1	Hs00610318_m1
TGF-β receptor 2	TGFBR2	Hs00559661_m1
18S	18S-rRNA	Hs03003631_g1
B2M	beta-2-microglobulin	Hs00187842_m1

Table 2.2 **TaqMan gene expression assays used in this study.** All assays were obtained from Applied Biosystems (Foster City, CA, USA) and were specific for the respective human mRNA.

2x TaqMan® Universal PCR Master Mix No AmpErase® UNG — Applied Biosystems (Foster City, CA, USA)

2x SYBR® Green Master Mix — Applied Biosystems (Foster City, CA, USA)

Gene	Forward primer (5'→3')	Reverse primer (5'→3')
PRAJA	TCGCCATTTTCCACTACTCGT	GTTCCCGAACTCTCGCTGT
ELF	AGCTGGAAGGCAGATTCAAG	CGTCCATCTCGAAGGTCAGT
Bim	TAAGTTCTGAGTGTGACCGAGA	GCTCTGTCTGTAGGGAGGTAGG
PAI-1	CACAAATCAGACGGCAGCACT	CATCGGGCGTGGTGAACTC
Smad4	GCTGCTGGAATTGGTGTTGATG	AGGTGTTTCTTTGATGCTCTGTCT
18S	AAACGGCTACCACATCCAAG	CCTCCAATGGATCCTCGTTA

Table 2.3 Primer sets for gene specific SYBR Green real time PCR.

2.1.5 Materials for SDS-PAGE gel electrophoresis and immunoblot analysis

2.1.5.1 Buffers and solutions for protein lysis and determination of concentration

RIPA buffer (Cell lysis buffer)

1,815 g Tris base
4.383 g Sodium chloride (NaCL)
6 mL Nonident P40
0.279 g EDTA, sodium salt
0.3 g SDS
1.6 g Deoxycholic acid, sodium salt
1x Protease inhibitor (see below)

Adjusted with ddH_2O to 300 mL, pH 7.2; stored at -20 °C;
Addition of 1x phosphatase inhibitor (see below) immediately prior use

Phosphatase Inhibitor Cocktail 2	Sigma Aldrich (St. Louis, Missouri, USA)
Protease Inhibitor, Complete	Roche (Mannheim, Germany)
Bovine serum albumin, Fraction V (BSA)	Merck (Darmstadt, Germany)
Protein Assay, DC	Bio-Rad (Munich, Germany)

2.1.5.2 Buffers, reagents and materials for SDS-PAGE gel electrophoresis and immunoblot analysis

10x Lämmli buffer

144 g Glycine
30.34 g Tris base (for electorphoresis)
100 mL 10 % SDS (for electrophoresis)

Adjusted with ddH_2O to 1 L

1x Lämmli buffer

100 mL	10x Lämmli buffer
900 mL	ddH_2O

Lämmli loading buffer, 5x

2.5 mL	β-Mercaptoethanol
2 g	SDS
10 mg	Bromphenol blue
6 mL	Tris-HCl (hydrochloric acid), 1 M, pH 6.8
200 µL	EDTA, 500 mM
10 mL	Glycerin
1.3 mL	ddH_2O

10x Towbin transfer buffer

250 mM	Tris base
1.920 M	Glycine

Adjusted with ddH_2O to 1 L

0.5x Towbin transfer buffer

50 mL	10x Towbin transfer buffer
200 mL	Methanol

Filled up with ddH_2O to 1 L

Protein ladder, PageRuler Plus prestained	Fermentas (St. Leon-Rot, Germany)
Nitrocellulose membrane, 0.45 micron	Pierce (Rockford, IL, USA)
Chromatography paper, 3MM Chr	Whatmann (Maidstone, England)
Sponge blotting pads	Invitrogen (Darmstadt, Germany)

2.1.5.3 Antibodies, buffers and reagents for protein detection

10x TBS

12.1 g	Tris base
87.66 g	Sodium chloride (NaCl)

Adjusted to pH 7.6 and filled up with ddH_2O to 1 L

TBST

100 mL	10x TBS
10 mL	10 % Tween20 solution (in ddH_2O)

Filled up with ddH_2O to 1 L

Epitope (target)	Species	Company	Cat.No	Dilution
Primary antibodies				
Akt	rabbit	Cell Signaling	9272	1:1000
Phospho-Akt (Ser473) (587F11)	mouse	Cell Signaling	4051	1:500
Bcl-2 (50E3)	rabbit	Cell Signaling	2870	1:1000
Bcl-XL (54H6)	rabbit	Cell Signaling	2764	1:1000
Phospho-c-Jun (Ser63)	rabbit	Cell Signaling	9261	1:1000
c-Myc (2Q329)	mouse	Santa Cruz	sc-70464	1:500
Cleaved Caspase-3 (Asp175) (5A1E)	rabbit	Cell Signaling	9664	1:1000
E-Cadherin	mouse	BD Bioscience	610181	1:1000
Phospho-ERK (E-4)	mouse	Santa Cruz	sc-7383	1:1000
GAPDH	rabbit	Santa Cruz	sc-25778	1:2000
p21WAF1/Cip1 (CP74)	mouse	Sigma Aldrich	P1484	1:1000
Phospho-p38 MAPK (Thr180/Tyr182)	rabbit	Cell Signaling	4631	1:1000
PARP	rabbit	Cell Signaling	9542	1:1000
PCNA (F-2)	mouse	Santa Cruz	sc-25280	1:1000
Smad2 (D43B4)	rabbit	Cell Signaling	5339	1:1000
Phospho-Smad2 (Ser465/467)	rabbit	Cell Signaling	3101	1:1000
Smad3	rabbit	Cell Signaling	9513	1:1000
Phospho-Smad3	rabbit	Epitomics	1880-1	1:1000
Smad4 (B-8)	mouse	Santa Cruz	sc-7966	1:1000
Secondary antibodies – horseradish peroxidase (HRP) conjugated				
goat anti-rabbit IgG-HRP	goat	Santa Cruz	sc-2301	1:10000
goat anti-mouse IgG-HRP	goat	Santa Cruz	sc-2005	1:10000

Table 2.4 **Primary and secondary antibodies used for immunoblot analysis.** Antibodies were obtained from Cell Signaling (Danvers, MA, USA), Santa Cruz Biotechnology (Santa Cruz, California, USA.), Sigma Aldrich (St. Louis, Missouri, USA), BD Bioscience (Heidelberg, Germany) or Epitomics (Burlingame, California, USA)

Ponceau S Red — Sigma Aldrich (St. Louis, Missouri, USA)

ECL solution

10 mL 0.1 M Tris-HCl buffer (pH = 8.5)

50 µL 250 mM Luminol

22 µL 90 mM p-Coumaric acid

3 µL Hydrogen peroxide solution 30 %

Freshly prepared

2.2 Methods

2.2.1 Cell Culture

All cell culture work was performed under sterile conditions using a laminar flow hood.

2.2.1.1 Cell Culture

Ten different liver cancer cell lines (chapter 2.1.3.1) and MFB-F11 cells were maintained in growth medium. Cells were cultured in filter cap tissue culture flasks at 37 °C in a humidified incubator with 5 % CO_2. Growth medium comprised high glucose DMEM medium, 2 mM L-glutamine and 10 % FBS and, in the case of MFB-F11 cells, 15 µg/mL hygromycin B. Cells were subcultured before reaching full confluency. For this, cells were washed with HBSS and collected in growth medium after detachment with 1x Typsin-EDTA. An appropriate amount of cells was used for further culturing or experiments. For experiments, cell numbers were determined using a Boyden chamber. Dead cells were identified using Trypan blue solution and ignored during cell counting.

2.2.1.2 Cryopreservation of cell lines

For long term storage, cells of a low passage number were collected (chapter 2.2.1.1) in growth medium, spun down (250xg, 5 min, room temperature) and resuspended in ice cold growth medium supplemented with 10 % dimethyl sulfoxide (DMSO, suitable for hybridoma). Cells were stored in cryo tubes at -20 °C for 4 h, kept at -80 °C over night and finally stored in liquid nitrogen. These cryopreserved cells were thawed at regular intervals to perform experiments within a similar passage range. For this, cell in cryo tubes were warmed to 37 °C in a water bath and immediately transferred to warm medium, spun down (250xg, 5 min) and resuspended in growth medium.

2.2.1.3 Mycoplasma detection

Each cell culture was tested for mycoplasma contamination at a low and high passage number, using the Venor GEM Mycoplasma Kit according to manufacturer's protocol. Briefly, cell culture supernatant was incubated at 95 °C for 5 min and cell debris was removed by centrifugation (13 000 rpm, 5 s). The test is a PCR (polymerase chain reaction) based detection of mycoplasma 16S RNA and includes an internal and a positive control to ensure a successful PCR. Together with the internal control DNA, cell culture supernatant or the

positive control was used to perform a PCR with the following conditions: 1 cycle at 94 °C for 2 min, 39 cycles at 94 °C for 30 s, 55 °C for 30 s and 72 °C for 30 s. PCR products were detected as described in 2.2.4.4. Mycoplasma negative samples resulted in one signal (internal control, 191 bp), while contaminated samples or the positive control showed a second signal at 265-278 bp (Figure 2.1).

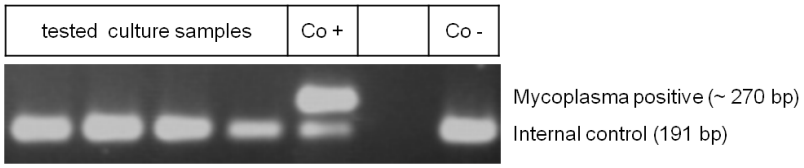

Figure 2.1 PCR for detection of mycoplasma contamination. Four examples of tested supernatants of HCC cultures are shown as well as the positive (Co+) and negative (Co-) controls.

2.2.2 Cell culture experiments

If not stated otherwise, cell line experiments were conducted in starvation medium (growth medium without FBS) and with a final confluency below 70-80 %. The cells were stored in the cell culture incubator between the different working steps. All experiments were performed within a passage number of 3-12 after thawing cryopreserved cells (see chapter 2.2.1.2).

2.2.2.1 Detection of promoter and transcriptional activity

2.2.2.1.1 Detection of Smad3/Smad4 reporter activity

To detect TGF-β induced Smad3/Smad4 transcriptional activity, an adenoviral construct carrying nine CAGA sequence repetitions within the firefly luciferase promoter region (Ad(CAGA)$_9$-MLP-Luc, described in [31]) was used for a luciferase promoter assay (hereafter named CAGA-Luc assay). 20 000 cells/cm² were allowed to attach to cell culture plates. Cells were then infected with the adenovirus for 2 h before washing twice with HBSS and adding starvation medium. To ensure equal and efficient infection, the cells were co-infected with an adenovirus carrying a β-galactosidase construct (described in [233]). The next day, medium was replaced with fresh starvation medium either containing 5 ng/mL TGF-β or not, and cells were disrupted in passive lysis buffer 9 h later. Each condition was performed in triplicates. Cell lysates were transferred to white microtiter plates. After addition of a luciferase substrate, luciferase activity was quantified by capturing luminescence with a microplate reader. Obtained values were first normalized to β-galactosidase activity (see 2.2.2.1.4) of the same sample, and afterwards, treated samples were normalized to untreated controls.

2.2.2.1.2 Detection of Smad2/Smad4 transcriptional activity

Unlike Smad3, activated Smad2 is unable to interact with DNA and needs additional assistance by, e.g., Fast-1 (chapter 1.1.2, page 3), which then recognizes an activin response element (ARE). Hence, a luciferase gene under the control of ARE and Fast-1 were introduced to cells to evaluate Smad2/Smad4 transcriptional activity. For this, cell lines were allowed to attach to a 1 cm² growth area over night before switching to 260 µL starvation medium. The cell confluency was between 70-80 % at that time. 0.3 µg ARE, 0.1 µg Fast-1 plasmid as well as 0.05 µg β-galactosidase control vector in 26 µL Opti-MEM medium were mixed with 0.4 µL Lipofectamine 2000 in 26 µL Opti-MEM medium and incubated for 20 min at room temperature. This mixture was then added dropwise to the cells and the transfection reaction was allowed to proceed for 5 h before replacing the starvation medium. The next day, starvation medium was renewed and either supplemented with 5 ng/mL TGF-β or not for 9 h, and thereafter, cells were collected in passive lysis buffer. Each treatment condition was performed in triplicates and the experiment was evaluated as described above. The detection of luciferase and β-galactosidase activity is described in chapter 2.2.2.1.1 and 2.2.2.1.4.

2.2.2.1.3 Smad7 promoter activity assay

After cell lines attached to a 1.9 cm² growth area, they were cultured in 500 µL starvation medium over night. Cell density did not exceed 70-80 %. For evaluation of Smad7 promoter activity, cells were transfected with a functional Smad7 promoter deletion mutant (p(-625 SacI)-Smad7prom-Luc), which was constructed using the 1321 bp rat Smad7 promoter region (-1276 to -41) [37]. Smad7 promoter (0.5 µg) and β-galactosidase (0.2 µg) plasmids were incubated with 0.8 µL Lipofectamine 2000 transfection reagent in 100 µL Opti-MEM medium for 20 min, before dropwise addition to the cell culture wells. After 6 h, the supernatant was replaced with starvation medium and the next day, cells were either left untreated or treated with 5 ng/mL TGF-β for 6 h. Cells were collected in passive lysis buffer. Each condition was performed in triplicates. Luciferase and β-galactosidase activities were evaluated as described in chapter 2.2.2.1.1 and 2.2.2.1.4.

2.2.2.1.4 β-galactosidase activity assay

β-galactosidase activity was evaluated using a β-galactosidase assay from Promega. 20 µL cell lysates or passive lysis buffer as a negative control were transferred to a clear microtiter plate and incubated with 20 µL assay buffer at 37 °C until a faint yellow color developed (30-60 min). Color development was stopped with 60 µL 1 M sodium carbonate and absorption at 420 nm was detected in a microplate reader.

2.2.2.2 RNAi knockdown of Smad2 and Smad3

Hep3B, HuH7 and PLC/PRF/5 cells were cultured in 1 cm² wells over night, before replacing growth medium with 260 µL starvation medium. For knockdown, siRNA (small interfering RNA) against Smad2, Smad3 or a non-specific sequence in 26 µL Opti-MEM medium was mixed with 0.5 µL RNAiMax in 26 µL Opti-MEM and incubated at room temperature for 20 min. This mix was added dropwise under careful agitation to cell cultures, reaching final siRNA concentration of 10 nM. Control wells were treated with the same mixture but without siRNA. After 6 h, starvation medium was replaced and, for HuH7 and PLC/PRF/5, supplemented with 1 % heat inactivated FBS (hiFBS). Two days later, starvation medium was renewed (1 % hiFBS for HuH7 cells) and cells were treated with or without 5 ng/mL TGF-β for 72 h. Medium for HuH7 contained 1 % FBS throughout the experiment, which leads to a faster dying out of the siRNA. Hence, a final siRNA concentration of 20 nM instead of 10 nM was applied. Each condition was performed in triplicates. Cell death and proliferation rates were evaluated performing a LDH assay as described in chapter 2.2.2.3, but with adjusted volumes for cell lysis (260 µL).

Knockdown efficiency was ensured with an immunoblot analysis for (phosphorylated) Smad2 and 3. For this, cells were disrupted in RIPA buffer after 1 h instead of 72 h TGF-β treatment (chapter 2.2.5).

2.2.2.3 LDH release as an indicator of cell death

Cell death leads to release of lactate dehydrogenase (LDH), a very stable protein. Hence, it can be used for determination of cell death rates. HCC cell lines were seeded in 96 well cell culture plates and maintained in growth medium over night. After a starvation period of 8 h, cells were cultured in 100 µL starvation medium with or without 5 ng/mL TGF-β. Medium for HCC-M and HuH7 cells was supplemented with 1 % hiFBS. After 72 h, 50 µL of supernatant was transferred to a clear microtiter plate. Cell layers were disrupted in 100 µL 1 % Triton X-100 in HBSS and 50 µL thereof were transferred to the microtiter plate. LDH amount in the supernatant and in cell lysates was quantified using a Cytotoxicity Detection Kit. 50 µL of a catalyst and dye solution mixture (ratio 1:45) was added to each well. Triton buffer and starvation medium with 0 % or 1 % hiFBS served as negative controls. After 10-20 min, absorption at 490 nm was detected with a microplate reader. The percentage of dead cells was calculated as follows. The untreated control sample was then defined as zero.

$$\frac{(Abs_{SN} - Abs_{blank-SN})}{((Abs_{SN} - Abs_{blank-SN}) + (Abs_{adh} - Abs_{blank-adh.}))} 100$$

$$= \frac{released\ LDH\ of\ dead\ cells}{total\ amount\ of\ LDH} 100 = cell\ death\ [\%]$$

SN = supernatant, adh = adherent cells, blank = negative control

For siRNA knockdown experiments (chapter 2.2.2.2), the cytotoxicity assay was additionally used to determine the relative amounts of viable cells. For this, the LDH content of viable (adherent) cells after TGF-β stimulation was normalized to the one without treatment:

$$\frac{Abs_{adh-treated} - Abs_{blank-adh}}{Abs_{adh-untreated} - Abs_{blank-adh}} 100 =$$

$$\frac{viable\ treated\ cells}{viable\ untreated\ cells} 100 = proliferation\ [\%]$$

adh = adherent cells, blank = negative control

2.2.2.4 MTT viability assay

Effects of TGF-β on proliferation were analyzed using an MTT viability assay. Cell lines were cultured in 0.38 cm² (100 µL) or 1 cm² (250 µL) cell culture wells for a 48 h or 6 day experiment, respectively. After attachment, cells were maintained in starvation medium containing 0.25 % FBS (1 % FBS for HCC-M and HuH7) over night and were then either treated with 5 ng/mL TGF-β or not in fresh medium. Starvation medium was supplemented with a low amount of FBS because cell lines may need some serum to gain proliferative capability. During the 6 day experiment, fresh FBS and TGF-β in 50 µL medium was added 3 days after start of treatment - using six-fold FBS and TGF-β concentrations to reach primary concentrations. At the end of the experiment, MTT solution was added at a final concentration of 500 µg/mL and viable cells were allowed to reduce yellow MTT solution to purple formazan crystals for 4 h. After removal of the supernatant, formazan crystals were resolved with a MTT solvent solution and absorption at 560 nm was evaluated using a microplate reader. MTT solvent was used as a negative control. The underlying assumption of this assay is that the MTT conversion in viable cells is not affected by (TGF-β) treatment. The effect of TGF-β on cell viability was calculated by normalizing data of treated samples to corresponding control samples.

2.2.2.5 Migration assay

A transwell assay was performed to analyze migratory capacity of HCC cell lines. Cell lines were cultured in cell culture dishes and in medium containing 3 % FBS over night. Subsequently, cells were starved for 24 h (1 % hiFBS for HCC-M and HuH7 cells), washed with HBSS, detached with 1x Trypsin-EDTA and spun down (200xg, 5 min). Single cell suspensions with 100 000 cells/mL were prepared using starvation medium with 1 % BSA. Transparent PET transwell cell culture inserts with a pore size of 8 µm were transferred to 24 well companion plates, which were filled with 750 µL medium containing 10 % hiFBS as an attractor for motile cells. Bubbles at the bottom of the insert were removed by careful tapping before transferring 250 µL cell suspension to the transwell inserts. Cell migration was allowed for 13 h. This was identified as a suitable time period to analyze and compare both, highly and less motile cell lines. Each test was performed in triplicates. Cells at the bottom and top of the membrane were detached by trypsinization and separately transferred to a white 96 well plate. After 10 min centrifugation at 500xg, the supernatant was discarded. The relative number of migrated (bottom) and non-migrated (top) cells was analyzed adding an ATP assay (CellTiter-Glo Assay) to the cells. 10 min later, luminescence intensity was determined using a microplate reader. The percentage of migrated cells was calculated by normalizing the amount of ATP in migrated cells to that in all cells (migrated and non-motile).

2.2.2.6 Detection of secreted TGF-β

TGF-β secretion by HCC cell lines was analyzed using the MFB-F11 reporter cell line. This cell line was generated by stable transfection of embryonic murine TGF-β-/- fibroblasts with a plasmid carrying the alkaline phosphatase under the control of Smad binding elements (SBE) [231]. Stimulation with TGF-β1-3 induces expression and secretion of the alkaline phosphatase (AP), whose activity can be visualized by addition of the AP substrate p-nitrophenyl phosphate and its conversion into yellow p-nitrophenol.

For each HCC cell line, 20 000 cells were allowed to attach to 1 cm² wells for 4 h before washing with HBSS twice and adding starvation medium without phenol red. The next day, starvation medium was replaced and collected 48 h later. Adherent cells were washed with HBSS and covered with 60 µL RIPA protein lysis buffer. Protein lysates and conditioned medium without cell debris were stored at -80 °C until further processing. Protein concentration was determined as described in chapter 2.2.5.2.

50 000 MFB-F11 cells/well were allowed to attach to 96 well plates for 2 h and starvation medium without phenol red was added after washing twice with HBSS. The next day, the

supernatant was removed to add 50 µL fresh phenol red free starvation medium. Each well was supplemented with 50 µL conditioned medium from the HCC cell lines or with 50 µL starvation medium containing known TGF-β concentrations (0-10 ng/mL). Additionally, latent TGF-β was activated as follows: 50 µL of the conditioned medium was incubated with 10 µL 1 N hydrochloric acid for 10 min before neutralization with 12 µL 1 N sodium hydroxide. 50 µL of this mixture was then added to the MFB-F11 cells. Each condition was tested in triplicates. MFB-F11 cells were incubated in a cell culture incubator to allow TGF-β induced production and secretion of alkaline phosphatase. After 48 h, 50 µL of this medium was transferred to a new microtiter plate and supplemented with 50 µL AP-substrate-buffer. Absorption of the colored product was detected at 420 nm at different time points (10 min to 3 days).

TGF-β concentration in conditioned medium was calculated using the TGF-β standard curve. A dilution factor was used for medium samples with fully activated TGF-β. Total amount of TGF-β in the supernatant was calculated and afterwards normalized to the total amount of protein in adherent cells (TGF-β [ng/$mg_{total\ Protein}$]).

2.2.3 Patient samples

Human HCC tissue samples and corresponding non-tumorigenic liver tissue, or RNA isolated from matched HCC/non-tumorigenic liver samples were kindly provided by different collaboration partners in Germany and China:

Dr. Thomas Weiß and the Center for Liver Cell Research (Department of Pediatrics and Juvenile Medicine, University of Regensburg Hospital, Regensburg, Germany) provided RNA samples isolated with a Qiagen-Kit (Hilden, Germany). The samples were collected by the Foundation Human Tissue and Cell Research (HTCR) in Regensburg, Germany. The experimental procedures were conducted according to the guidelines of the charitable state controlled foundation HTCR. All patients provided informed patient's consent, which was approved by the local ethical committee of the University of Regensburg.

Prof. Dr. Otto Kollmar (current address: Department of General and Visceral Surgery, University Hospital Göttingen, Göttingen, Germany) and the Department of General, Visceral, Vascular and Pediatric Surgery (University of Saarland, Homburg/Saar, Germany) provided tissue samples. All patients provided informed consent for tissue procurement, which was approved by the local ethics committee.

Prof. Heike Allgayer and Dr. Jörg Leupold (Department of Experimental Surgery and Molecular Oncology of Solid Tumors, Medical Faculty Mannheim, University of Heidelberg

and German Cancer Research Center, Heidelberg, Germany) provided tissue samples. Tissues were collected from HCC patients at the Department of Surgery (University Hospital Mannheim, University of Heidelberg, Germany). All patients gave informed patient's consent and the tissue procurement was approved by the local ethical committee.

Prof. Chun Fang Gao and Dr. Xing Gu (Department of Laboratory Medicine, Eastern Hepatobiliary Hospital, Second Military Medical University, Shanghai, China) provided raw data of TaqMan real time PCR experiments for Smad7, 18S rRNA and β2-microglobulin. The specimens enrolled in this study were collected from September 2007 to December 2008 in Shanghai Eastern Hepatobiliary Surgery Hospital (EHBH, Shanghai, China). All patients signed informed consents and the experiments were conducted in accordance with the official recommendations of the Chinese Community Guidelines.

Immediately after (partial) hepatectomy, tissue samples were snap-frozen in liquid nitrogen and stored at -80 °C until further procedure. RNA isolation was performed as described in chapter 2.2.4.1 if not stated otherwise.

2.2.4 mRNA isolation and expression analysis

2.2.4.1 RNA isolation

2.2.4.1.1 RNA isolation from tissue using TRIzol reagent

50-100 mg of frozen human liver samples was homogenized in 1 mL TRIzol® reagent using an Ultra-Turrax T25 and stored on ice for 15 min before removal of cell debris by centrifugation (10 min, 4 °C, 12 000xg). The room temperature adjusted supernatant was vigorously mixed with 200 µL chloroform for 15 s, incubated at room temperature for 2 min and spun down (15 min, 12 000xg, 4 °C) to reach phase separation. The topmost phase, containing RNA, was transferred to a fresh tube and mixed with 500 µL of isopropanol. After 10 min of incubation, the precipitated RNA was collected by centrifugation (10 min, 12 000xg, 4 °C). The RNA pellet was washed twice with 75 % ethanol (centrifugation at 10 000xg and 4 °C for 5 min), dried at room temperature and resolved in 100-300 µL RNase free water. RNA was stored at -80 °C until further processing.

2.2.4.1.2 RNA isolation from cell cultures using an RNeasy Kit

To isolate RNA from HCC cell lines, they were allowed to attach to 6 well cell culture plates using growth medium. After starvation over night, starvation medium was replaced and

5 ng/mL TGF-β was added 0 h, 2 h or 24 h before collecting the samples. RNA was isolated using the RNeasy Kit from Qiagen according to the manufacturer's protocol. Briefly, adherent cell layers were washed with HBSS, collected in RLT lysis buffer supplemented with 1 % β-mercaptoethanol and stored at -80 °C until further processing. The lysate was mixed with the same volume of 70 % ethanol and loaded to an RNeasy spin column, followed by a 30 s centrifugation step at 13 000 rpm. Subsequently, the column was washed once with 700 µL RW1 and twice with 500 µL RPE buffer, including a centrifugation step (see above) between each washing step. 40 µL of RNAse free water was added to the column and RNA was collected by centrifugation into a fresh tube. The RNA was stored at -80 °C until further processing.

2.2.4.2 RNA gel electrophoresis

For the determination of RNA concentration and quality, 2 µL of the RNA solution was loaded to a NanoQuant plate and analyzed in a microplate reader. Molten 1 % agarose in RNase free 1x MOPS buffer was poured to a gel casting system with a well comb and was allowed to polymerize for 30 min. 200 ng RNA was mixed with RNA loading buffer and incubated at 68 °C for 10 min. These samples were loaded onto the gel and separated in 1x MOPS buffer by applying 7 mV/(cm electrode distance) for 1 h. Ethidium bromide stained RNA was visualized with a UV transilluminator system. Visible 28S and 18S ribosomal RNA (rRNA) bands, with the last one about half as intense as the former, indicated a good RNA integrity. cDNA was only used if a high-quality and similar RNA integrity and no DNA contamination was ensured.

2.2.4.3 Reverse transcription

Reverse transcription (RT) of RNA to cDNA was performed using the Omnitect Reverse Transcription Kit (Qiagen). To disintegrate possible DNA contaminations, 1 µg RNA in 12 µL RNase free water and 2 µL gDNA wipe out buffer was incubated at 42 °C for 2 min using a PCR thermal cycler. After the addition of 6 µL of a master mix comprising 5x buffer (with dNTPs and Mg^{2+}), primer and reverse transcriptase, the RT reaction was performed at 42 °C for 1 h before heat inactivating the enzyme (5 min, 95 °C). An efficient and equal RT reaction was ensured by detection of 18S rRNA using conventional PCR technology. Afterwards, Real time PCR was used for comparative expression analysis of various genes (see below).

2.2.4.4 Conventional PCR

To amplify parts of the 18S rRNA sequence, one PCR reaction comprised 2 ng cDNA, 1 µL of a 10 µM forward/reverse primer (1:1) mix (Table 2.3, page 29), 0.4 µL of a 10 mM dNTP solution, 0.5 U FastStart Taq DNA polymerase, 2 µL 10x Buffer with $MgCl_2$.and was filled up with double distilled water to 20 µL. In a PCR thermocycler, the sample was first incubated at 95 °C for 3 min, followed by 15 cycles of 30 s at 95 °C (denaturation), 30 s at 60 °C (annealing) and 1 min at 72 °C (elongation). After a final incubation step of 5 min at 72 °C, the samples and a DNA marker of known size were mixed with DNA loading buffer and loaded to a gel (1 % agarose in 1x TAE buffer and 2 µL/100 mL ethidium bromide), which was placed in an agarose gel electrophoresis system filled with 1x TAE buffer. DNA separation by size was accomplished by applying 5-10 V/(cm electrode distance) for 45-60 min. The ethidium bromide stained DNA was detected using a UV transilluminator. Equal transcription efficiency for different samples was assumed if the detected signal intensities of the amplified 18S rRNA cDNA were comparable.

2.2.4.5 TaqMan and SYBR Green real time PCR analysis

Expression levels of different TGF-β signaling related genes were examined using TaqMan® or SYBR® Green real time PCR analysis.

2.2.4.5.1 TaqMan Real Time PCR

Aqueous 1 ng/µL cDNA solutions were used for the detection of mRNA levels of various genes, whereas lower cDNA concentrations (5 pg/µL) were applied for analysis of 18S rRNA expression. A TaqMan master mix of an adequate volume for all samples (Table 2.5) was prepared and 18 µL thereof was transferred to a suitable real time PCR plate. After addition of 2 µL cDNA or a negative control, the Real time PCR plate was sealed with a clear adhesive foil and centrifuged for 10 s at 1000 rpm.

TaqMan master mix	
Component	**Volume for one 20 µL reaction**
TaqMan probe	1 µL
2x TaqMan Master Mix	10 µL
ddH_2O	7 µL

SYBR Green Master mix	
Component	**Volume for one 20 µL reaction**
Forward primer (5 µM)	0.4 µL
Reverse primer (5 µM)	0.4 µL
2x SYBR® Green Master Mix	10 µL
ddH_2O	7.2 µL

Table 2.5 Composition of master mixes for TaqMan and SYBR Green real time PCR

The gene specific TaqMan probes used for this study are listed in Table 2.2 (page 28). Using an AbiPrism 7000 real time PCR cycler, the PCR conditions were as follows: 10 min at 95 °C (activation of DNA polymerase) and 40 cycles of 15 s at 95 °C (denaturation) and 1 min at 60 °C (annealing and elongation). Each sample was analyzed in triplicates and evaluated as described below (chapter 2.2.4.5.3).

2.2.4.5.2 SYBR® Green PCR analysis

In general, the experimental setup for SYBR Green real time PCR analysis was the same as for TaqMan Real time PCR analysis (see above). One exception was the use of a SYBR Green (Table 2.5, right) instead of the TaqMan master mix. The used primer pairs for specific cDNA detection are listed in Table 2.3 (page 29). The PCR conditions were as described in the previous chapter. To exclude possible unwished signals of primer dimers or unspecific primer binding, a dissociation curve between 60 °C and 90 °C was included at the end of each experiment. Samples were tested in triplicates and evaluated as described below.

2.2.4.5.3 Evaluation of real time PCR results

The fluorescence signal of TaqMan dyes or DNA intercalated SYBR Green was detected after each elongation step. The threshold for collection of Ct values was set within the linear rise of the curve. Each sample was measured in triplicates. The data were analyzed according to the ΔΔCt method:

$$\frac{\left(Ct_{GOI} - Ct_{ref}\right)_{treated}}{\left(Ct_{GOI} - Ct_{ref}\right)_{untreated}} = \Delta\Delta Ct$$

$$changes\ in\ expression = 2^{-\Delta\Delta Ct}$$

GIO = gene of interest, ref = reference gene

18S rRNA was identified as suitable reference gene by comparison of its Ct values in all cell lines: The mean Ct values (of 3-4 experiments) were calculated for each cell line and varied between 19.6 and 20.2 with a standard error below 0.36 in all cases. TGF-β treatment did not alter 18S rRNA values within one cell line, as seen in variations of the Ct values below 0.4 cycles.

2.2.5 SDS-PAGE gel electrophoresis and immunoblot analysis

2.2.5.1 Protein lysates of cultured cells

HCC cell lines were allowed to attach to 9.6 cm² cell culture wells before replacing growth medium with starvation medium. The next day, cells were treated with 5 ng/mL TGF-β 0 h, 1 h, 3 h, 8 h, 24 h or 48 h before collecting the cells. For a comparison of basal protein levels, cells were incubated in starvation medium for 24 h. the end of an experiment, cells were washed with HBSS and disrupted in ice-cold RIPA buffer containing phosphatase and protease inhibitors. Cells were stored at -80 °C until further processing and for a better cell disruption. Cell lysates were scraped with a rubber policeman, transferred to a collection tube and spun down to remove cell debris (15 min, 13 000 rpm, 4 °C). After determination of protein concentrations, proteins were separated by an SDS-PAGE gel electrophoresis and immobilized on a membrane for immunodetection of protein levels (see below)..

2.2.5.2 Determination of protein concentration

Protein concentrations were determined using a BC protein assay, which is based on the Lowry assay. The principle of this assay is the reaction of amino acids with an alkaline copper tartrate and Folin reagent, which results in a reduction of Folin to a blue product. 2 µL of protein samples or of a BSA (bovine serum albumin) standard curve with known concentrations (0-10 mg/mL) were transferred to a microtiter plate and supplemented with 20 µL of a mix of 1000 µL solution A and 20 µL of solution S (alkaline copper tartrate). 200 µL solution B (Folin reagent) was added and after 10-15 min, the absorbance was detected at 690 nm using a microplate reader. Each sample was measured in triplicates and unknown protein concentrations were calculated using the BSA standard curve.

2.2.5.3 Sample preparation for immunoblot

For denaturation of disulfide bonds, a mixture of 20-30 µg protein lysate and 6 µL reducing protein loading buffer was incubated at 95 °C for 10 min and stored on ice. Within the next hour, protein samples were loaded to an SDS-PAGE gel for protein separation (see below).

2.2.5.4 Preparation of SDS-polyacrylamide gels and gel electrophoresis

Protein separation by size was achieved performing an SDS-PAGE (sodium dodecyl sulfate-polyacrylamide gel electrophoresis). For this, 1.5 mm thick Bis-acrylamide (12 %) gels were

poured in gel casting systems from Bio-Rad: The separating gel (Table 2.6, see below) was freshly prepared and immediately casted between two glass plates, leaving enough space for the stacking gel. This separating phase was covered with isopropanol to ensure a sharp and linear edge. The gel was allowed to polymerase for 30 min before isopropanol was removed. The space between the two glass plates was filled up with the freshly prepared stacking gel (Table 2.6) and a comb with 15 slots was added. After polymerization for 45-60 min, the gels were installed in an electrophoresis module. The space between two gels as and the running chamber itself was filled with 1x Lämmli buffer (page 29). The comb was carefully removed and the wells were washed thoroughly before a protein marker of known sizes and samples were loaded to the gels. Protein alignment in the collection phase was allowed at 40 V. Once the running front reached the separating gel, the voltage was increased to 80-110 V.

Separating gel, 12 %	
Acrylamide	2.6 mL
1.5 M Tris-HCl, pH 8.8	1.6 mL
ddH_2O	2.2 mL
SDS (10%)	66.7 µL
TEMED	6.0 µL
APS (10%)	40 µL

Stacking gel	
Acrylamide	0.3 mL
1M Tris-HCl pH 6.8	0.5 mL
ddH_2O	1.1 µL
SDS (10%)	19.1 µL
TEMED	3.4 µL
APS (10%)	22.9 µL

Table 2.6 Composition of separating and stacking gel for SDS-PAGE gel electrophoresis

2.2.5.5 Western transfer

Immunoblot (Western blot) analysis was used to immobilize proteins on a nitrocellulose membrane (0.45 micron, Pierce, Rockford, IL). A sandwich was prepared, with the gel and the membrane in the middle, followed by three chromatography papers (3MM Chr, Whatmann, Maidstone, England), and blotting pads on both sides. To build this Western sandwich, the different layers were wetted in 0.5x Towbin transfer buffer (page 30) and bubbles between the layers were carefully removed to ensure accurate protein transfer. The transfer was performed in a blotting module filled with 0.5x Towbin transfer buffer, with the membrane closer to the anode and the gel closer to the cathode. For protein transfer, 250-300 mA per membrane was applied over a time period of 4 h.

2.2.5.6 Immunodetection of proteins

Membrane bound proteins were temporarily stained with Ponceau S Red solution to ensure equal loading and satisfying blot quality and to identify possible transfer mistakes. The

membrane was washed in TBST (page 30) and blocked with 5 % non fat dried milk in TBST for 1 h at room temperature. After washing with TBST, the membrane was incubated with a protein specific (first) antibody overnight at 4 °C and was then washed again (3x 5 min) to remove unbound antibodies. The membrane was incubated with a species specific (second) antibody conjugated to a horseradish peroxidase (HRP). Antibodies are listed in Table 2.4 (page 31). After 1-2 h at room temperature, the membrane was washed three times in TBST. All washing and incubation steps were conducted under agitation on a shaker. Horseradish peroxidase activity was detected by wetting the membrane with ECL solution and capturing the resulting chemiluminescence using a luminescent image analyzer.

For further analysis with the same membrane, the antibodies associated to the membrane were detached. For this, the membrane was washed 2 min in TBST, 2 min in distilled water and subsequently incubated in aqueous 0.2 N sodium hydroxide solution for 5 min. After washing with water and TBST, the membrane could be used again.

2.2.6 Statistical Analysis

Cell line data are presented as the mean ± the standard error (SE) of at least three independent experiments, if not stated otherwise. In some cases, statistically significant differences were identified by Student's *t*-test. Correlation analysis was performed by calculating the Pearson correlation coefficient *r*.

For human HCC patient samples, a chi-square (X^2) analysis was performed to identify possible associations between different Smad7 expression levels and clinicopathological characteristics. A 2x2 table was used and patients were grouped as: Smad7 overexpression or no Smad7 overexpression (unchanged or reduced mRNA levels).

For all tests, significant levels are indicated as * $p < 0.05$, ** $p < 0.01$ and *** $p < 0.001$.

3 RESULTS

3.1 Heterogeneous cytostatic effects of TGF-β in HCC cell lines

TGF-β exerts anti-proliferative and pro-apoptotic effects on hepatocytes (chapter 1.2). Cancer cells frequently develop resistance to these effects. Therefore, the behavior of nine different HCC (HCC-M, HCC-T, HepG2, Hep3B, HuH7, FLC-4, PLC/PRF/5, HLE and HLF) and hepatoblastoma cell line HuH6 regarding proliferation and survival upon TGF-β treatment was investigated.

3.1.1 Divergent effects of TGF-β on proliferation in different HCC cell lines

Liver cancer cell lines were cultured at a low density and treated with TGF-β for 2 or 6 days. Upon TGF-β stimulation, the different cell lines showed various responses ranging from induction of growth arrest to stimulation of proliferation (Figure 3.1, right side).

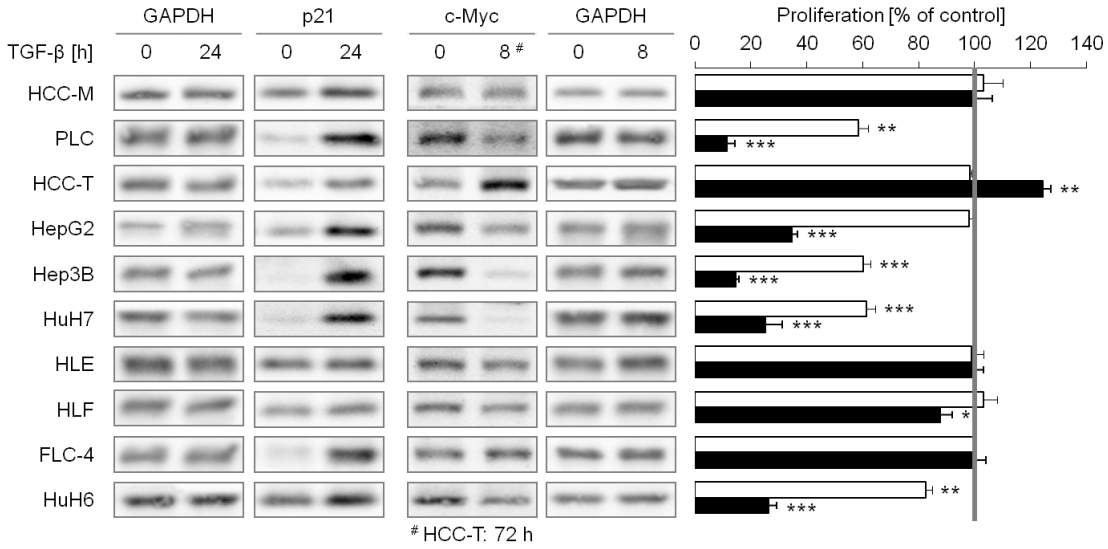

Figure 3.1 **Ambiguous effects of TGF-β on proliferation in HCC cell lines.** (Left) HCC cell lines were either treated with 5 ng/mL TGF-β or left untreated for indicated time points. Changes in c-Myc and p21 expression were detected using immunoblot analysis with GAPDH as a loading control. In line with the late proliferative response in HCC-T cells (right diagram), changes in c-Myc levels were also delayed (after 72 h instead of 8 h). Results were confirmed with a second independent experiment. (Right) After TGF-β treatment for 0 (grey line), 2 (white bars) or 6 days (black bars), cell proliferation was evaluated by MTT assays. Treated samples were normalized to control samples of the same cell line. Significant differences are indicated as * $p < 0.05$, ** $p < 0.01$ and *** $p < 0.001$ (Student's *t*-test). Results are shown as means +SE.

Overall, proliferation rates of four cell lines (HCC-M, HLE, HLF and FLC-4) remained unaltered following TGF-β treatment. The cytokine marginally reduced proliferation in HLF cells after 6 days of TGF-β treatment. In other cells, TGF-β interfered with proliferation,

interestingly, with different sensitivities. The strongest effects of TGF-β were observed in PLC/PRF/5, Hep3B and HuH7 cells, as seen by reduction of cell viability to 60 % after 2 days and to 11-25 % after 6 days. TGF-β triggered a delayed anti-proliferative response in HepG2 and HuH6 cells with no or minor growth inhibition after 48 h, but a pronounced induction of growth arrest after 6 days (35 % and 26 % viable cells). In contrast to all other cell lines analyzed, HCC-T cells significantly ($p < 0.01$) increased cell division to 124 % upon long term TGF-β treatment (6 days).

The protein p21 is involved in cell cycle control and is described as an indicator of growth arrest. In contrast, c-Myc is able to encourage proliferation (Chapter 1.2). Immunoblot (Western blot) analysis (Figure 3.1, left) revealed a strong TGF-β dependent increase of p21 and decrease of c-Myc levels in cell lines which were sensitive to TGF-β induced growth arrest: Hep3B, HuH7, PLC/PRF/5, HepG2 and, with a lower intensity, HuH6 cells. TGF-β also moderately enhanced p21 levels in HCC-M, HCC-T and FLC-4 cells, which were insensitive to TGF-β mediated inhibition of proliferation. c-Myc levels, however, were not affected by TGF-β in those cell lines. In line with the pro-proliferative effect of TGF-β in HCC-T cells, TGF-β increased c-Myc protein levels after 72 h.

3.1.2 Varying sensitivities regarding TGF-β induced cell death in HCC cell lines

TGF-β is a well recognized mediator of cell death, but this signaling branch is often disrupted in cancer (chapter 1.2 and 1.4.2). To evaluate effects of TGF-β on cell death, HCC cell lines were treated with TGF-β for 3 days and LDH release was quantified. LDH is a prominent and very stable enzyme in the liver and therefore is a good tool to evaluate cell damage.

Cell death was calculated as ratio of released LDH of dying cells to total amounts of viable and dying cells. Untreated samples were defined as zero to achieve a better comparability between the cell lines. Figure 3.2 shows that four cell lines, HCC-T, HLE, HLF and FLC-4, were resistant against TGF-β induced cell death, whereas minor inductions of cell death were detected in HepG2 and HuH6 cells (increase of 7.0 % and 4.5 %). In contrast, TGF-β strongly enhanced death rates of Hep3B, HuH7 and PLC/PRF/5 cells to 29.8 %, 36.5 % and 19.5 %, respectively. In those three cell lines, the high sensitivity towards TGF-β caused cell death was mirrored in cleavage and thereby activation of caspase 3 (a member of the apoptotic cascade) and in the proteolytic degradation of caspase target PARP (immunoblot in Figure 3.2). TGF-β did not alter caspase 3 and PARP in all other cell lines. Interestingly, HCC-M cells responded to TGF-β with a reduction of basal cell death rates.

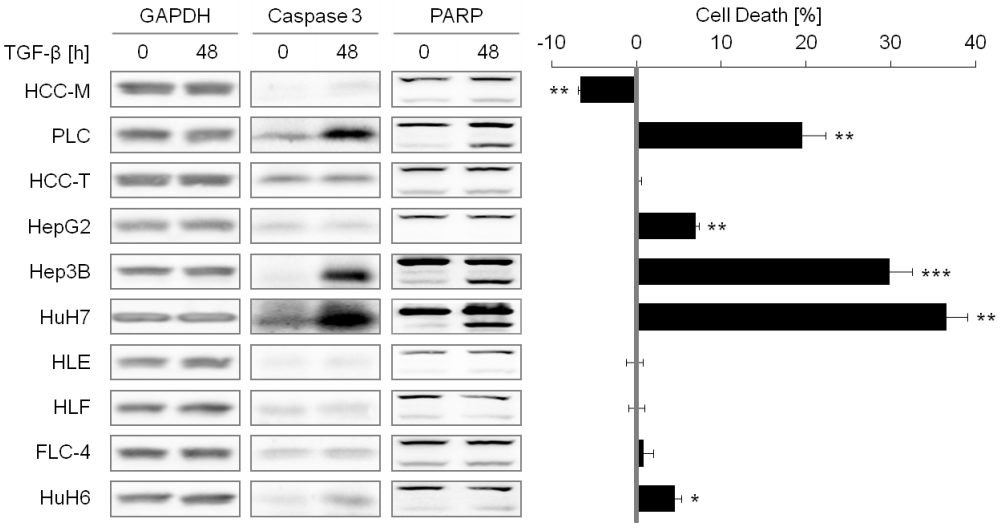

Figure 3.2 TGF-β induces cell death in Hep3B, HuH7 and PLC/PRF/5 cells. (Left) Immunoblot analysis of PARP and caspase 3 cleavage using GAPDH expression as a loading control was conducted after 48 h TGF-β treatment. Untreated samples were used as controls. In the case of HuH7 cells, the control sample was treated with TGF-β for 3 h. The blots show representative results of at least two independent tests. (Right) Cell death induced by 5 ng/mL TGF-β over 72 h (filled bars) was quantified by detecting the ratio of LDH release to total amount of LDH. Untreated samples were defined as 0 (grey line) and treated samples are shown as filled columns. The results are shown as mean +/- SE of at least three independent experiments. Significant differences are indicated as * $p < 0.05$, ** $p < 0.01$ and *** $p < 0.001$ (Student's *t*-test).

In summary, results shown in chapter 3.1.1 and 3.1.2 identify two different groups, showing either resistance or sensitivity towards TGF-β induced cytostasis. Hep3B, HuH7 and PLC/PRF/5 cells underwent strong induction of cell death, accompanied by growth arrest, while HepG2 and HuH6 cells mainly reacted with proliferation inhibition. All other cell lines showed resistance against the described effects, with HCC-T even showing increased cell division and HCC-M a reduced basal cell death upon TGF-β treatment.

3.2 Endogenous and TGF-β dependent changes in expression of canonical TGF-β signaling components in HCC cell lines

Mature TGF-β dimers mainly signal through a heterotetrameric receptor complex composed of TGF-β receptor II and I, which transfer the signal into the cell by phosphorylation of receptor (R)-Smads 2 and 3. Activated R-Smads then form a transcription factor complex with Smad4. This signaling cascade is effectively blocked by Smad7 (chapter 1.1.1 and 1.1.2). The experiments described above revealed resistance against cytostatic effects of TGF-β in many HCC cell lines. Hence, a detailed analysis of canonical TGF-β signaling components was performed to delineate the underlying mechanism of these findings.

3.2.1 Basal expression analysis of TGF-β signaling components

A comparative analysis of endogenous expression levels of TGF-β signaling components was performed to investigate the impact on observed cytostatic effects of TGF-β in the different cell lines.

3.2.1.1 Varying endogenous Smad7 levels in HCC cell lines correlate with TGF-β1 expression

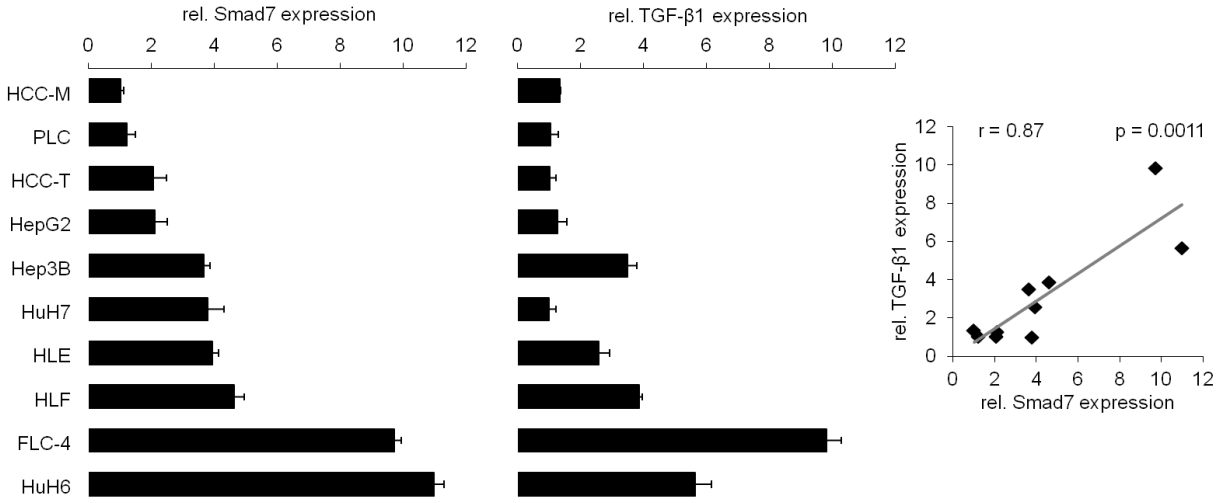

Figure 3.3 Smad7 mRNA levels correlate with TGF-β1 expression in HCC cell lines. Relative Smad7 (left) and TGF-β1 (middle) expression levels were detected using TaqMan real time PCR. Expression of 18S rRNA was used as a reference gene. The results are pictured as mean +SE of at least three independent experiments. A strong correlation (right) of Smad7 and TGF-β1 expression was identified by calculating the Pearson coefficient (r = 0.87; p = 0.0011).

The quantity of the TGF-β cytokine and its inhibitory opponent Smad7 are two major factors which decide the outcome of activated TGF-β signaling. Real time PCR analysis of Smad7 revealed a strong variation in relative mRNA levels in the different HCC cell lines. It ranged from 1 fold in HCC-M cells, rising over PLC/PRF/5, HCC-T, HepG2 (2.1 fold), Hep3B (3.7 fold), HuH7, HLE and HLF cells to 4.6 fold and to 9.7 and 11.0 fold in FLC-4 cells and in the hepatoblastoma cell line HuH6, respectively (Figure 3.3, left diagram). TGF-β1 is the predominant isoform in the liver. Similar to Smad7, it was heterogeneously expressed in the different cell lines, being lowest in HuH7 cells and highest in the cell line FLC-4 with 9.8 fold increased levels when normalized to HuH7 cells (Figure 3.3, middle). Here, relative TGF-β1 expression in HuH7, HCC-T, PLC/PRF/5, HepG2 and HCC-M cells varied between 1-1.34 fold, whereas medium levels of 2.6 to 3.9 fold were identified for HLE, Hep3B and HLF cells. HuH6 and FLC-4 featured highest TGF-β1 mRNA levels (5.7 and 9.8 fold). Interestingly, TGF-β1 expression significantly (r = 0.87, p = 0.0011) correlated with Smad7 mRNA levels, as identified by calculating the Pearson correlation coefficient (Figure 3.3, right).

3.2.1.2 TGF-β receptor I, Smad2 and Smad4, but not TGF-β receptor II and Smad3 are overall evenly expressed

Figure 3.4 shows basal mRNA expression levels of the TGF-β receptor I (TβRI) and II (TβRII). Real time PCR analysis identified HCC-M as the cell line with highest TβRI mRNA levels, which were 5.6 fold increased in comparison to HLE cells (Figure 3.4, left). Expression levels among the other cell lines were relatively stable, ranging from 1 fold in HLE to 2.4 fold in HuH7 cells, with FLC-4 as an outlier (2.9 fold). In contrast, TβRII mRNA levels (middle diagram), normalized to its expression in HCC-M cells, varied strongly in the different cell lines. TβRII expression was increased in HLF, FLC-4, HuH6, HLE (1.6-3.3 fold) and Hep3B and HuH7 cells (about 5 fold) when compared to HCC-M and HCC-T cells (1-1.2 fold).

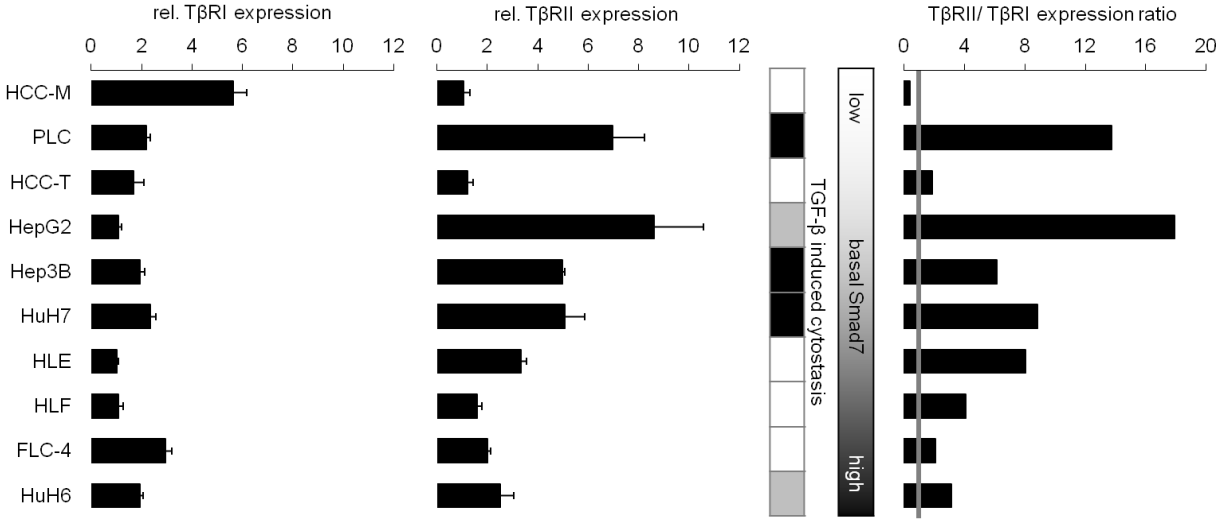

Figure 3.4 Expression of TGF-β Receptor 1 (TβRI) is relatively stable while receptor 2 (TβRII) levels are heterogeneous in HCC cell lines. Expression levels of TβRI (left) and TβRII (middle) were detected using TaqMan real time PCR with 18S rRNA expression as a reference. Shown experiments represent the mean + SE of three independent experiments. In the table, cell lines marked as black showed TGF-β induced cell death and growth inhibition whereas cells highlighted as grey mainly reacted with the latter one. In a second calculation, TβRII expression was normalized to TβRI mRNA of the cell line to identify the TβRII/TβRI ratio (right).

However, highest TβRII amounts were detected in PLC/PRF/5 and HepG2 cells with 7.0 and 8.6 times elevated levels, respectively. Interestingly, except for HCC-M and HCC-T cells, TβRII expressions were elevated in cell lines with low Smad7 mRNA levels (compare to Figure 3.3 or table in Figure 3.4). After exclusion of HCC-M and HCC-T, a significant negative correlation was observed between Smad7 and TβRII mRNA levels (r = -0.72, p = 0.044, not shown). Further, TβRII expression was highest in cells responsive to TGF-β mediated cytostasis (table in Figure 3.4 or Figure 3.1 and 3.2), namely PLC/PRF/5, HepG2, Hep3B and HuH7. Only HuH6 cells expressed lower TβRII levels than HLE, the cell line of the non-responders with the highest expression. Noteworthy, TβRII expression was higher than TβRI in all but HCC-M cells (Figure 3.4, right diagram).

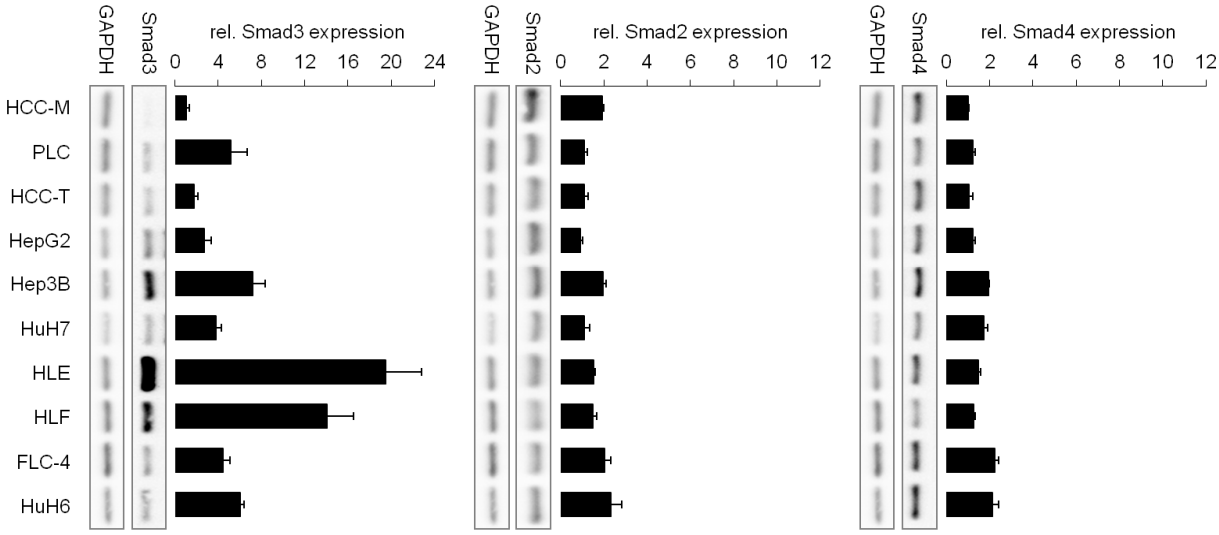

Figure 3.5 Smad2 and Smad4 are equally expressed, while Smad3 levels strongly vary in different HCC cell lines. Relative Smad3 (left), Smad2 (middle) and Smad4 (right) mRNA and protein levels were detected using either real time PCR with 18S rRNA as a reference gene or Western blot analysis with GAPDH as a loading control. Real time PCR results are presented as mean +/- SE of at least three independent results. Western Blot results show one representative of two independent experiments.

Upon activation of the TGF-β receptor complex, receptor Smads are phosphorylated and form heteromeric transcription factor complexes with Smad4. Therefore, the impact of basal R-Smad2 and 3 and common-mediator Smad4 expression on different sensitivities towards TGF-β induced apoptosis and growth arrest (Chapter 3.1) was evaluated. Immunoblot as well as real time PCR analysis revealed rather stable expression levels of Smad2 and Smad4 between the cell lines (Figure 3.5). Smad2 mRNA levels (middle diagram) were highest in HuH6 (2.6 fold increase) when compared to HepG2 cells, whereas Smad4 expression levels ranged from 1 fold in HCC-M to 2.2 fold increase in FLC-4 cells. In contrast to Smad2 and Smad4, heterogeneous amounts of Smad3 mRNA and protein were detected in the different cell lines (Figure 3.5, left diagram). No correlation to the observed cytostatic behavior was detectable. Relative to HCC-M cells, Smad3 mRNA levels were 1.8-7.2 times increased in HCC-T, HepG2, HuH7, FLC-4, HuH6, PLC/PRF/5 and Hep3B cells, but the highest expressions were detected in HLE and HLF cells (14.0 and 19.5 fold). Altogether, those findings were confirmed by immunoblot analysis, which identified the strongest Smad3 signal intensities for Hep3B, HLF and HLE cells and the lowest intensities in HCC-M cells.

3.2.2 Effects of TGF-β on expression of its canonical signaling components

Regulation of TGF-β signaling occurs via different TGF-β dependent mechanisms. After analyzing basal levels of TGF-β signaling components, the impact of TGF-β1 stimulation on their expression was the next focus of investigation.

3.2.2.1 TGF-β induces its type II but not type I receptor in cells sensitive to TGF-β induced cytostasis

Effects of TGF-β on the expression of its receptors were investigated using real time PCR analysis. HCC cell lines were treated with TGF-β for 24 h, and TβRI and TβRII mRNA levels were compared to untreated control samples.

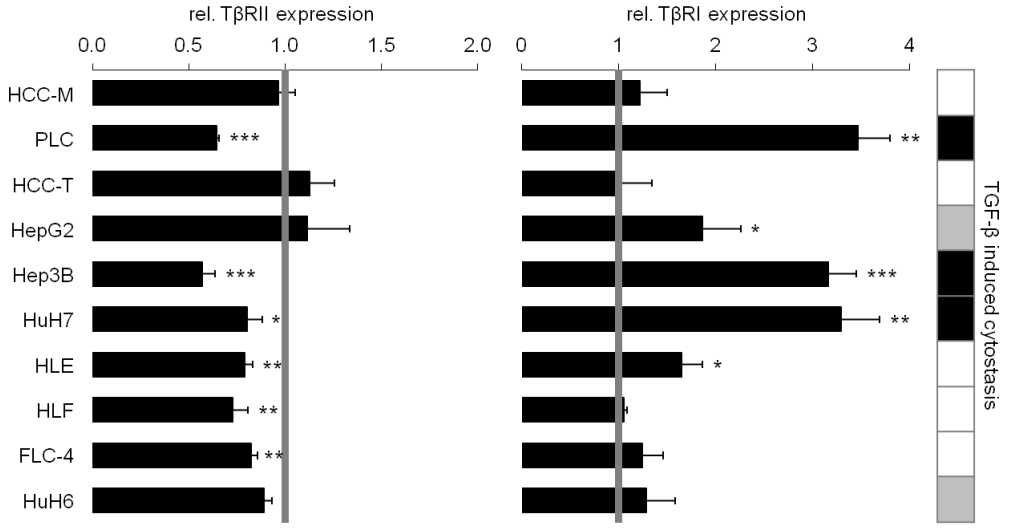

Figure 3.6 TGF-β modifies TβRI but not TβRII expression in HCC cell lines. Liver cancer cell lines were treated with (filled bars) or without (grey line) 5 ng/mL TGF-β for 24 h. Real time PCR detecting TβRII (left) and TβRI (middle) mRNA levels was performed using 18S rRNA as a reference gene. In the table (right), cell lines sensitive to TGF-β induced growth arrest but not cell death are marked as grey, whereas black represents cells reacting with both. Real time PCR experiments are presented as mean +/- SE of at least three independent experiments. Significant differences are labeled as * $p < 0.05$, ** $p < 0.01$, *** $p < 0.001$ (Student's *t*-test).

TGF-β stimulation resulted in minor inhibition of TGF-β receptor II expression in all but HCC-M, HCC-T and HepG2 cells. This effect was strongest in PLC/PRF/5 and Hep3B cells with a significant repression to 0.6 fold ($p < 0.001$; Figure 3.6, left). In contrast, TGF-β significantly induced TβRI expression by a factor of 3.3-3.5 in HCC cell lines (Hep3B, HuH7 and PLC/PRF/5) which were sensitive to TGF-β induced cell death (Figure 3.6, right diagram and table). Additionally, a TGF-β dependent 1.7-1.9 fold increase of TβRI mRNA levels was observed in HLE and HepG2 cells. In all other cell lines, TGF-β did not alter TβRII expression, including HuH6 cells, which were responsive to TGF-β induced growth arrest.

3.2.2.2 TGF-β alters Smad3, but not Smad2 or Smad4 expression

Smad2, Smad3 and Smad4 are the main signaling mediators of TGF-β inside the cells and their expressions after stimulation with TGF-β in comparison to untreated controls were therefore carefully analyzed for the different liver cancer cell lines. As demonstrated in Figure

3.7 (left and middle), Smad2 and Smad4 mRNA were not altered decisively upon 24 h TGF-β treatment. The cytokine slightly inhibited Smad2 expression in HCC-M cells (0.7 fold, $p < 0.05$), whereas a marginal upregulation was found in HepG2 and HuH6 (1.3 fold, $p < 0.01$ and < 0.05) cells. Similarly, Smad4 levels varied between 0.8 and 1.1 fold expression regulations by TGF-β, with a negligible but significant induction in HepG2 and Hep3B cells. The finding that external TGF-β stimulation did not influence Smad2 and Smad4 levels, was confirmed on the protein level by performing immunoblot analysis after 24 h of TGF-β treatment (Figure 3.8).

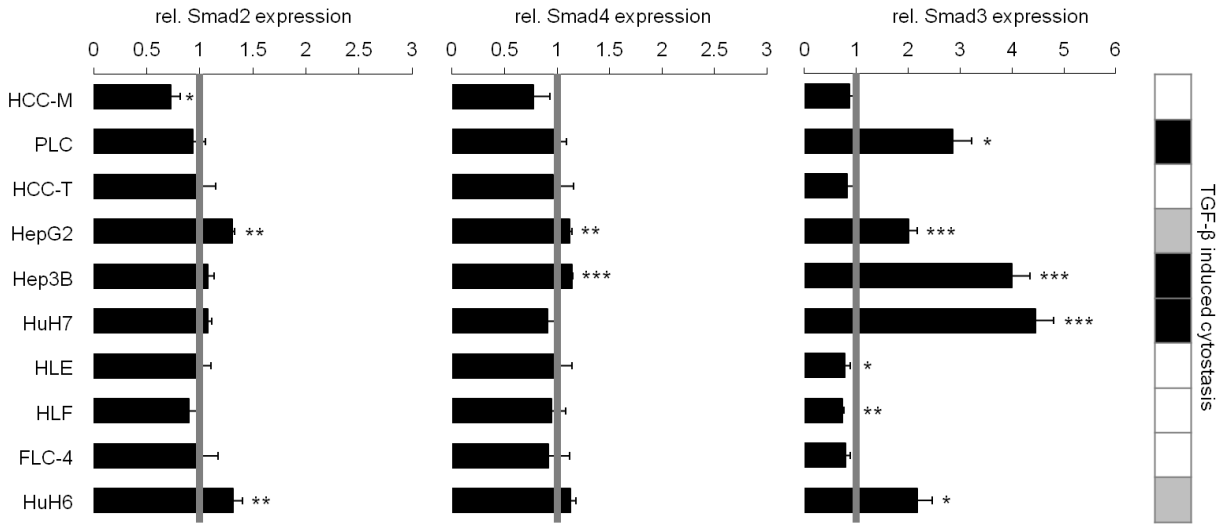

Figure 3.7 TGF-β induces Smad3, but not Smad2 and Smad4 expression in HCC cell lines sensitive to TGF-β induced cytostasis. HCC cell lines were treated with (filled bars) or without (grey line) 5 ng/mL TGF-β for 24 h. Expression levels of Smad2 (left), Smad4 (middle) and Smad3 (right) were detected using real time PCR with 18S rRNA expression as a reference gene. In the table, cell lines marked as black showed TGF-β induced cell death and growth inhibition whereas cells marked as grey mainly reacted with the latter one. Results are shown as mean + SE from at least two independent experiments. Significances are indicated as * $p < 0.05$, ** $p < 0.01$, *** $p < 0.001$ (Student's *t*-test).

In contrast, TGF-β considerably enhanced Smad3 mRNA levels (Figure 3.7, right diagram) in cell lines with a cytostatic TGF-β response (compare to table in Figure 3.7 or chapter 3.1). It resulted in a significant 2.0-2.2 fold increase of Smad3 expression in HepG2 and HuH6 cells ($p < 0.05$), which showed a TGF-β mediated inhibition of proliferation. This effect was even more pronounced in cell lines which additionally died upon TGF-β treatment. Here, TGF-β enhanced Smad3 expression by the factor 2.9-4.5 in PLC/PRF/5, Hep3B and HuH7 cells. Interestingly, no TGF-β dependent changes or a rather faint inhibition of Smad3 expression was observed in cell lines resistant to TGF-β induced cytostasis, such as HCC-M, HCC-T, HLE, HLF and FLC-4 cells. Most significant repression was found in HLE and HLF cells with about 0.75 fold expression when compared to untreated samples.

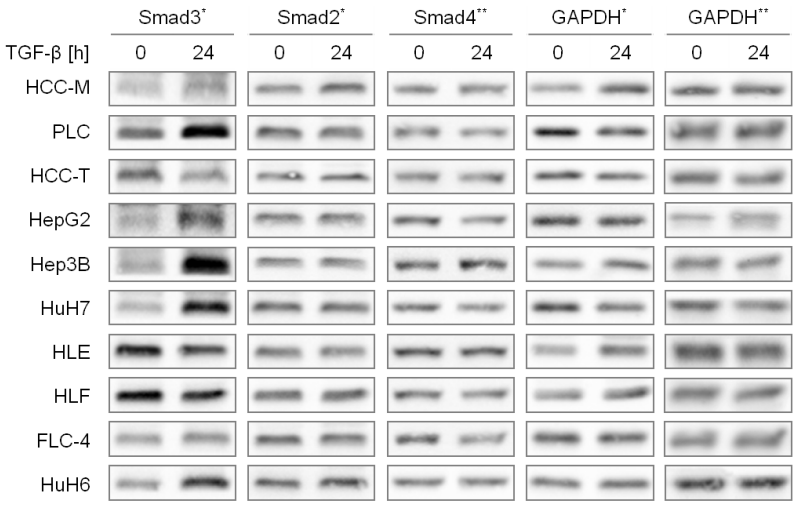

Figure 3.8 **TGF-β alters Smad3 but not Smad2 and Smad4 protein levels.** Smad2, Smad3 and Smad4 protein expression in control samples and cells treated with TGF-β for 24 h was evaluated by immunoblot analysis using GAPDH as a loading control. * and ** indicate which GAPDH belongs to Smad2 and Smad3 or Smad4, respectively. The results show one representative of two independent experiments.

These findings were confirmed by immunoblot analysis (Figure 3.8), revealing a distinct increase of Smad3 protein levels in PLC/PRF/5, HepG2, Hep3B, HuH7 and HuH6 cells, while those in HCC-M, HCC-T and FLC-4 cells remained stable upon TGF-β treatment for 24 h. Furthermore, a minor TGF-β mediated decrease of Smad3 protein amounts was in line with slightly reduced Smad3 expression in HLE and HLF cells (compare Figure 3.8 to 3.7).

3.2.2.3 TGF-β induced Smad7 expression is highest in cell lines with low basal Smad7 expression

Smad7 is a potent inhibitor of canonical TGF-β signaling, and its expression is induced by TGF-β in a negative feedback loop. Given that Smad7 in turn may exert significant influence on TGF-β outcome, TGF-β induced Smad7 expression was investigated.

Real time PCR analysis identified different Smad7 inductions upon 2 h of TGF-β administration in various cell lines (Figure 3.9, upper left). Interestingly, when excluding HCC-M and HCC-T cells, basal (Figure 3.3 or gradient in Figure 3.9) and induced Smad7 mRNA levels showed a strongly negative correlation to each other (Pearson coefficient r = -0.74, p = 0.034; Figure 3.9 lower left). This implies that Smad7 induction is higher in cell lines with low endogenous expression and the other way around. HCC-M and HCC-T cells differed from this behavior, as seen in low basal Smad7 levels but almost no induction by TGF-β (< 1.5 fold; Figure 3.9, upper left). With that, they were in the same range as FLC-4, HLF and HuH6 cell, which had high basal Smad7 levels and a TGF-β dependent 1.2-1.8 fold induction. In PLC/PRF/5, HepG2 or Hep3B cells with rather low endogenous Smad7

transcription, TGF-β strongly elevated Smad7 expression by a factor of 9.4, 6.6 and 5.1, respectively. Consistently, TGF-β moderately increased Smad7 expression to 3.2 and 2.6 fold in HuH7 and HLE cells, respectively; two cell lines with medium basal Smad7 levels.

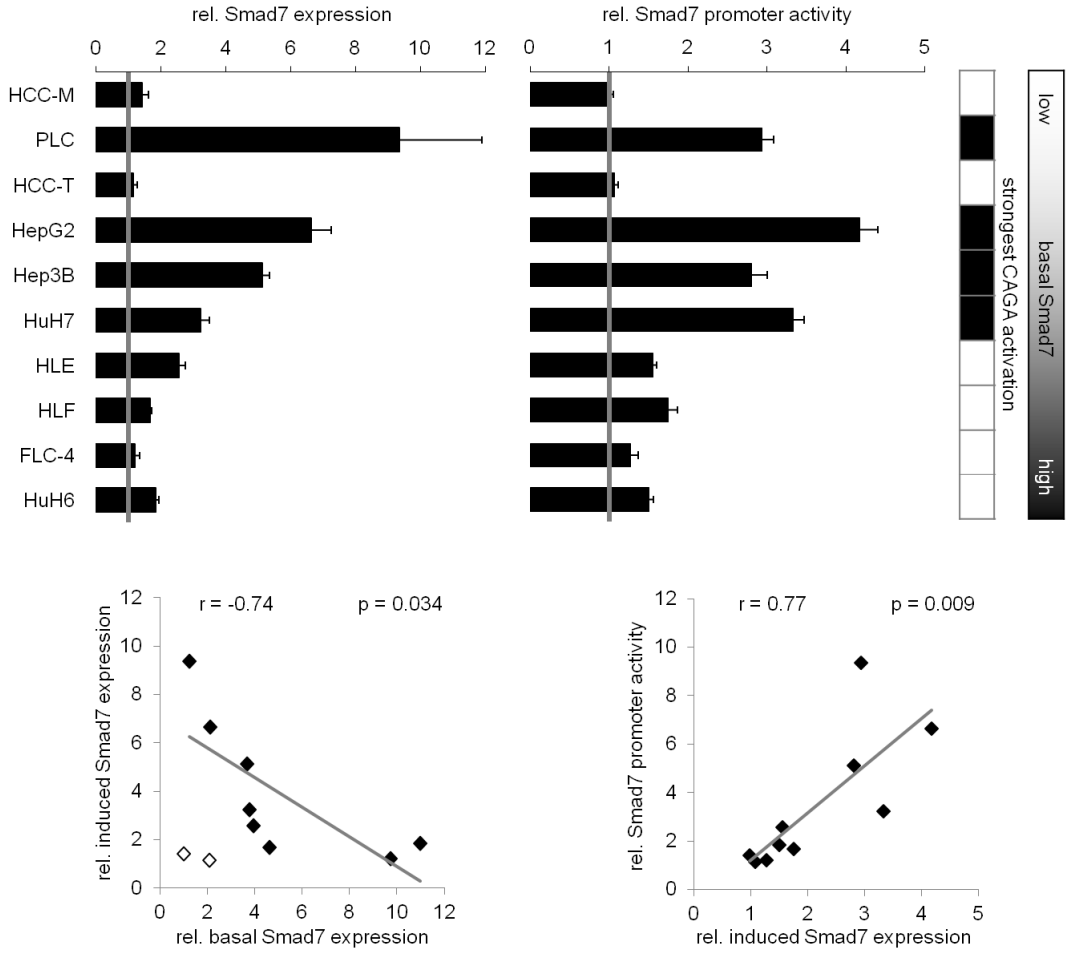

Figure 3.9 TGF-β induced expression of target gene Smad7 is lowest in cell lines with high basal expression. (Upper left diagram) HCC-T cells were either treated with 5 ng/mL TGF-β (filled bars) or left untreated (grey line) for 2 h. Relative Smad7 expression levels were evaluated using real time PCR with 18S rRNA as a reference gene. (Upper right diagram) HCC cells were transfected with a Smad7 promoter reporter assay, which was evaluated after 6 h of stimulation with or without 5 ng/mL TGF-β. TGF-β treated samples (filled bars) were normalized to the corresponding untreated control (grey line). Results show the mean +SE of at least three independent experiments. (Right table) Cell lines with the strongest Smad3/Smad4 transcriptional activity (Figure 3.11, page 58) are marked as black. The gradient stands for increasing basal Smad7 expression. (Lower diagrams) Correlation analysis was performed by calculation of the Pearson coefficient *r* between relative TGF-β induced Smad7 mRNA levels and basal Smad7 expression (left) as well as relative Smad7 promoter activity (right). In the left diagram, HCC-M and HCC-T cells, which were excluded from the analysis, are shown as open squares.

Next to analysis of Smad7 mRNA levels, a reporter assay was performed, using the firefly luciferase gene under control of parts of the human Smad7 promoter (Figure 3.9, upper right diagram). This promoter fragment is sufficient for TGF-β induced activity [37]. Data were acquired in collaboration with Jasmin Fabian from the same group. Reporter assay analysis validated the results of real time PCR. 6 h after TGF-β stimulation, there was no elevation of

promoter activity in HCC-M and HCC-T cells, but a 2.8-4.1 fold increase in Hep3B, PLC/PRF/5, HuH7 and HepG2 cells when compared to untreated controls. In all other cell lines, TGF-β treatment resulted in only minor inductions (1.3-1.8 fold). Correlation analysis confirmed a strong similarity between the results of Smad7 mRNA and promoter activity analysis (Pearson coefficient $r = 0.77$, $p < 0.01$; Figure 3.9, lower right). Furthermore, TGF-β most efficiently induced Smad7 transcription in cell lines with a high induced Smad3/Smad4 transcriptional activity (CAGA activation; table in Figure 3.9 or Figure 3.11, page 58).

In summary, the results presented in chapter 3.2 demonstrate that Smad7 expression strongly correlated with TGF-β1 mRNA levels. Interestingly, except for HCC-M and HCC-T, TGF-β's ability to induce Smad7 expression was reduced with rising endogenous Smad7 transcription. Overall, TβRI expression was rather stable between the various cell lines and, in general, lower than TβRII. The latter was predominantly expressed in cell lines sensitive to TGF-β induced cytostasis and expression remained unaltered following TGF-β treatment. Interestingly, TGF-β1 enhanced TβRI mRNA levels in exactly those cell lines. Finally, Smad2 and Smad4 expression was stable, both endogenously and after TGF-β treatment. In contrast, Smad3 was expressed heterogeneously in different HCC cell lines, but did not correlate with TGF-β sensitivity. However, Smad3 expression was induced by TGF-β only in cell lines which were sensitive to TGF-β mediated cytostasis.

3.3 Effects of TGF-β on Smad2 and Smad3 activity in HCC cell lines

Modified levels of TGF-β signaling components do not necessarily reflect changes in signal transduction intensity. Consequently, an analysis of R-Smad activation and functionality was conducted.

3.3.1 TGF-β enhances Smad2 and Smad3 activity in HCC cell lines

Intracellular TGF-β signaling is implemented by receptor mediated phosphorylation and thereby activation of receptor Smads, mainly Smad2 and Smad3 (chapter 1.1.2). Hence, an analysis of the intensity and duration of R-Smad activation was important for a detailed delineation of TGF-β signaling in HCC cell lines.

Immunoblot analysis suggests a strong variation in durations of TGF-β dependent Smad2 activation in the different cell lines, ranging from 1 h to 48 h (Figure 3.10, left). By trend, cell

lines with high Smad7 expression showed a transient activation of Smad2 for 1 h, which was clearly reduced after 3 h, as seen in HLE, HLF, FLC-4 and HuH6 cells. In contrast, TGF-β treatment in HCC-M and HCC-T, but also PLC/PRF/5 cells with low Smad7 mRNA levels resulted in a prolonged Smad2 activation of up to 48 h. HepG2 and Hep3B cells displayed an exception, with rather short signaling but low Smad7 expression in HepG2 cells and higher Smad7 and longer signaling duration in Hep3B cells. Overall, calculation of the Pearson coefficient suggest a negative, but insignificant correlation between the duration of the Smad2 activation and Smad7 mRNA levels (r = -0.55, p = 0.102).

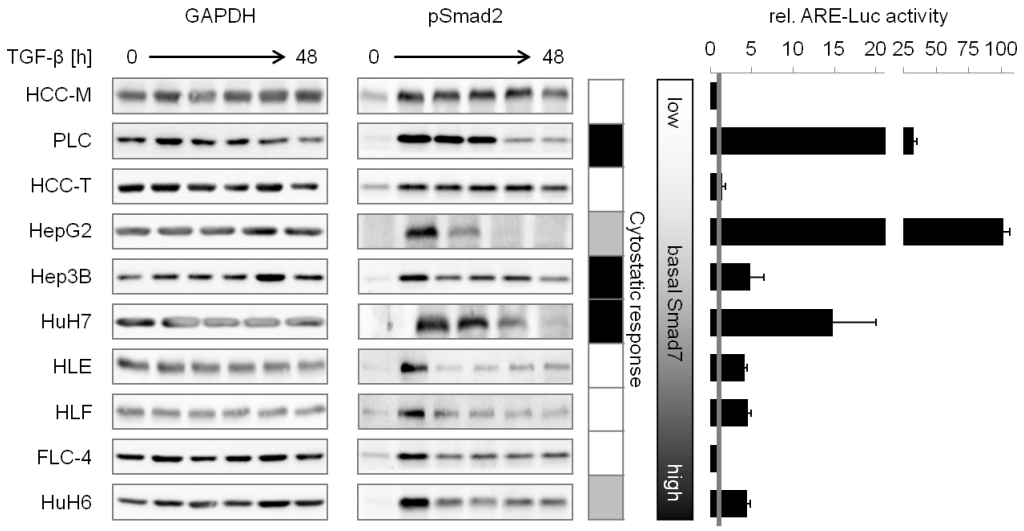

Figure 3.10 TGF-β induced activation of Smad2 is heterogeneous in different HCC cell lines but weakly correlates with Smad7 expression. (Left) HCC cell lines were treated with 5 ng/mL TGF-β 0, 1, (3), 7, 24 and 48 h before cell lysis. Immunoblot analysis of phosphorylated Smad2 and GAPDH as a reference was performed. The immunoblots show one representative example of at least two independent experiments. The table characterizes the cell lines regarding cytostatic response, with cells showing TGF-β induced growth arrest in grey and cell lines additionally reacting with cell death in black. The gradient from white to black displays increasing basal Smad7 expression levels. (Right) Cell lines were transfected with a plasmid carrying a luciferase gene under the control of ARE. Smad2 transcriptional activity was detected 9 h after treatment with (filled bars) or without (grey line) 5 ng/mL TGF-β. Results are presented as the mean +/-SE of three independent experiments.

Activated Smad2 forms a transcription factor complex with Smad4, which then, together with DNA binding proteins such as Fast-1, regulates gene expression by binding to an activin responsive element (ARE; chapter 1.1.2, page 3). As the formation of this complex and its binding to DNA can be affected by many factors, it was indispensable to analyze Smad2 transcriptional activity after TGF-β treatment using an ARE-luciferase reporter assay. TGF-β strongly induced luciferase activity by a factor of 14.8, 32.7 and 102.1 in cytostasis sensitive HuH7, PLC/PRF/5 and HepG2 cells, respectively (Figure 3.11, right). HuH6 and Hep3B cells, which were responsive to TGF-β induced cytostasis, showed similar inducibility in resistant HLE and HLF cells (4.1-4.8 fold). Despite a clear activation of Smad2, TGF-β was unable to

markedly induce Smad2 transcriptional activity in HCC-M, HCC-T and FLC-4 cells. However, preliminary data using a TβRI inhibitor (data not shown) suggest that this pathway is endogenously activated in those cell lines, as the inhibitor reduced basal Smad2 transcriptional activity to 10 %. In line with that, basal activity was lowest in cells with the highest inducibility by TGF-β, namely HepG2 and PLC/PRF/5.

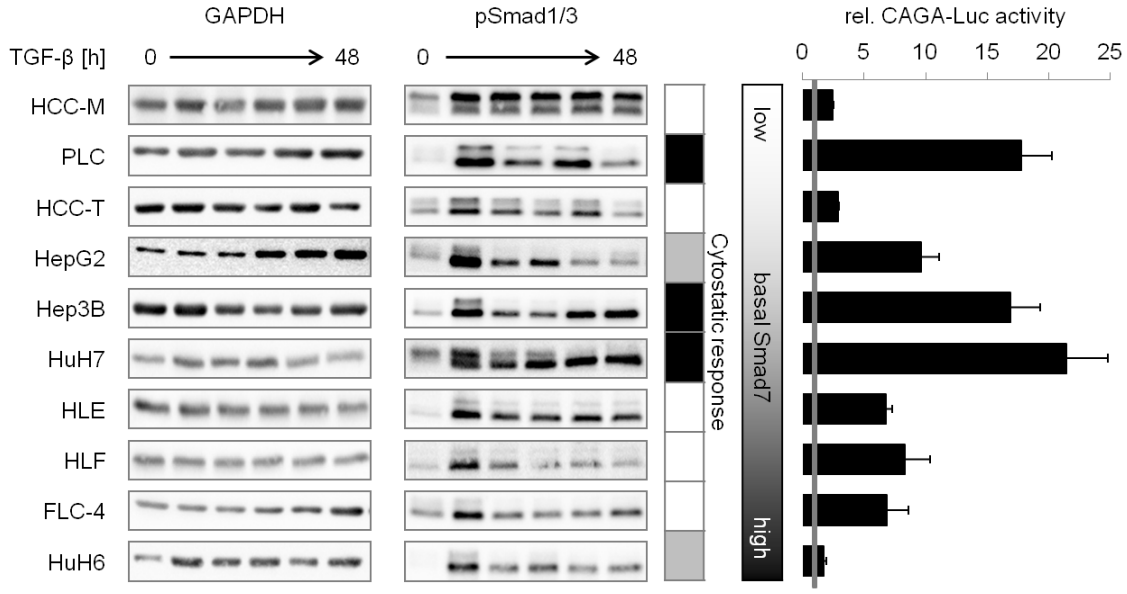

Figure 3.11 TGF-β mediated Smad3 activation is prolonged but does not correlate to Smad3 transcriptional activity in HCC cell lines. (Left) HCC cell lines were treated with 5 ng/mL TGF-β 0, 1, 3, 7, 24 and 48 h before cell lysis. Afterwards, immunoblot analysis of phosphorylated Smad1 (upper band) and 3 (lower band) as well as GAPDH as a loading control was performed. The immunoblot represents two independent experiments. (Middle) The table characterizes the cell lines regarding cytostatic response, with cells showing TGF-β induced growth arrest in grey and cell lines additionally reacting with cell death in black. The gradient from white to black displays increasing basal Smad7 expression levels. (Right) Cell lines were infected with an adenovirus encoding a luciferase gene under the control of a CAGA response element. Smad3/Smad4 transcriptional activity was detected 9 h after treatment with (filled bars) or without (grey line) 5 ng/mL TGF-β. Results are presented as mean + SE of three independent test.

Immunoblot analysis shows that TGF-β mediated Smad3 phosphorylation did not correlate as clearly with basal Smad7 levels as Smad2 activation (Figure 3.11). Except for HepG2, HLF and FLC-4 cells, TGF-β induced Smad3 activation was prolonged and lasted for up to 48 h. No correlation to the cytostatic TGF-β response was observed (Figure 3.11, table). Finally, TGF-β stimulation resulted in a transient Smad1 activation in all but HCC-M cells, which showed considerably prolonged signal duration until at least 48 h of TGF-β treatment.

Smad3 activation results in the formation of a transcription factor complex, which regulates gene expression by binding to a CAGA element (chapter 1.1.2, page 3). To analyze whether TGF-β activated Smad3 signaling is interrupted downstream of the R-Smad activation, a CAGA-luciferase reporter assay with or without TGF-β stimulation for 9 h was performed. Although TGF-β strongly induced Smad3 phosphorylation, the resulting Smad3/Smad4

transcriptional activity was low (1.7-2.8 fold) in HuH6, HCC-M and HCC-T in comparison to untreated controls (Figure 3.11, right diagram). A TβR1 inhibitor was unable to reduce basal Smad3 transcriptional activity as dramatically as in the case of Smad2 (preliminary data, not shown), indicating lower endogenous Smad3 activation. FLC-4, HLE, HLF and HepG2 showed a TGF-β dependent 6.8 to 9.7 fold increase of basal CAGA-Luc activity. However, highest inductions by a factor of 16.9-21.4 were found in Hep3B, PLC/PRF/5 and HuH7 cells. These were cell lines with relatively low amounts of TGF-β and Smad7 mRNA and with sensitivity towards TGF-β induced cell death (table in Figure 3.11 and Figure 3.3).

3.3.2 Induction of Smad3 target genes Bim and PAI-1 by TGF-β correlates with Smad3/Smad4 transcriptional activity

The previous results demonstrate that TGF-β induced cytostasis correlated with increased Smad3 transcriptional activity, which was accompanied by a stronger induction of the TGF-β target gene Smad7. To strengthen these observations, I examined the impact of TGF-β on further Smad3/Smad4 target genes, Bim and PAI-1.

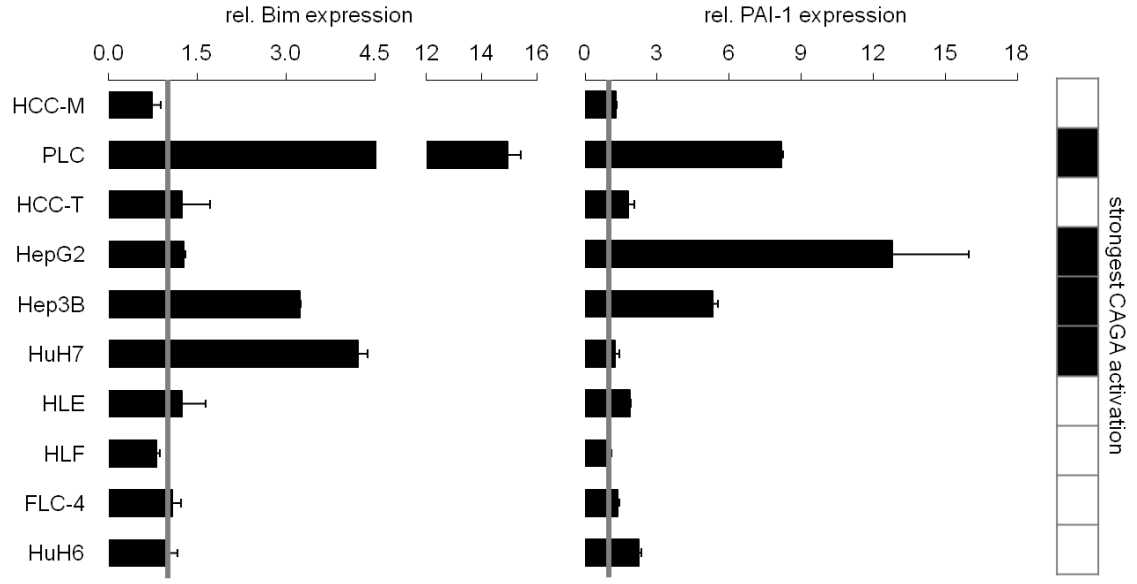

Figure 3.12 TGF-β induces Smad3/Smad4 target genes Bim and PAI-1 in HCC cell lines with high CAGA activity. Real time PCR against Bim (left) and PAI-1 (middle) was performed after stimulation with (filled bars) or without (grey line) 5 ng/mL TGF-β for 24 h and 2 h, respectively. 18S rRNA was used as a reference gene. Data are presented as the mean + SE of three independent experiments. (Right) The table demonstrates which cell lines showed a strong TGF-β induced Smad3/Smad4 transcriptional activity (CAGA-Luc assay, Figure 3.11).

Expression of pro-apoptotic Bim is induced Smad3 dependently during TGF-β mediated activation of the apoptotic cascade in hepatocytes [71, 234]. Real time PCR experiments after 24 h of TGF-β stimulation (Figure 3.12) revealed an induction of Bim expression in HCC

cell lines which were responsive to TGF-β caused cell death, namely Hep3B, HuH7 and PLC/PRF/5 (3.2, 4.2 and 14.9 fold when normalized to untreated controls). TGF-β was unable to enhance Bim expression in all other cell lines, including HepG2 cells with good inducibility of CAGA-Luc activity. In contrast, Bim expression was weakly inhibited by TGF-β to 73 % and 81 % in HCC-M and HLF ($p < 0.05$) cells.

Another Smad3 target gene is plasminogen activator inhibitor-1 (PAI-1). TGF-β induces PAI-1 expression during EMT in hepatocytes [139, 140]. In the analyzed liver cancer cell lines, TGF-β strongly enhanced PAI-1 mRNA levels in PLC/PRF/5, Hep3B and HuH7 cells (three out of four cell lines with the highest CAGA-Luc activity measured). In comparison to untreated control samples, TGF-β led to a 5.3, 8.2 and 12.8 fold induction of PAI-1 in Hep3B, PLC/PRF/5 and HepG2 cells, respectively, while it was below 2.2 fold in all other cell lines, including HuH7 cells.

In conclusion, studies on R-Smad proteins show that TGF-β enhances C-terminal phosphorylation of Smad2 and Smad3 in all HCC cell lines analyzed. The duration of Smad2, but not Smad3 activation is by trend negatively correlated with Smad7 mRNA levels. Smad3 phosphorylation was mostly prolonged but did not correlate with inducibility of CAGA activity, which was higher in cell lines with low Smad7 expressions. On the other hand, Smad3/Smad4 transcriptional activity was accompanied by Smad3 target gene expression and induction of cytostasis by TGF-β.

3.4 Regulation of TGF-β induced cytostasis

3.4.1 Endogenous expression of proteins involved in survival signaling or growth control

To investigate if the HCC cell lines are primed to the different cytostatic responses, basal levels of proteins, which are known to be involved in survival signaling and growth control, were analyzed: phosphorylation of ERK, c-Jun, and Akt (lower band) and endogenous levels of Akt as well as anti-apoptotic Bcl-2 and Bcl-XL. Figure 3.13 demonstrates that there was no survival signaling status indicating a coherent regulation mechanism of cytostatic TGF-β effects in all cell lines tested. High Akt phosphorylation (lower band) was only detected in HCC-T, Hep3B and FLC-4 cells, and no connection to the TGF-β induced cytostatic response could be drawn. Similarly, basal Akt levels, which were lower in HuH7 and HuH6 but also in HCC-M and FLC-4 cells when compared to the other cell lines, did not indicate cytostatic responsiveness.

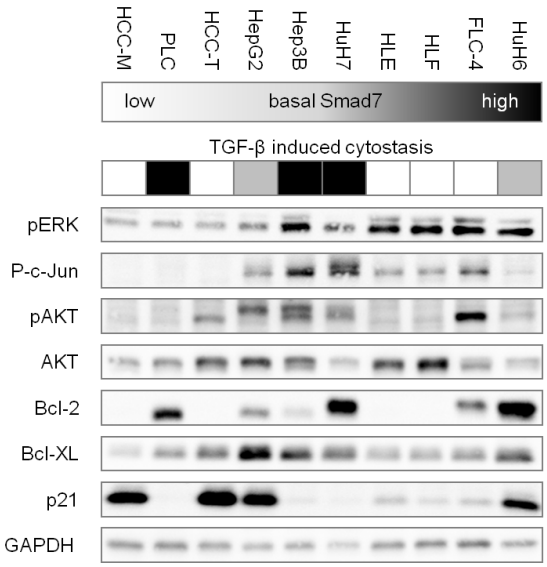

Figure 3.13 Endogenous expression levels of different survival and growth regulating factors. HCC cell lines were cultured in starvation medium for 24 h. Immunoblot analysis was conducted to detect phosphorylated ERK, c-Jun and Akt (lower band) as well as total Akt, Bcl-2, Bcl-XL and p21. GAPDH was used as a loading control. The blots show representative results of two independent experiments. The table characterizes the cell lines regarding cytostatic response, with cells showing TGF-β induced growth arrest in grey and cell lines additionally reacting with cell death in black. The gradient from white to black displays increasing basal Smad7 expression levels.

Anti-apoptotic Bcl-2 levels were elevated in cell lines with a cytostatic TGF-β response, but also in FLC-4 cells. In contrast, the other anti-apoptotic member of the Bcl-2 family, Bcl-XL, was present in all analyzed cell lines, with high levels in HepG2 and Hep3B and rather low amounts in HCC-M, HLE, HLF, and PLC/PRF/5 cells. Phosphorylation and consequently activation of ERK and c-Jun did not correlate to TGF-β dependent cytostasis. However, interestingly, the phosphorylation status of both proteins was higher in cell lines with increased Smad7 mRNA levels (Figure 3.13, gradient). Only phospho-c-Jun in HuH6 cells deviated from this observation. Finally, p21 was predominantly found in cell lines with low Smad7 expression. Here, HuH6 with high p21 and Smad7 levels and PLC/PRF/5 with low basal Smad7 mRNA but also low p21 protein levels were an exception.

3.4.2 TGF-β induced cytostasis is Smad3 dependent

TGF-β strongly enhanced Smad3 expression and its transcriptional activity in HCC cell lines which were sensitive to TGF-β mediated cytostasis. Strongest effects were observed in PLC/PRF/5, Hep3B and HuH7 cells, which did not only show TGF-β dependent growth inhibition but also induction of apoptosis. Because TGF-β mediated apoptosis is Smad3 dependent in hepatocytes [67], the role of Smad3 during TGF-β induced cytostasis was further delineated and was compared to Smad2. For this, RNA interference technology was used to target Smad2 and Smad3 mRNA. The knockdown was established over 48 h before

continuous stimulation with TGF-β for 72 h. Efficient knockdown was ensured by immunoblot analysis after 1 h of TGF-β treatment (Figure 3.14, left). siRNA against Smad2 and Smad3 significantly reduced corresponding R-Smad levels as well as their phosphorylation by TGF-β. Admittedly, both siRNAs showed some cross reactivity with the other R-Smad's mRNA, with stronger effects of Smad2 siRNA on Smad3.

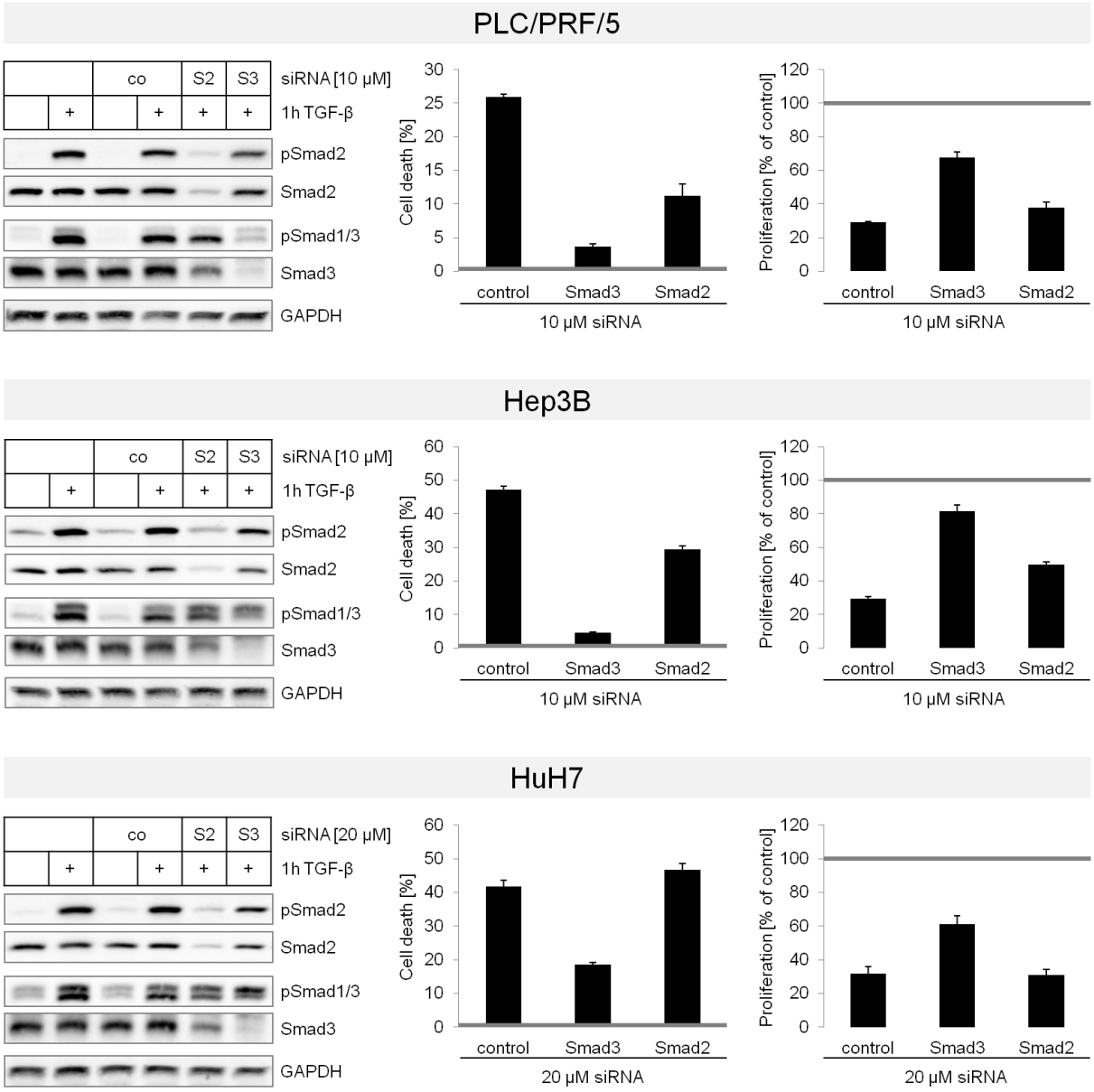

Figure 3.14 TGF-β induced cell death is Smad3 but not Smad2 dependent. PLC/PRF/5 (upper panel), Hep3B (middle panel) were treated with 10 µM, HuH7 (lower panel) with 20 µM siRNA against Smad2 (S2) or Smad3 (S3). An unspecific siRNA sequence (co) was used as a control. Knockdown was established for 48 h and afterwards, each condition was either treated with or without 5 ng/mL TGF-β for 1 h (immunoblot) or 3 days (cell death and proliferation). (Left) Immunoblot analysis was performed to detect phosphorylated and total Smad2 and Smad3 (lower band for pSmad1/3) as well as GAPDH as a loading control. (Middle) Cell death rates were detected using an LDH assay. Untreated cells for each siRNA condition were defined as 0 (grey line). TGF-β treated samples are shown as filled bars. (Right) The same assay, but only LDH content in viable cells, was used to evaluate proliferation rates. TGF-β treated (bars) cells were normalized to untreated (grey line) cells for each siRNA condition. The results show one representative of two independent experiments.

Figure 3.14 demonstrates that Smad3 knockdown, in contrast to Smad2 knockdown, efficiently blocked TGF-β induced cell death (middle) and growth arrest (right) in PLC/PRF/5, Hep3B and HuH7 cells. In PLC/PRF/5 cells, Smad3 siRNA reduced TGF-β mediated cell death from 26 % to 4 %, whereas it was decreased to 11 % in cells with Smad2 knockdown. However, Smad2 siRNA also reduced Smad3 protein levels, which may be the reason for the observed protective effect. Smad3 knockdown additionally interfered with TGF-β induced growth arrest in PLC/PRF/5 cells (right diagram). It restored TGF-β decreased proliferation from 29 % to 68 %, while Smad2 siRNA resulted in only minor effects (38 %).

Basal Smad3 levels were higher in Hep3B compared to PLC/PRF/5 cells (Figure 3.5). This explains why the observed cross reactivity of Smad2 siRNA was not as strong in Hep3B as in PLC/PRF/5 cells (Figure 3.14). Smad3 knockdown almost completely abolished TGF-β induced cytostasis in Hep3B cells. Smad3 siRNA efficiently counteracted TGF-β induced cell death from 47 % to 2 % and restored cell viability from 29 % to 82 %. In contrast, interference with Smad2 translation still resulted in TGF-β induced cell death to 28 % and growth arrest to 50 %. In HuH7 cells, inhibition of Smad3 transcription bisected TGF-β induced cell death from 42 % in control cells to 19 %. Furthermore, it interfered with TGF-β mediated growth arrest leading to 61 % viable cells instead of only 32 % in control samples. Smad2 knockdown, however, did not alter the cytostatic TGF-β response in HuH7 cells.

3.4.3 Potential regulation of Smad3 by PRAJA and ELF

ELF (β2-Spectrin) may be involved in the nuclear translocation of the Smad3/Smad4 complex and is therefore a potential regulator of Smad3 dependent TGF-β signaling [182]. Downregulation of ELF displays one mechanism to avoid cytostatic effects of TGF-β. PRAJA initiates ubiquitination and proteasomal degradation of ELF and thereby regulates its activity [183]. Hence, high PRAJA expression may lead to low ELF levels, which in turn results in reduced Smad3 transcriptional activity. Consequently, expression levels of both proteins were comparatively analyzed.

The table and right diagram of Figure 3.15 highlight that the ELF/PRAJA ratio of the relative expression levels is, except for FLC-4 cells, lowest in cells with an established resistance against TGF-β induced cytostasis. This is mainly based on varying endogenous ELF expression levels between the different cell lines. It was lowest in HLE, HCC-T, HLF and HCC-M cells (1.0-1.3 fold, normalized to HLE), which were all resistant against TGF-β induced cytostasis (Figure 3.15, left diagram and table). In contrast, elevated mRNA levels were found in cell lines responsive to TGF-β mediated cell death and growth arrest. Here, medium ELF expression was detected in PLC/PRF/5, HepG2 and HuH6 cells (2.5-6.0 fold),

while highest ELF mRNA levels were assigned to HuH7 and Hep3B cells (7.8 and 11.3 fold). Among the top six ELF expressions, only FLC-4 cells were resistant against TGF-β induced cytostasis, with a 5.5 times higher ELF expression than HLE cells. However, expression of PRAJA (Figure 3.15, middle diagram), which induces degradation of the ELF protein, was also 2 times increased in FLC-4 cells in comparison to TGF-β sensitive Hep3B cells.

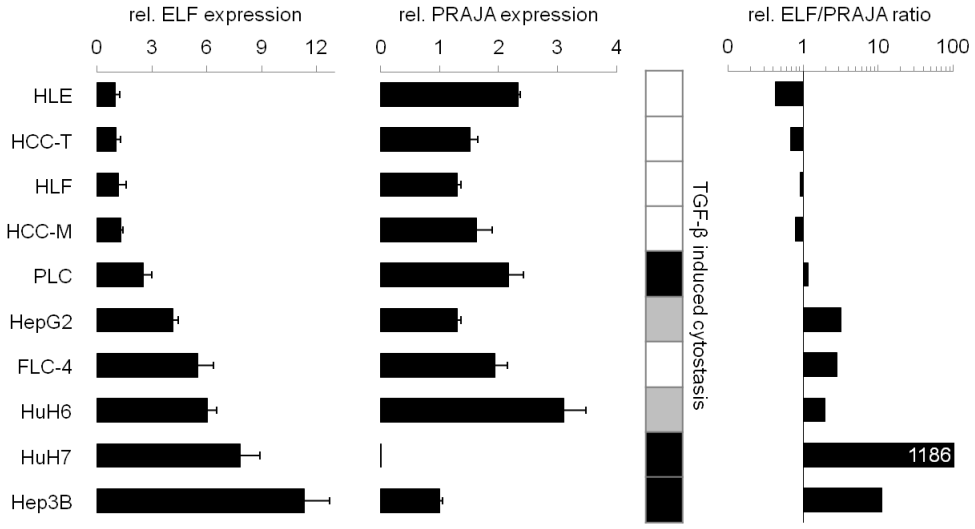

Figure 3.15 Basal mRNA levels of PRAJA and ELF in HCC cell lines. Liver cancer cell lines were cultured in starvation medium for 24 h and afterwards, relative ELF (left) and PRAJA (middle) expression were detected using real time PCR with 18S rRNA as a reference gene. Results are presented as mean + SE of three independent experiments. (Middle) The table highlights cell lines sensitive to proliferation inhibition by TGF-β alone (grey) or in combination with induction of cell death (black). (Right)The right diagram presents the ELF/PRAJA ratio of the relative expression levels shown left.

Similar to Hep3B, other TGF-β cytostasis sensitive cell lines expressed likewise low amounts of PRAJA, and it was almost lost in HuH7. Cytostasis resistant HLF, HCC-T, HCC-M and HLE cells with low ELF mRNA levels expressed low to moderate PRAJA levels (1.3-1.6 fold, and 2.3 fold in HLF cells). Finally, PLC/PRF/5 as well as HuH6 cells showed with 2.2 and 3.1 times elevated levels a rather high PRAJA expression. In general, Ct values for ELF were lower in HCC cell lines than the ones for PRAJA, suggesting that more ELF than PRAJA mRNA was present (not shown).

In conclusion, the data in chapter 3.4 demonstrate that common survival factors such as ERK, Akt or Bcl-2 and Bcl-XL did not correlate with the cytostatic TGF-β response in ten different HCC cell lines. In contrast, the finding that TGF-β mediated Smad3 transcriptional activity and inducibility of its target genes correlated with TGF-β induced cytostasis (chapter 3.3) was in line with the observation that knockdown of Smad3, but not Smad2, led to reduction of TGF-β induced cell death and growth arrest. One possible mechanism of the observed resistance in other cell lines could be the ratio between ELF and PRAJA, which was mostly lower than in sensitive cell lines.

3.5 Basal cell migration is highest in cell lines with high Smad7 expression and low TGF-β induced cytostasis

To acquire motility is an important step of cancer cells to move to new areas and to increase malignancy. An *in vitro* transwell migration assay was performed to characterize the ten liver cancer cell lines in regard of migratory capacity. Figure 3.16 demonstrates that three cell lines showed high cell motility (left diagram). While more than 40 % of HLE, HLF and FLC-4 cells migrated within 13 h, all other cell lines showed low motility with migration rates below 7 %. Interestingly, all three highly motile cell lines featured high Smad7 mRNA levels (Figure 3.16, gradient). Only TGF-β sensitive HuH6 cells with the highest Smad7 expression was rather immotile.

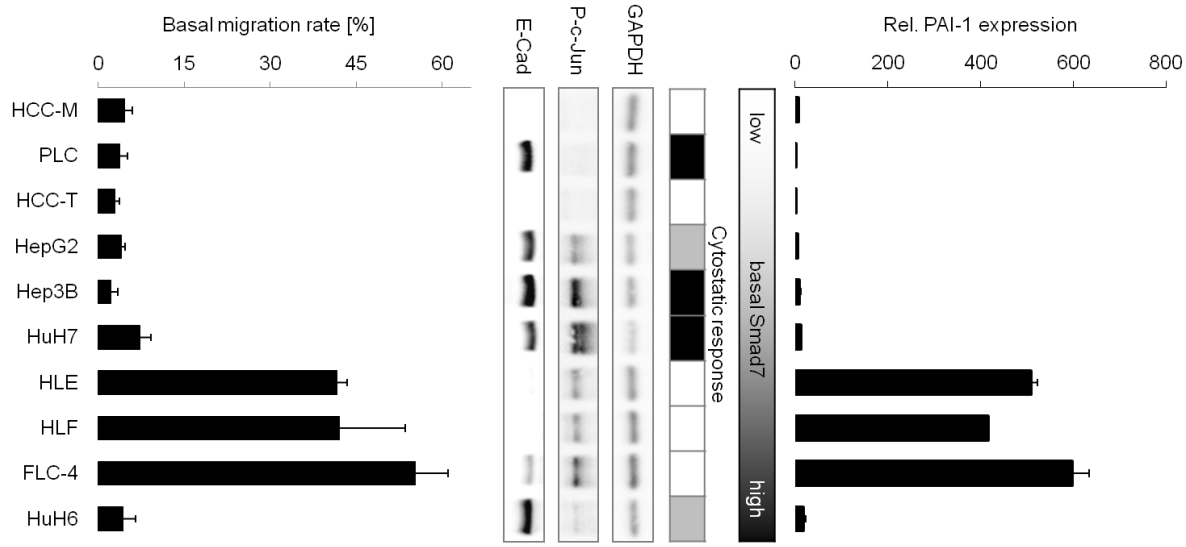

Figure 3.16 Migration capacity comes along with high Smad7 and low E-Cadherin levels. (Left) Basal migration rate of HCC cell lines was evaluated using a transwell assay. (Middle) HCC cell lines were cultured in starvation medium for 24 h and subsequently, protein levels of E-Cadherin, phosphorylated c-Jun and GAPDH as a loading control were detected using Western blot analysis. The table at the right shows cell lines sensitive to TGF-β induced growth arrest (grey) and additionally cell death (black). The gradient displays increasing Smad7 mRNA levels from white to black. (Right) Cell lines were cultured in starvation medium for 24 h. Real time PCR analysis was performed to detect endogenous PAI-1 expression using 18S rRNA as a reference gene. The diagrams present the mean + SE of at least two independent experiments. Western blots show one representative of at least two independent experiments.

Cancer cells of epithelial origin have to detach from the tight epithelial network to gain migratory capacity. Usually, epithelial-to-mesenchymal transition (EMT) is the underlying process, leading to adaption of a mesenchymal phenotype with higher degrees of freedom. TGF-β is an important regulator of EMT, which is accompanied by downregulation of epithelial markers such as E-cadherin and an induction of various matrix regulating genes, e.g., PAI-1 [139, 140]. Immunoblot analysis (Figure 3.16, middle) revealed that highly motile HLE, HLF and FLC-4, but also HCC-M and HCC-T cells possessed low or undetectable

E-cadherin levels. In contrast, E-cadherin was heavily expressed in immotile PLC/PRF/5, HepG2, Hep3B, HuH7 and HuH6 cells. High cell motility was accompanied by a strong overexpression of EMT marker PAI-1, as seen in 420-600 times higher PAI-1 mRNA levels in HLF, HLE and FLC-4 when compared to PLC/PRF/5 cells. In all other cell lines, PAI-1 expression did not exceed a 17 fold increased level (right diagram).

JNK signaling is an important non-canonical TGF-β signaling pathway and has been associated with TGF-β induced apoptosis and growth arrest, but also with TGF-β mediated proliferation, dedifferentiation and invasion. Furthermore, some of those observations have been linked to Smad7 [81, 114, 235]. Interestingly, Except for HuH6 cells, basal c-Jun phosphorylation was in general elevated in cell lines with increased Smad7 expression, including cells with a high motility (Figure 3.16, middle). In contrast, c-Jun activation was not detectable in HCC-M, HCC-T and PLC/PRF/5 with low Smad7 expression.

Serum TGF-β levels increase during liver disease progression and malignant hepatocytes start to produce the cytokine in relevant amounts themselves [158, 236, 237]. Next to its anti-tumorigenic functions, TGF-β is a well known booster of cancer progression as it may induce pro-tumorigenic processes, such as migration, invasion and metastasis (chapter 1.4). TGF-β is secreted as an inactive form and is activated by several proteins and factors (chapter 1.1.1). Hence, secretion of active and total amounts of TGF-β by HCC cell lines was of interest (Figure 3.17).

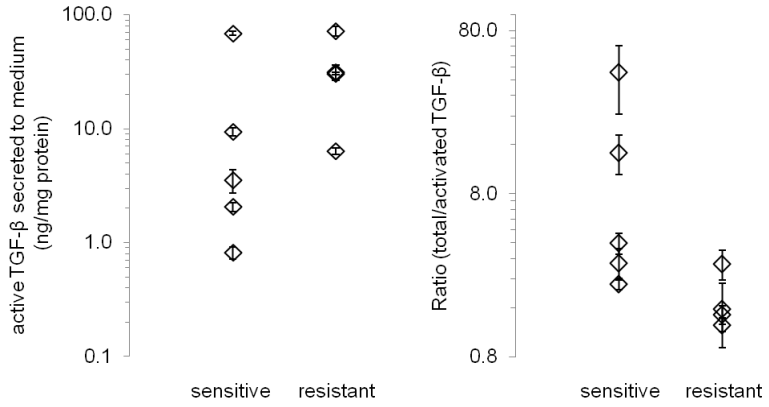

Figure 3.17 Active TGF-β levels are higher in HCC cell lines insensitive to TGF-β induced cytostasis. (Left) TGF-β reporter cell line MFB-F11 was used to evaluate the total amount of active TGF-β secreted to the medium by liver cancer cell lines. Secreted TGF-β was normalized to protein content in adherent cells. Cells were grouped in cell lines sensitive (HepG2, HuH6, PLC/PRF/5, HuH7 and Hep3B) or resistant (HCC-T, FLC-4, HLE and HLF) to TGF-β induced growth arrest and cell death. (Right) In addition to mature TGF-β, the total amount of TGF-β was detected after activation of latent TGF-β. The diagram shows the ratio of total to active TGF-β. The data are presented as mean +/- SE of three independent experiments.

TGF-β amounts in the medium were normalized to the total protein amount of adherent cells and for further evaluation, cells were grouped in cell lines sensitive (HepG2, HuH6,

PLC/PRF/5, HuH7 and Hep3B) or resistant (HCC-T, FLC-4, HLE and HLF) to TGF-β induced cytostasis. HCC-M cells were excluded from this experiment because some component of the conditioned medium interfered with the assay. Sensitive cells secreted by trend lower amounts of active TGF-β in comparison to resistant cell lines (left diagram). However, this finding was only significant ($p = 0.032$) when Hep3B cells, the sensitive cell line with the highest active TGF-β levels, were excluded. Lowest amounts of mature TGF-β in cell lines resistant to TGF-β induced cytostasis were detected in HCC-T cells, which showed similar levels to TGF-β sensitive cells. Furthermore, the right diagram of Figure 3.17 demonstrates that resistant HCC cell lines activated TGF-β at a higher percentage. The ratio of total to activated TGF-β is by trend lower in these cells when compared to cell lines sensitive to cytostatic effects of TGF-β.

In summary, migratory capacity in HCC cell lines correlated with reduced E-cadherin levels, high c-Jun activation as well as elevated Smad7 and PAI-1 expression and, by trend, more activated TGF-β in the medium.

3.6 Smad7 overexpression in human liver cancer samples

TGF-β signaling is frequently defective during hepatocarcinogenesis. Smad7 is an important modulator, but also cross-talk mediator, of TGF-β signaling (chapter 1.1.4 and 1.4.). Hence, Smad7 expression in human HCC samples was compared to “normal” (non tumorigenic) liver tissue from the same patient. Expression analysis of 133 samples from China and Germany was performed, of which 6 Chinese samples were not compared to matching normal liver samples but to the mean of two samples from other patients without HCC. Information about the patients is summarized in Table 3.1.

For expression analysis of Smad7, real time PCR was performed and 18S rRNA was used as a reference gene. Calculated Smad7 expression in tumors was normalized to Smad7 expression of the corresponding non-tumorigenic liver specimen. Samples were only included in the study if Ct-values of 18S rRNA were similar (within 1 cycle) in matched tumorigenic and adjacent liver tissue samples, or, as in seven cases, when larger differences were confirmed with a second reference gene (β2-microglobulin). Smad7 overexpression was assumed when the expression levels in tumorigenic tissue was more than 1.2 fold increased as compared to the control tissue.

	Chinese specimen	German specimen
Total	63	70
Gender		
Male	51	36
Female	4	18
Unknown	8	16
Age (mean)	25-75 years (49.0)	20-80 years (61.1)
> 50	42.6 %	82.5 %
≤ 50	57.4 %	18.5 %
Unknown	7	15
Etiology		
HBV	61	5
HCV	1	3
HBA	0	2
Alcohol	4 (all HBV)	12 (1x HBV, 1x HCV)
Cirrhosis - yes/no	51/10	17/48
Unknown	2	5
Tumor size		
> 5 cm	34	33
≤ 5 cm	21	15
Unknown	8	22
Cell differentiation		
Well - moderate (G1/2)	36	24
Poor - undifferentiated (G3/4)	19	22
Unknown	8	24
AFP (ng/ml)		
> 50	34	15
≤ 50	20	21
Unknown	9	34

Table 3.1 Clinicopathological variables of HCC patients from Germany and China.

Unchanged levels were defined as mRNA levels between 0.8 and 1.2 fold, whereas a reduction of expression to less than 0.8 fold was rated as repressed. Figure 3.18 shows that Smad7 mRNA levels were elevated in the majority (58.6 %) of all analyzed HCC samples, while they were repressed in only 24.1 % and unchanged in 17.3 %. A more detailed analysis revealed that Smad7 overexpression in HCC varied from 1.22 to 38.7 fold, in which half of the samples (51.2 %) expressed levels between 2 and 10 fold. 28.2 % were only slightly elevated with Smad7 mRNA being 1.2 to 2 fold increased. After all, about one fifth of all Smad7 overexpressing HCC samples possessed very high levels (>10 fold). In contrast, cancer specimens with reduced Smad7 expression were less spread and only one showed

expression below 0.1 fold. Similar to the Smad7 overexpressing samples, the majority of all samples with reduced Smad7 (56.2 %) expression exhibited 2-10 times reduced Smad7 levels (0.5-0.1 fold). However, compared to HCC samples with slightly elevated Smad7 levels (28.2 %), a higher percentage of HCCs (40.6 %) showed a minor Smad7 repression with less than two-fold inhibition (> 0.5 fold).

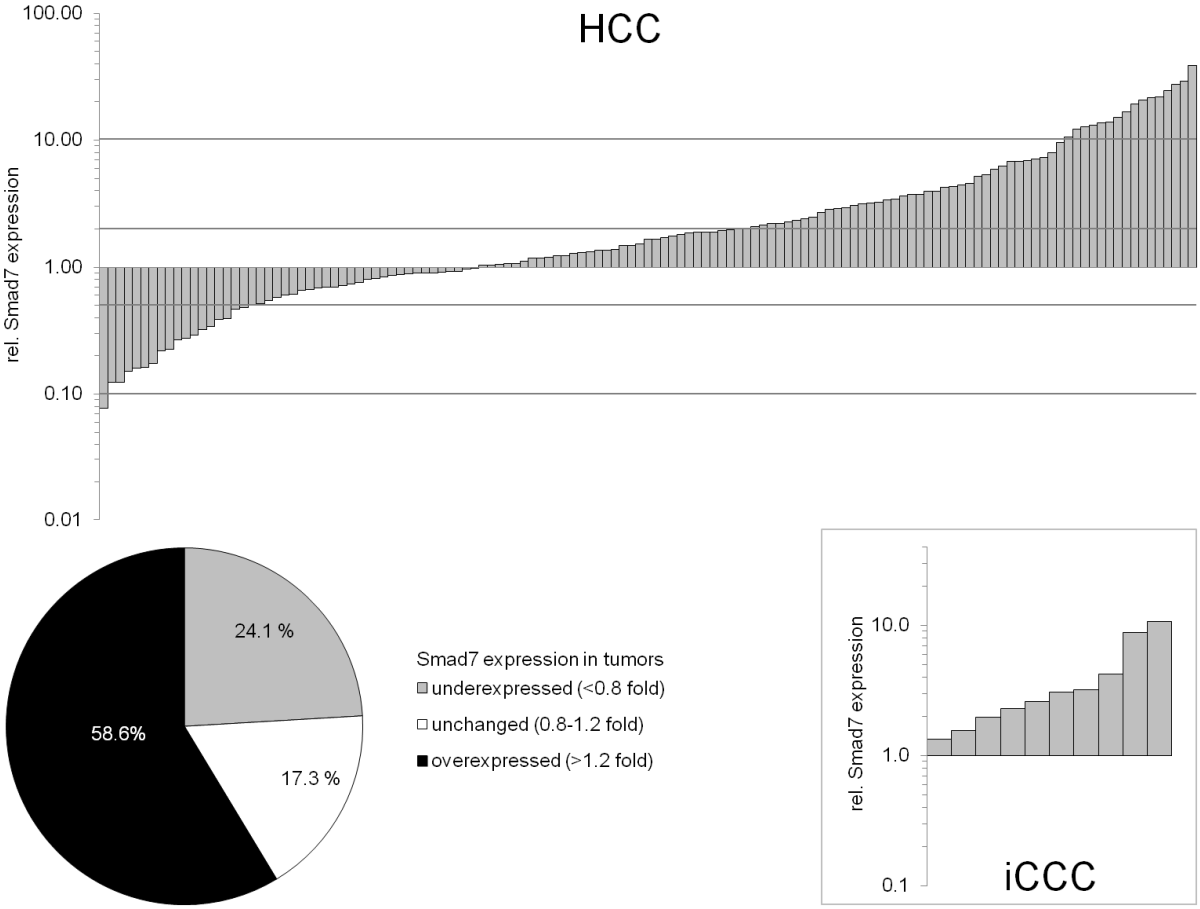

Figure 3.18 Smad7 expression is increased in hepatocellular and intrahepatic cholangiocellular carcinoma. Real time PCR expression analysis of Smad7 and 18S rRNA as a reference gene was performed for 133 matched normal liver and HCC (upper diagram) or intrahepatic cholangiocarcinoma (iCCC, lower right) patient samples. The grey lines in the upper diagram indicate 2 or 10 times increased or reduced Smad7 expression. Six analyzed HCC samples were compared to the mean of two normal liver samples from other persons. Four cancer/adjacent liver tissue samples included in the HCC analysis were of mixed origin (HCC/iCCC). The circle diagram shows the percentage and number of HCC samples with underrepresented, overexpressed or unchanged Smad7 levels.

Next to biopsies of hepatocellular carcinoma, a limited number of intrahepatic cholangiocarcinoma (iCCC), a cancer of the liver bile duct system accounting for about 5-10 % of all primary liver cancers [238], were analyzed. Interestingly, Smad7 levels were increased in all iCCC samples investigated when compared to adjacent liver tissue, ranging from 1.3 to 10.7 fold (Figure 3.18, lower right diagram).

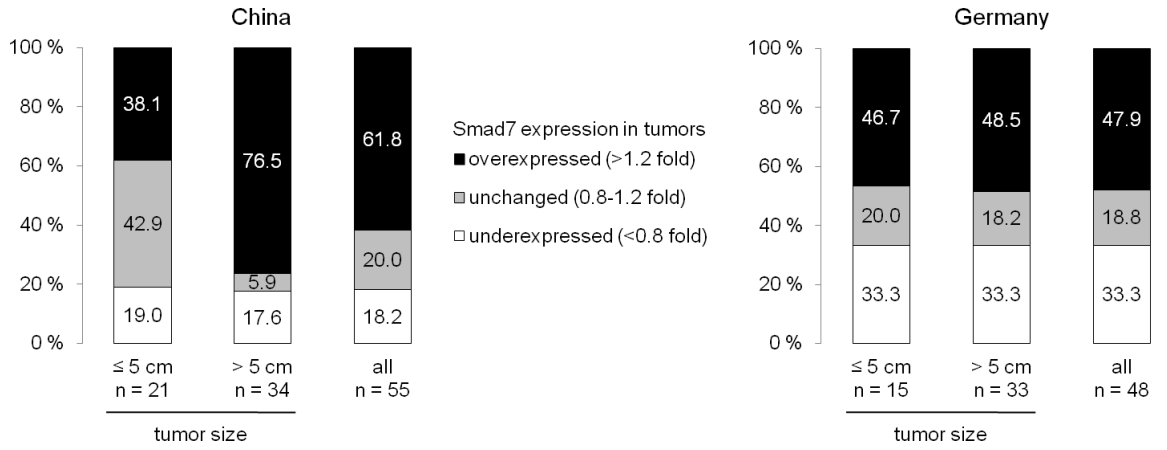

Figure 3.19 Smad7 expression correlates with tumor size in HCC patient samples from China. Information about tumor size was available for 103 of 133 HCC samples as contained in Figure 3.18. 55 HCC samples from China (left) and 48 from Germany (right) were grouped in tumors smaller than/equal to or bigger than 5 cm. Diagrams show percentages of samples with increased (black), decreased (white) or unchanged (grey) Smad7 levels for small and large tumors as well as for the sum of both groups.

Seventy paired HCC/"normal" liver samples were obtained from Germany and 63 from China. The majority of Chinese samples were evaluated in collaboration with Prof. Gao and Dr. Gu (Department of Laboratory Medicine, Eastern Hepatobiliary Hospital, Second Military Medical University, Shanghai, China). Overexpression of Smad7 was found in 54.3 % and 63.5 % of German and Chinese samples, respectively (not shown). Comprehensiveness of patient data was varying for the different patient samples. Hence, correlation analysis between Smad7 expression and different clinical data was only conducted for tumor size and cell differentiation. Tumor size was known for 103 patients, 55 from China and 48 from Germany (Figure 3.19), in which Smad7 was overexpressed at a lower frequency when compared to all samples: 47.9 % and 61.8 % instead of 54.3 % and 63.5 %, respectively. The samples were sorted in two groups, at which one contained samples with tumors sized bigger than 5 cm (largest dimension), while tumors smaller or equal to 5 cm were allocated to the second group. Interestingly, there was a strong difference in the Smad7 pattern in samples collected in China (Figure 3.18, left diagram), whereas in those from Germany, percentages of unchanged, elevated or decreased Smad7 were similar in the two groups. In Chinese samples, overexpression was found in only 38.1 % of small tumors but in a remarkable 76.5 % of large HCCs. This increase in overexpression was mainly at the expense of unmodified Smad7 levels. For Chi-Square analysis the samples within one group (small versus large tumor) were sorted in samples with or without Smad7 overexpression. Differences in the Chinese sample set turned out to be significant ($X^2 = 8.1$, $p = 0.004$). Hence, Smad7 overexpression significantly correlated with tumor size in Chinese but not German ($X^2 = 0.01$, $p = 0.91$) HCC tissue samples. In line with that, Smad7 overexpression in intrahepatic CCC from Germany strongly correlated to increasing tumor size ($r = 0.82$,

$p < 0.01$; data not shown). Correlation analysis between cell grading and Smad7 expression identified similar Smad7 expression patterns in well/moderately differentiated and poorly differentiated/undifferentiated HCC specimens of China as well as Germany ($X^2 = 0.47$, $p = 0.49$ and $X^2 = 0.03$, $p = 0.87$). Noteworthy, HCC in samples from Germany did not arise from HBV or HCV infection in most cases, whereas the broad majority of the Chinese samples were collected from patients with HBV infection (Table 3.1).

In summary, the evaluation of HCC patient samples from Germany and China show that Smad7 is frequently overexpressed in tumorigenic tissue with a strong correlation to increased tumor size in Chinese samples. This can possibly be ascribed to HBV infection as cancer etiology.

4 DISCUSSION

4.1 TGF-β signaling patterns in liver cancer cell lines

TGF-β is a well known inducer of growth arrest and apoptosis in various cell types, e.g., epithelial cells and hepatocytes [71, 123, 124], and, hence, a suppressor of tumor development in different cancer systems. Intriguingly, TGF-β was shown to exert protumorigenic functions in various tumors, including HCC (chapter 1.4). It is thought that neoplastic cells may develop different responses to this ambiguous role of TGF-β. The impairment of TGF-β signaling key components results in total inhibition of TGF-β signaling. Abrogation of components further downstream, however, may specifically amputate cytostatic TGF-β signaling while protumorigenic pathways are still functional.

In this study, nine different HCC cell lines (HCC-M, HCC-T, HepG2, Hep3B, HuH7, PLC/PRF/5, HLE and HLF) and the hepatoblastoma cell line HuH6 were analyzed with respect to integrity and functionality of TGF-β signaling, with a special focus on cytostatic effects of TGF-β (summarized in Figure 4.1, page 84).

4.1.1 Cytostatic TGF-β impact varies in HCC cell lines

The anti-tumorigenic character of TGF-β is frequently lost in cancers. TGF-β levels in serum are rising during progression of liver disease [236, 237]. Therefore, the cytostatic response of different HCC cell lines to continuous TGF-β stimulation was evaluated (Figure 3.1 and 3.2) and could be roughly assigned into two groups. TGF-β rapidly induced cell death and growth arrest in Hep3B, HuH7 and PLC/PRF/5, whereas HepG2 and HuH6 cells solely responded with a delayed inhibition of cell growth. Inhibition of proliferation was accompanied by repression of pro-proliferative c-Myc and induction of anti-proliferative p21. Moreover, TGF-β dependent cleavage of PARP and Caspase-3, and enhanced Bim expression (Figure 3.12) indicated an involvement of the apoptotic cascade in the observed induction of cell death. The second group consisted of cell lines which were resistant against TGF-β induced cytostasis: HCC-M, HCC-T, FLC-4, HLE and HLF. In two of these cell lines, TGF-β even exerted pro-proliferative (HCC-T) or anti-apoptotic (HCC-M) effects. In line with this, TGF-β was first identified as a growth factor which induces proliferation in mesenchymal cells [185]. Since then, tumors of epithelial origin were found to acquire this behavior in response to TGF-β [186, 239]. This emphasizes findings that cancer cells may use TGF-β for their own benefit, once the cytostatic TGF-β branch is disrupted.

TGF-β induces cell death and growth arrest in Hep3B, HuH7 and PLC/PRF/5 and inhibits proliferation in HepG2 cells.	[174, 187, 240-244]
HLE and HLF cells are resistant against TGF-β induced cytostasis	[242]
TGF-β enhances proliferation in HCC-M and HCC-T cells	[239]

Table 4.1 Publications regarding cytostatic TGF-β response in HCC cell lines used in this study.

The described TGF-β responses were already known for most cell lines and could be confirmed by the results of this study (Table 4.1). A notable exception was the HCC-M cell line, for which a weak pro-proliferative effect of TGF-β was described [239]. In contrast, the MMT assay used in this study suggested unaltered proliferation. Proliferation analysis using an LDH assay, however, indicated an increase of viable HCC-M cells to 108 % ($p = 0.016$, data not shown) after three days TGF-β treatment. HuH6 and FLC-4 are cell lines not well analyzed regarding their TGF-β response. To my knowledge, this is the first time that effects of TGF-β on proliferation and apoptosis were delineated in these two cell lines.

4.1.2 Contribution of canonical TGF-β signaling components to cytostatic response and conversion to a more malignant phenotype

TGF-β exerts its anti-tumorigenic functions via different canonical and non-canonical mechanisms. To identify possible underlying reasons for the observed resistances, a detailed dissection of canonical TGF-β signaling was performed.

4.1.2.1 TGF-β receptors

Mature TGF-β dimers activate canonical signaling through inducing the formation of a heteromeric receptor complex. Altogether, endogenous mRNA levels of TGF-β receptor II (TβRII) were elevated in liver cancer cell lines which were responsive to cytostatic effects of TGF-β (Figure 3.4). The second component of the receptor complex, TβRI, was characterized by a more stable basal expression. These results suggest that the quantity of TβRII may dictate the cell fate upon TGF-β treatment. In fact, hepatocyte proliferation in growing livers is enhanced in heterozygous TβRII knockout mice as compared to wild type animals. Further, the knockout animals are more responsive towards chemically induced liver cancerogenesis [245]. In line with that, TGF-β receptor levels increase in primary rat hepatocytes during culture, which correlates with a rising sensitivity towards growth inhibition by TGF-β [246].

The TβRII/TβRI mRNA ratio pointed out that basal TβRII expression was higher than that of TβRI in most HCC cell lines. Overall, this ratio was higher in cytostasis sensitive cell lines in comparison to resistant cells (Figure 3.4). TGF-β impact on TGF-β receptor expression created a totally different picture (Figure 3.6). Minor inhibition of TβRII expression was observed in most cell lines after stimulation with TGF-β, whereas TβRI mRNA levels were strongly increased in cell lines responding to TGF-β with cell death induction (Hep3B, HuH7, and PLC/PRF/5). Different TGF-β type I receptors compete for the same type II receptor. In the case of TβRII, TβRI (ALK5) is the main mediator of TGF-β signaling. However, ALK1, ALK2 and ALK3 are also able to interact with TGF-β activated TβRII, leading to phosphorylation of Smad1 and Smad5. This process, which is linked to proliferation, anchorage-independent growth and migration, is TβRI dependent and simultaneously leads to decreased TβRI signaling via Smad2 and Smad3 [21-24]. TGF-β induced Smad1 phosphorylation in all cell lines analyzed (Figure 3.11), suggesting an activation of a type I receptor other than TβRI. The observed induction of TβRI expression may therefore result in a higher probability of TβRI-TβRII-complex formation, possibly leading to higher susceptibility to TGF-β induced apoptosis and growth arrest. Conversely, low TβRII levels and unresponsiveness to TGF-β induced TβRI expression may provide protection against TGF-β induced cytostasis. The role of TβRI during hepatocarcinogenesis is still unsolved as conflicting findings have been described [243, 247]. In line with the result presented here, a reduction of TβRII levels is frequently found in HCC [158, 174, 243, 247], but mainly during advancing dedifferentiation [174], questioning its importance for establishing a resistance against cytostatic effects of TGF-β during early hepatocarcinogenesis. These observations coincide with the results presented here and elsewhere [174], in which the highest TβRII expression was observed in well differentiated cell lines (in this study: Hep3B, HepG2, PLC/PRF/5 and HuH7).

In conclusion, downregulation of TGF-β receptor II and inhibition of TGF-β dependent inducibility of TGF-β receptor I may protect HCC cell lines against cytostatic effects of TGF-β. A shift of TβRI towards other TGF-β type I receptors may provide a mechanism that directs TGF-β signaling towards tumorigenic effects.

4.1.2.2 TGF-β and Smad7

TGF-β1, according to current knowledge, is the main player of the three cytokine isoforms in the liver and initiates canonical signaling and cross-talk to other signaling pathways. Smad7 is able to counteract canonical TGF-β signaling at several levels (chapter 1.1.4.1) and to direct the effects of TGF-β in different directions (chapter 1.1.4.3). Therefore, basal Smad7

as well as autocrine TGF-β1 levels are important modulators of TGF-β signaling. Smad7 mRNA levels varied considerably between the ten different liver cancer cell lines but, interestingly, strongly correlated with TGF-β1 expression (Figure 3.3). Cell lines which were sensitive to TGF-β mediated cytostasis expressed comparably low Smad7 and TGF-β levels. In the group of resistant cell lines, only HCC-M and HCC-T showed similar low levels of TGF-β and Smad7. Those two cell lines took an exceptional position throughout almost the whole study, which will be discussed in detail in chapter 4.1.2.4. HuH6 cells with a moderate sensitivity to TGF-β induced growth arrest showed high Smad7 and TGF-β1 expression, but rather low amounts of mature TGF-β levels (Figure 3.17) in the medium. HuH6 cells are derived from a hepatoblastoma [225] and therefore, may behave differently from HCC cell lines. Low Smad7 levels in TGF-β sensitive cell lines suggest that Smad7 overexpression inhibits TGF-β induced cytostasis in HCCs. Indeed, protective effects of Smad7 against cytostatic TGF-β functions were shown in Hep3B and HuH7 cells [116, 241]. Once cytostatic effects of TGF-β are inhibited, cancer cells may benefit from tumorigenic TGF-β processes (chapter 1.4.1 and 1.4.2). In line with that, endogenous activation of latent TGF-β was by trend increased in HCC cell lines with an established resistance against TGF-β induced cytostasis (Figure 3.17). These findings suggest the following mechanism in HCC cell lines. Elevated Smad7 expression provides protection against cytostatic effects of TGF-β and hence allows increased activation of mature TGF-β. However, this enhanced turnover of TGF-β requires intensified production of the cytokine, which explains elevated TGF-β mRNA levels and the observed positive correlation to Smad7. In fact, elevated TGF-β levels is a common feature in various cancer entities [153-157], including HCC, in which malignant hepatocytes were identified as one source of TGF-β production [158, 159].

The amount of active TGF-β is increased in invasive HCC cell lines [192] and TGF-β serum levels in HCC patients correlate with invasiveness [248]. Further, autocrine TGF-β signaling was identified as important for increased cell motility, as a TβRI inhibitor (LY2109761, inhibits canonical and non-canonical signaling [249]) restores expression of E-cadherin and efficiently inhibits migration and invasion of HLE and HLF cells *in vitro* and metastasis of HLE cells *in vivo* [191, 250]. Consistently, the three HCC cell lines with a high migratory capacity (HLE, HLF and FLC-4, Figure 3.16) secreted the largest amounts of mature TGF-β within the TGF-β induced cytostasis resistant group. This motile phenotype was accompanied by low E-cadherin, high PAI-1 and Smad7 expression and high c-Jun activation. Interestingly, activation of the JNK pathway by TGF-β is Smad7 dependent and linked to TGF-β induced motility [81, 251] (further discussed in chapter 4.1.3.2). Further, PAI-1 and active c-Jun correlate with low grade differentiation and poor prognosis in human HCC, respectively [79, 252, 253], which is in agreement with the results presented here. Some immotile cell lines

showed high c-Jun activity as well, but no repression of E-cadherin. In contrast, HCC-M and HCC-T cells featured low levels of epithelial marker E-cadherin, but also of Smad7 and active c-Jun. Overall, the findings suggest that migratory capacity of HCC cell lines coincidences with repression of the epithelial marker E-cadherin and with enhanced levels of Smad7, active c-Jun and mesenchymal marker PAI-1. Interestingly, all those factors can directly or indirectly be regulated by TGF-β, which is in line with rather high levels of mature TGF-β in the supernatant of motile cells.

4.1.2.3 Receptor-Smads and Smad4

TGF-β induces phosphorylation and, thereby, activation of receptor (R-) Smads, which then form a transcription factor complex with Smad4. Analysis of R-Smad2 and 3, and common mediator Smad4 in HCC cell lines suggests that basal expression levels did not contribute to the observed differences in cytostatic TGF-β response (Figure 3.5). Smad2 and Smad4 mRNA and protein were equally distributed between the different cell lines. In contrast, Smad3 levels varied strongly but without any correlation to inducibility of cytostasis by TGF-β. TGF-β dependent induction of Smad3 expression, however, was exclusively found in cell lines which were sensitive towards TGF-β induced cytostasis, while mRNA levels of Smad2 and 4 remained unaltered (Figure 3.7 and 3.8). This indicates a higher relevance of Smad3 than Smad2 for cytostatic effects of TGF-β, which was confirmed using RNA interference technology in Hep3B, HuH7 and PLC/PRF/5 cells. TGF-β strongly induced cytostasis in these cell lines. Smad3, unlike Smad2, knockdown efficiently inhibited TGF-β induced cell death and partly restored the original proliferation rates. In agreement with this, Smad3, unlike Smad2, was identified as a main mediator of TGF-β induced apoptosis and growth arrest in hepatocytes and Hep3B cells [67, 128, 129]. Furthermore, Smad3 knock-down increases susceptibility to chemically induced liver tumors *in vivo*, probably due to protection against induction of cytostasis by elevated TGF-β levels in neoplastic areas [129]. Intriguingly, Smad3 mutations are not reported for HCC [254]. Smad2 mutations are detected in 5 % and, although reduced levels of Smad4 occur frequently, a depletion of Smad4 protein is observed in only 10 % of all HCCs [173, 255]. Accordingly, other mechanisms than R-Smad or Smad4 mutations likely contribute to the development of resistances against cytostatic effects of TGF-β (e.g., Smad7 overexpression, TβRII downregulation).

R-Smads are activated by phosphorylation at the C-terminus. TGF-β induced Smad2 activation was found in all cell lines (Figure 3.10 and 3.11), but with varying signal durations. Smad2 phosphorylation was by trend prolonged in cell lines with lower Smad7 expression and transient in cells with elevated Smad7 mRNA levels. This negative correlation between Smad7 and the duration of Smad2 activation suggests that Smad7 is able to not only inhibit

R-Smad activation, but also alter canonical TGF-β response by abbreviation of Smad2 activation. TGF-β signaling can be disrupted at various levels (chapter 1.1.4.3). Hence, it was of interest if the inducibility of R-Smads correlates with their transcriptional activity. TGF-β induced Smad2 transcriptional activity was high in some, but not all, cytostasis sensitive cell lines (HuH7, PLC/PRF/5 and HepG2). Contrarily, it was not inducible in resistant HCC-M, HCC-T and FLC-4 cells, but preliminary experiments suggest a high autocrine stimulation of Smad2 (but not Smad3) transcriptional activity (data not shown). TGF-β quickly induced Smad3 phosphorylation in all cell lines. Nevertheless, in contrast to Smad2, the signal duration was prolonged in most cell lines (Figure 3.11) and therefore did not correlate with the Smad7 expression. TGF-β induced Smad3 transcriptional activity, however, was highest in all cell lines sensitive to cytostatic effects of TGF-β, showing a better coincidence with inducibility of cytostasis than the one of Smad2. This is in line with the results of the Smad2/3 knockdown experiments (see above).

Functions of Smad2 and, especially, Smad3 dependent TGF-β signaling can be divergent and context dependent [128, 256-258], highlighting the necessity to carefully analyze each signaling branch in the HCC cell lines. In pancreatic cancer cells with TGF-β induced transient Smad2 activation, the cytostatic sensitivity is decreased as compared to cell lines with prolonged Smad2 signaling. This transient Smad2 response results in reduced effects of TGF-β on expression of cell cycle control proteins (e.g., induction of p21), while the TGF-β induced expression of other target genes, such as Smad7 and PAI-1, is not affected [259]. As discussed above, elevated basal Smad7 expression resulted in transient Smad2 activation by TGF-β, which was accompanied by resistance against cytostatic effects of TGF-β and reduced (but in most cases not depleted) Smad2 transcriptional activity in HCC cell lines. Similarly, TGF-β induced Smad3 transcriptional activity was reduced but seldom lost in those cell lines. Downregulation of TGF-β receptor II, as seen in various cancers, may not only interfere with the cytostatic TGF-β branch, but also with pro-tumorigenic signaling. Smad7, on the other hand, is not only an inhibitor of canonical signaling, but also an important scaffold protein for several non-canonical TGF-β pathways, which mostly exert protumorigenic effects (chapter 1.1.4 and 3.4.1). Hence, Smad7 overexpression could display a mechanism to attenuate a TGF-β signal below the threshold for cytostasis induction, while more sensitive or cross-talking pathways are still functional. This could be of importance as, for example, TGF-β induced Smad3 activity is not only linked to induction of cell death, but also to EMT in hepatocytes [128]. This hypothesis is supported by the fact that HCC cell lines with high Smad7 levels tended to a) express increased levels of TGF-β (Figure 3.3) and b) activate the latent cytokine at a higher rate (Figure 3.17Figure 3.17). These enhanced TGF-β levels could in turn be used to induce protumorigenic effects of

TGF-β (e.g., migration, see chapter above) in an autocrine manner via non-canonical but also via (not fully abrogated) canonical signaling pathways.

Taken together, the results discussed in chapter 4.1.2.2 and 4.1.2.3 indicate that attenuation of canonical TGF-β signaling may offer a protection against cytostatic effects of the cytokine, whereas other TGF-β features could remain functional. By this, TGF-β, which mainly acts as a tumor suppressor in normal epithelial cells, can be converted into a tumor promoter in cancers of epithelial origin. Interestingly, elevated TGF-β expression predominantly occurs in cell lines with a resistance against TGF-β induced cytostasis and coincides with high Smad7 levels, which may attenuate TGF-β signaling.

4.1.2.4 HCC-M and HCC-T – cell lines with a special TGF-β signature

Overall, the cell lines can be grouped in cells being responsive or resistant to TGF-β induced cytostasis, which is accompanied by specific features (overview and discussion in chapter 4.1.4). HCC-M and HCC-T cells, however, combined characteristics of both groups. They shared low Smad7 mRNA levels and a prolonged TGF-β induced activation of Smad2 with TGF-β sensitive HCC cell lines, but they were resistant against TGF-β mediated cytostasis and had many other similarities to cell lines expressing high levels of Smad7. For example, they expressed low levels of TβRII and were unresponsive to TGF-β mediated target gene induction (Smad3, PAI-1, Smad7 and TβRI), repression of c-Myc and induction of p21. Interestingly, out of all cell lines analyzed, only HCC-T and HCC-M cells showed even inverted effects of TGF-β in regard of cytostasis, as seen in increased proliferation in HCC-T and reduced basal cell death in HCC-M cells upon stimulation with TGF-β.

The outcome of a TGF-β signal can be dependent on the amount of TβRII (chapter 4.1.2.1). HCC-M and HCC-T expressed the lowest TβRII levels of all cell lines analyzed. Repression of TβRII, as alternative to overexpression of Smad7, possibly provides another mechanism to establish a resistance against cytostatic effects of TGF-β, which could result in a signal below the threshold for induction of cytostasis. However, TGF-β treatment led to prolonged phosphorylation of Smad2 and 3 (Figure 3.10 and 3.11), indicating a successful signal transmission into the cell. Both cell lines, nevertheless, were under the top three with the lowest TGF-β induced Smad2 and Smad3 transcriptional activity (Figure 3.10 and 3.11). Noteworthy, preliminary data suggest a high autocrine Smad2, but not Smad3 transcriptional activity (data not shown). These results imply a functional Smad2 pathway and, in contrast, aberrant Smad3 signaling, which is disrupted downstream of Smad3 activation. In line with that, TGF-β induced apoptosis of hepatocytes is linked to Smad3 [67]. The observed

resistance to TGF-β induced cell death in HCC-T and HCC-M cells may be related to a low ELF/PRAJA ratio (Figure 3.15). ELF assists with the nuclear translocation of Smad3, but has no impact on Smad2 signaling. Because PRAJA mediates proteasomal degradation of ELF and Smad3 (detailed discussion in chapter 4.1.3.3), low ELF and high PRAJA levels (low ratio) may result in reduced Smad3 signaling downstream of its activation, while Smad2 signaling is not affected.

4.1.3 Impact of cross-talk components and signaling regulators on TGF-β induced cytostasis

So far, besides direct modulations of TGF-β signaling components, various other mechanisms were identified that shed light on how cancer cells circumvent TGF-β induced anti-tumorigenic effects. The following chapters will discuss a potential involvement of those mechanisms in the analyzed HCC cell lines.

4.1.3.1 Bcl-2 family and p21 – proteins with direct impact on cell survival and proliferation

The Bcl-2 family consists of pro- (e.g., Bim) and anti-apoptotic (e.g., Bcl-2 and Bcl-XL) family members, and the balance between those two groups can decide cell fate. Endogenous levels of anti-apoptotic Bcl-XL did not correlated with inducibility of apoptosis by TGF-β in the liver cancer cell lines analyzed. Surprisingly, anti-apoptotic Bcl-2 was by trend higher expressed in cell lines sensitive towards TGF-β mediated cell death. However, TGF-β decreases Bcl-2 and Bcl-XL levels during induction of apoptosis in hepatocytes, while expression of pro-apoptotic Bim is increased [71, 130]. Similarly, TGF-β strongly enhanced Bim expression in HCC cell lines responsive to TGF-β induced cell death (Figure 3.12), which probably contributes to switch the balance from survival towards cell death.

Expression of p21, an inhibitor of the cell cycle, is induced during TGF-β mediated growth arrest [34, 36, 135]. In contrast, c-Myc usually exerts pro-proliferative functions and may be downregulated by TGF-β [137, 138]. Smad7 inhibits basal and TGF-β induced p21 expression and has opposing effects on c-Myc in human adenocarcinoma cell lines [235]. Accordingly, HCC cell lines with a responsiveness to TGF-β mediated regulation of c-Myc and p21 (Figure 3.1) expressed, in general, low Smad7 levels (Figure 3.3). Furthermore, except for PLC/PRF/5 and HuH6 cells, basal p21 protein levels were high in cell lines with decreased Smad7 amounts (Figure 3.13). This is in line with the described suppressive effects of Smad7 on p21 and on TGF-β induced growth arrest.

4.1.3.2 The TGF-β-MAPK- and Akt-axis

Next to Smad dependent signaling, TGF-β utilizes various non-canonical signaling cascades, including several survival pathways, in a cell type and circumstance dependent manner (chapter 1.1.3).

Cross-talk with the Ras-Raf-MEK-ERK pathway

Cross-talk of TGF-β with ERK signaling is well recognized and is involved in EMT, migration and invasion of various normal and (epithelial) cancer cells [62, 63, 251, 260]. In human HCC, MEK1/2 (MKK1/2) and ERK expression and phosphorylation are linked to proliferation and disease progression [261, 262]. Furthermore, hyperactive Ras activates ERK and thus inhibits TGF-β induced cytostasis in immortalized hepatocytes, while the EMT process remains functional and is even enhanced [263]. In the liver cancer cell lines analyzed, endogenous ERK phosphorylation increased with rising Smad7 mRNA levels and was well detectable in motile and TGF-β induced cytostasis resistant HLE, HLF and FLC-4 cells (Figure 3.13). However, similar activity was also found in TGF-β sensitive Hep3B, HuH7 and HuH6 cells. Interestingly, EGF receptor HER2, via Ras-Raf-ERK, is able to induce Smad7 expression in different cancer cell lines [109]. Even though HER2 overexpression is seldom found in HCC [264, 265], these publications demonstrate a possible impact of ERK on Smad7 levels. ERK hyperactivity is found in 39-100 % of all HCCs, especially in those related to HBV or HCV [180, 252, 261, 262, 266, 267]. Interestingly, TGF-β itself is able to induce ERK activity [59-61]. In the analyzed HCC cell lines, TGF-β1 expression correlated with Smad7 expression and, by trend, survival. Furthermore, ERK activation was increased in cell lines with enhanced Smad7 expression. Hence, it would be interesting to analyze if enhanced Smad7 expression in the HCC cell lines can be ascribed to increased ERK activity, and if the high TGF-β expression itself contributes to this by induction of ERK.

The TAK1-MKK-JNK pathway

Except for the hepatoblastoma cell line HuH6, amounts of activated c-Jun were also increased in cell lines with elevated Smad7 expression (Figure 3.13). TGF-β induces MAPK JNK, an upstream signaling component of c-Jun, in epithelial and mesenchymal cells [65, 67]. Interestingly, Smad7 is probably an important scaffold protein, which facilitates the interaction of TβRI with upstream components (TRAF6-TAK1-MKK) of JNK and c-Jun [68] (chapter1.1.4.3). This possibly explains the elevated c-Jun activation in HCC cell lines with high Smad7 expression. Smad7 overexpression in the well differentiated colon adenocarcinoma cell line FET results in a more malignant and faster growing phenotype *in vivo*. This is accompanied by basal c-Jun phosphorylation, which is further enhanced by TGF-β treatment. Simultaneously, growth limiting TGF-β signaling is repressed [235].

Similarly, JNK is crucial for TGF-β induced breast cancer cell motility *in vitro* [251]. Positive phospho-c-Jun staining is found in human HCC and its intensity is increasing during dedifferentiation [252]. Other potentially pro-tumorigenic effects of c-Jun in the liver were discovered in mice, as seen in reduced proliferation, increased apoptosis and impaired liver regeneration after knockdown of c-Jun in hepatocytes [268]. Consistently, high c-Jun phosphorylation and Smad7 and TGF-β1 expression were detected in HCC cell lines with a high migratory capacity and resistance against cytostatic effects of TGF-β (Figure 3.16). However, similar c-Jun activation was also observed in some cytostasis sensitive cell lines. c-Jun is a component of stress response pathways and hence, has been linked to anti-tumorigenic effects as well. Smad7 is able to induce c-Jun activity in epithelial kidney and lung cell lines, which is linked to increased apoptosis after serum starvation [114]. Hence, the cross-talk between TGF-β/Smad7 and JNK is context dependent, which possibly explains the hyperactivity of c-Jun found in both, Smad7 overexpressing cell lines insensitive and responsive to TGF-β induced cell death.

R-Smad linker phosphorylation by ERK and JNK signaling pathways

As discussed above, TGF-β may impact ERK and JNK signaling. Intriguingly, those pathways are in turn able to directly modify Smad activity by phosphorylation of specific sides within the Smad linker regions (chapter 1.1.3). EGF stimulation, for example, leads to the phosphorylation of ERK consensus sites and results in retention of Smad2 and 3 in the cytoplasm [78]. During HCV related liver disease progression in patients, TGF-β signaling is switched from C-terminal to JNK-dependent linker phosphorylation of Smad3. Furthermore, patients with fibrosis carry a higher risk to suffer from cancer if this Smad3 linker phosphorylation is elevated. Inhibition of JNK activity interferes with TGF-β induced Smad3 linker phosphorylation and invasion in primary hepatocytes. In parallel, the growth limiting TGF-β branch (C-terminal Smad3 phosphorylation and p21 induction) remains functional and its activity is even enhanced after inhibition of JNK [81]. Similar findings were made in HBV related liver disease progression [82]. These observations suggest that canonical TGF-β signaling does not only suffer from a shift towards non-canonical signaling, but that this shift may result in an additional interference with (ERK) or modification of (JNK) R-Smad signaling. Hence, to fully delineate R-Smad signaling in the used liver cancer cell lines, an analysis of linker phosphorylation and the contribution of JNK and ERK, but also of TGF-β itself is indispensable.

The PI3K/Akt signaling pathway

TGF-β modulates Akt signaling in certain contexts. In several cell types, TGF-β stimulates Akt activity, resulting in enhanced survival and induction of proliferation and EMT [69-72]. In

contrast, in cells in which the cytostatic TGF-β branch dominates, TGF-β induced apoptosis is accompanied by inhibition of Akt activation [73, 74]. Hepatocytes cultured on a stiff matrix are characterized by fast dedifferentiation and decreased TGF-β induced apoptosis when compared to well differentiated hepatocytes cultured between two soft collagen layers (collagen sandwich). This reduced sensitivity to cytostatic effects of TGF-β can be attributed to enhanced basal and TGF-β induced Akt phosphorylation [71]. Consistently, Akt is overexpressed and hyperactive in HCC [179, 180]. Akt interacts with Smad3 and interferes with its phosphorylation and thus activation. TGF-β, in turn, inhibits the formation of the Akt-Smad3 complex. Hence, the ratio between Akt and Smad3 may determine the sensitivity or resistance against TGF-β induced cell death [177, 178]. Comparison of the different HCC cell lines showed that basal Akt protein levels were rather stable while Smad3 levels varied, although without any correlation to the cytostatic TGF-β response. However, Smad3 expression and transcriptional activity was elevated by TGF-β in cell death sensitive cells lines (Figure 3.13), which may result in an additional shift of the Akt/Smad3 towards functional Smad3. This is coherent with an observation that introduction of Akt into Hep3B cells inhibits TGF-β induced apoptosis [176].

4.1.3.3 PRAJA and ELF as regulators of Smad3 distribution

ELF and PRAJA offer another explanation for different intensities of TGF-β induced Smad3 dependent cytostasis despite universal activation of Smad3. ELF interacts with Smad3 and escorts the active Smad3/Smad4 complex into the nucleus [182]. ELF is underrepresented in human HCCs. Furthermore, heterozygous ELF knockout mice spontaneously develop HCC [184]. E3 ligase PRAJA TGF-β dependently interacts with ELF and initiates ubiquitination and degradation of ELF and Smad3. The grade of degradation and, thus, interference with Smad3 signaling is dependent on the amount of PRAJA [183], suggesting that the ELF/PRAJA ratio may define the fate of a cell upon TGF-β stimulation. During liver regeneration, reduced ELF and increased PRAJA levels facilitate hepatocyte proliferation due to interference with growth limiting effects of TGF-β. Consistently, ELF siRNA interferes with TGF-β induced growth arrest and apoptosis in the hepatocyte cell line AML-12 [183, 269]. ELF expression strongly varied between the different HCC cell lines analyzed (Figure 3.15). In agreement with the discussed publications, five out of six liver cancer cell lines with the highest ELF/PRAJA ratio showed responsiveness to TGF-β induced cell death or growth arrest. Interestingly, PRAJA is neither able to interact with Smad2 nor to induce degradation of Smad2 or Smad4 [182, 183]. The different roles of Smad2 and Smad3 during hepatocarcinogenesis are, until now, not fully understood. However, Smad3 seems to be the main mediator of TGF-β induced cytostasis in hepatocytes and in the cell lines analyzed (see

chapter 4.1.2.3). A shift of the ELF/PRAJA balance towards PRAJA offers a mechanism to specifically attenuate or shut down (dependent on the ELF/PRAJA ratio) Smad3 signaling, while the Smad2 pathway remains functional. Both Smad2 and Smad3 have been linked to tumor progression in various cancers (chapter 4.1.2.3). Hence, further studies are needed to investigate the role of both R-Smads during liver cancer initiation and progression and if, e.g., an attenuation of Smad3 signaling (as observed in this study; Figure 3.11) instead of a complete disruption not only inhibits cytostatic effects of TGF-β, but in parallel allows pro-tumorigenic effects.

In conclusion, TGF-β develops complex cross-talking networks with various pathways in a cellular and context dependent manner. An acquisition of resistance against cytostatic effects of TGF-β is a common feature of tumorigenesis. One possible mechanism to establish such resistance is a reduction of ELF levels, leading to attenuated Smad3 signaling. Another frequent observation is a shift from canonical, with often anti-tumorigenic functionalities, to non-canonical TGF-β signaling (ERK, JNK), which usually exerts tumor-promoting tasks. Elevated Smad7 levels possibly contribute to this rearrangement of TGF-β signaling. The final outcome of TGF-β in HCC cell lines likely depends on the balance of the different pathways, which complicates interpretation of the results.

4.1.4 Clustering of HCC cell lines based on cytostatic TGF-β response

As discussed above, TGF-β may exert ambiguous functions during hepatocarcinogenesis. In HCC, a resistance against anti-tumorigenic effects of TGF-β is frequently developed, while pro-tumorigenic functions are preserved. This results in a switch of TGF-β from a tumor suppressor to a potential tumor promoter.

This study extends a first characterization of early and late TGF-β signatures in HCC [270] and offers an in-depth analysis of nine HCC and one hepatoblastoma cell lines regarding basal and induced TGF-β signaling and its impact on cell death and proliferation. The results are summarized in Figure 4.1 and suggest that the HCC cell lines can be in sorted into three groups.

Group I: Responsiveness to TGF-β induced cytostasis

The first group consists of HepG2, PLC/PRF/5, Hep3B and HuH7 cells. All cell lines were sensitive to TGF-β induced growth arrest and, except for HepG2, cell death. This phenotype was in general accompanied by relatively low endogenous TGF-β1 and Smad7 expression

but high mRNA levels of its type II receptor (TβRII). TGF-β stimulation resulted in a) induction of TβRI and Smad3 expression, b) by trend, prolonged Smad2 phosphorylation, c) enhanced Smad3/4 transcriptional activity and d) induction of TGF-β target gene expression (Smad7, PAI-1, Bim). Interestingly, all cell lines of this group have been reported to belong to the group of HCC cell lines expressing early TGF-β-responsive genes (early TGF-β signature), which correlated with a better prognosis in HCC patients [270].

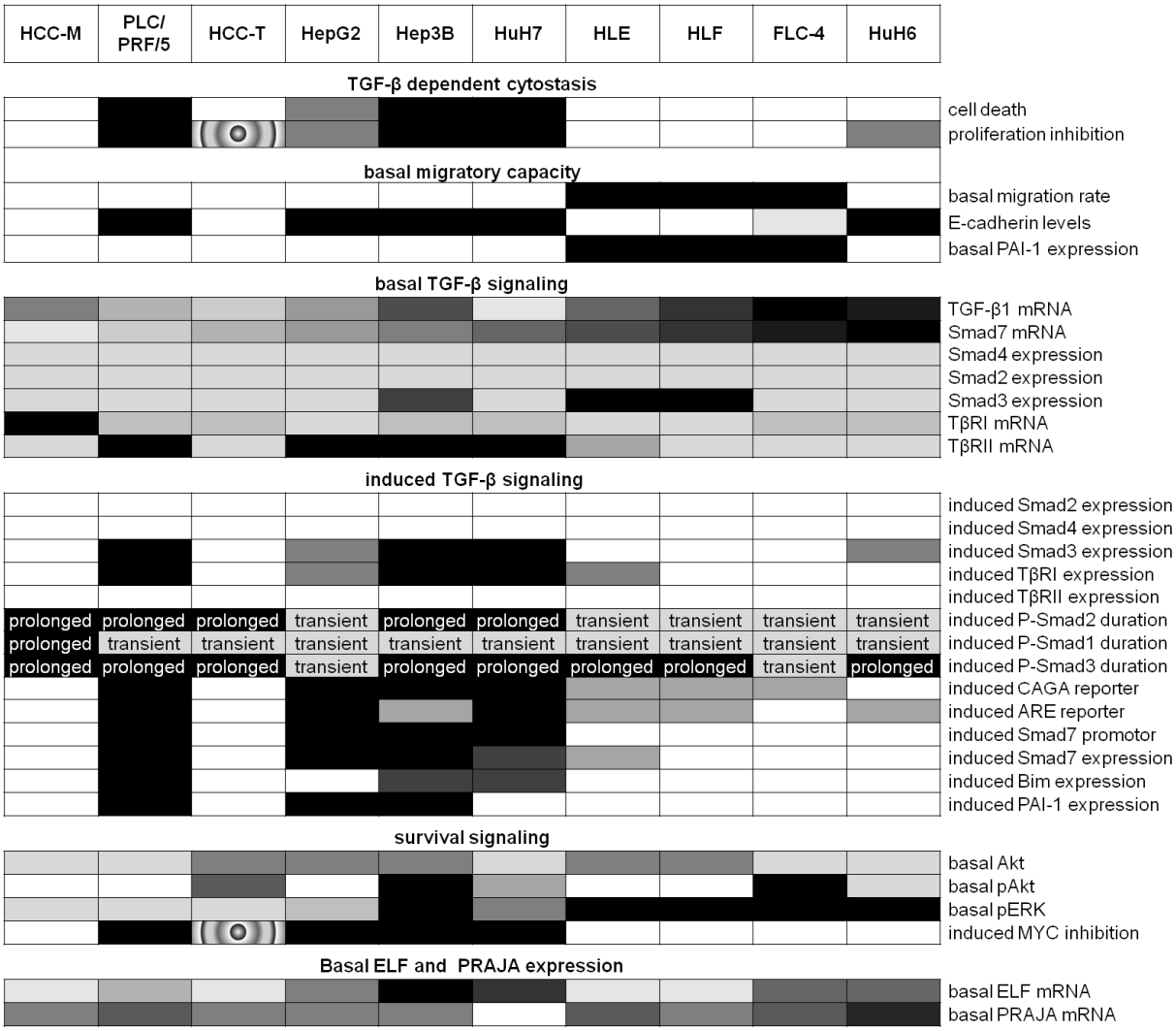

Figure 4.1 Overview of endogenous expression levels and responses to TGF-β stimulation in liver cancer cell lines. (TGF-β dependent cytostasis, basal migratory capacity, induced TGF-β signaling and inhibition of c-Myc expression) The darker the field, the stronger the reaction, or as in the case of proliferation, the earlier the observed TGF-β mediated reaction emerged. Patterned fields highlight cell lines in which TGF-β resulted in opposite effects compared to the other cell lines. (Basal TGF-β signaling, survival signaling and ELF and PRAJA expression) The different gray scales represent different basal expression levels with increasing darkness for higher expression.

Group II: Resistance against cytostatic effects of TGF-β

The second group, consisting of HLE, HLF, FLC-4 and to some extent HuH6, exhibited contrary behavior. Except for a delayed inhibition of proliferation in HuH6 cells, TGF-β was

unable to initiate any cytostatic responses. Furthermore, those cell lines expressed relatively high levels of TGF-β1 and Smad7 but low levels of TβRII when compared to group I. TGF-β treatment a) induced only short-term (transient) phosphorylation of Smad2, b) resulted in relatively low induction of Smad2 or Smad3 transcriptional activity and c) failed to intensively induce TβRI expression and target genes such as Smad7, PAI-1 or Bim. Further basal ERK activation was increased when compared to group I and, except for HuH6, cell lines of this group had a high migratory capacity, which was accompanied by low E-cadherin and high basal PAI-1 expression and c-Jun activation. The special position of HuH6 in this group might be explained by the different origin (hepatoblastoma). Furthermore, HLE and HLF cells are assigned to the subgroup with a late TGF-β signature, which correlated with higher basal invasion (in line with the migrative phenotype observed in this thesis) and poorer prognosis [270]. The cell line FLC-4 probably belongs to the same group as its behavior coincided with HLE and HLF cells. HuH6 was described as a cell line expressing early TGF-β-responsive genes [270], which could be another explanation for the outlying behavior of these cells.

Group III: HCC-M and HCC-T cells

Figure 4.1 further highlights that HCC-M and HCC-T cells exhibited outlying behavior, possessing characteristics of both groups described above. Like cell lines from group II, they had low levels of TβRII and were completely resistant against TGF-β induced cytostasis, whereas they expressed similar low levels of Smad7 and TGF-β1 to TGF-β sensitive cell lines (group I). Compared to sensitive cell lines from the first group, TGF-β1 mediated induction of a) Smad3 or TβRI expression, b) Smad3 or Smad2 transcriptional activity and c) TGF-β target genes was strongly reduced, just as in group II.

The impression, that the cell lines can be divided into three groups, two main groups and HCC-M and HCC-T cells, was confirmed by a hierarchical cluster analysis, which integrated all findings in regard to TGF-β signaling, its cytostatic effects and regulation (Figure 4.2, kindly provided by Dr. Coulouarn, INSERM, UMR991, University of Rennes 1, Pontchaillou University Hospital, Rennes, France).

HCC cell lines are an extensively used tool in liver cancer research. However, due to the diversity of different HCC cell lines, many contrary results on cellular processes and underlying mechanisms have been published so far. The results of this study will help to deepen the understanding of human hepatocarcinogenesis in regard of cytostatic TGF-β signaling and the frequently occurring shift from anti- to pro-tumorigenic effects of TGF-β. It offers an itemized and comparative description of the role of TGF-β signaling components during different cellular cytostatic TGF-β responses. This facilitates the correct choice of cell lines to analyze specific aspects of HCC initiation and progression.

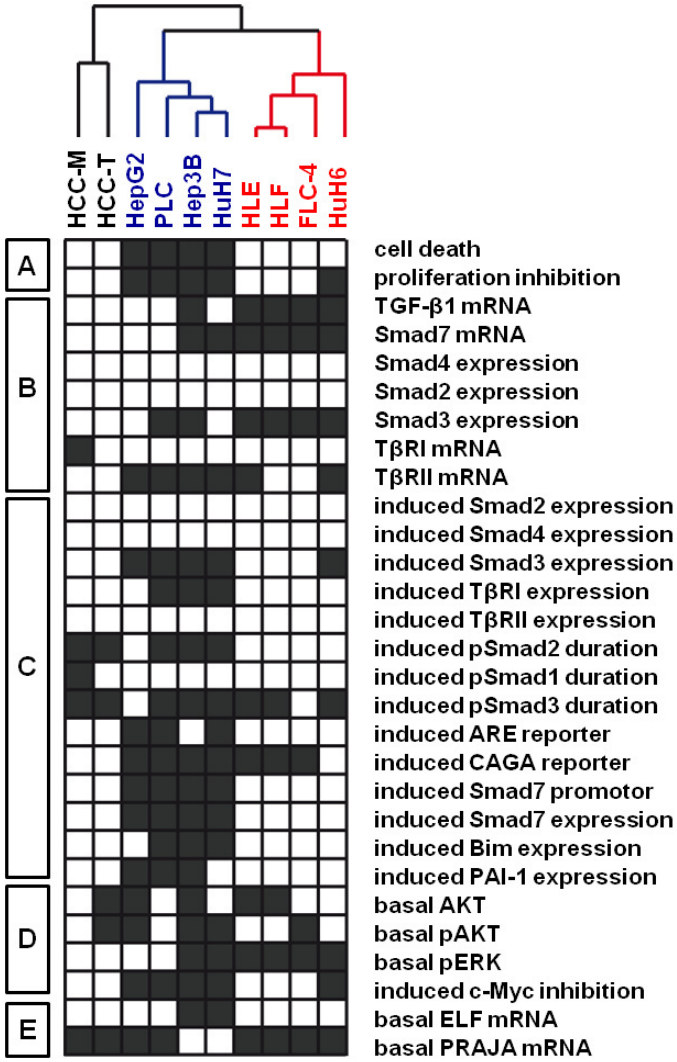

Figure 4.2 **Hierarchical clustering analysis of liver cancer cell lines regarding TGF-β signaling and cytostatic response.** Cytostatic TGF-β signaling related findings of this study (overview in Figure 4.1) in one hepatoblastoma and 9 HCC cell lines were converted into an all-or-none fashion (black/white) to generate a matrix, which was then structured using a hierarchical clustering algorithm. Like in Figure 4.1, the different observations were assembled as followed (left side): (A) TGF-β induced cytostasis (black: cell death > 5 %, growth inhibition > 50 %), (B) basal TGF-β signaling (black: rel. expression ($2^{-\Delta\Delta Ct}$) > 2.5 for all, but > 4 for Smad3), (C) induced TGF-β signaling (black: rel. induction of expression ($2^{-\Delta\Delta Ct}$) > 2, induction of CAGA and Smad7 promoter and expression > 2.8, induction of ARE reporter > 5, prolonged Smad phosphorylation), (D) survival signaling (black: increased or decreased (c-Myc) immunoblot signal), (E) basal ELF and PRAJA expression (black: rel. expression ($2^{-\Delta\Delta Ct}$) > 6 (ELF) or > 1.2 (PRAJA)). Clustering analysis was performed by using Cluster 3.0 software and the data were further visualized with TreeView 1.6 [270].

HCC is one of the most common and deadliest cancers worldwide with, until now, limited treatment options. Hence, new therapeutic approaches are urgently needed. Targeting TGF-β signaling is not only in constant discussion for treatment strategies against HCC, but also against other liver diseases such as fibrosis or cirrhosis. The described ambiguous functionality of TGF-β, however, strongly complicates development of reliable therapies, which therefore requires an exact knowledge about the time point of the switch from anti- to

pro-tumorigenic TGF-β features. The results of this PhD thesis highlight different possible mechanisms of resistance against cytostatic effects of TGF-β, which might need different therapeutic targeting. Hence, the study offers for the first time the possibility of a systematic assortment of cell lines as investigation tools. Once pro-tumorigenic TGF-β functionality is carefully deciphered as well, the cell lines can be sorted into groups of different TGF-β signature. Hopefully, this knowledge will then help to test new therapeutic strategies in the different cell lines in order to identify suitable, but also to exclude risky, approaches for the different groups.

4.2 Smad7, a potential oncogene in liver cancer samples

Aberrations of Smad2 and 4 are frequently found in different cancers (chapter 1.4.2). In contrast, basal Smad2, Smad3 (unlike induced) and Smad4 levels did not contribute to different cytostatic TGF-β responsiveness in HCC cell lines, and alterations of the proteins play minor roles in human HCC (chapter 4.1.2.1). TβRII reduction, on the other hand, was found in a subset of 25 % - 50 % of HCCs [174, 181]. However, this occurred during loss of differentiation, suggesting that it is a rather late event during hepatocarcinogenesis. TβRII is a key component for canonical, but also for non-canonical TGF-β signaling. Hence, deletion of TβRII possibly shuts down both, cytostatic and protumorigenic TGF-β signaling. As TGF-β is frequently over-presented in HCC tissue [158, 159, 236, 237], it is likely that other strategies can be found in HCC, which include functional pro-tumorigenic but defective anti-tumorigenic TGF-β signaling.

Smad7 is a potent inhibitor of TGF-β signaling and is able to exert its functions at different levels of the TGF-β signaling cascade (chapter 1.1.4.1). In parallel, it may interact with several other pathways (chapter 1.1.4.3). The results from the 10 different liver cancer cell lines suggest that Smad7 could be involved in developing a resistance against TGF-β mediated cytostatic effects (chapter 4.1.2.2). In line with that, Smad7 is involved in cancerogenesis of various tumors (chapter 1.4.3). Mostly, elevated Smad7 levels are linked to tumor progression and eventually correlate with increased tumor size, higher malignancy or poorer prognosis [208-216, 218-220] . Opposite findings were demonstrated for a few tumor species, in which Smad7 exerted protective effects in human patient samples or in murine cancer models [120, 206, 207, 217]. Analysis of a limited number of human HCC specimens suggests overexpression of Smad7 in HCC. Immunhistochemical analysis showed positive staining for Smad7 in 64 % of HCCs and in only 36 % of adjacent tissues [159]. In another study, Smad7 protein was present in 61 % of advanced HBV related HCCs

(but not in dysplastic nodules) with no significant differences between tumor size, differentiation or vascular invasion. Interestingly, reduced TGF-β receptor II mRNA levels predominantly occurred in HCCs with no detectable Smad7 levels [181], underlining the hypothesis of two alternative mechanisms to develop resistance against cytostatic TGF-β signaling. Independent of the endogenous Smad7 expression, TβRII mRNA levels were reduced in all TGF-β resistant HCC cell lines when compared to the sensitive ones (Figure 3.4). However, in agreement with the results presented by Park et al [181], this reduction was lowest in HCC-M and HCC-T cells with very low Smad7 mRNA levels. To confirm the relevance of Smad7 during hepatocarcinogenesis, an expression analysis of 133 HCCs and matched non-tumorigenic liver tissues from Germany and China was performed. Smad7 was overexpressed in 59 % of all HCCs (Figure 3.18), with a modestly higher frequency in samples collected in China when compared to those from Germany. Unlike Park et al., we found a significant ($p = 0.004$) correlation between Smad7 and increasing tumor size in samples from China, whereas no differences were found in tissues from Germany. Chinese samples mainly derived from patients with HBV infection, just as in the cohort of Park et al., while tissues collected in Germany were mostly hepatitis negative. The discussed *in vitro* data demonstrate that TGF-β signaling outcome is not only dependent on the expression signature of its signaling components, but also on various cross-talks with other pathways. HBV and HCV related HCC, for example, is linked to activated ERK [180, 262, 266, 267], which is known to enhance Smad7 [109]. Hence, a comparative analysis of different TGF-β cross-talk pathways and Smad7 expression in HCC would be interesting. Furthermore, it should be evaluated if Smad7 and HBV exert synergistic effects on proliferation. Another *in vitro* finding was that highly motile HCC cell lines showed increased Smad7 expression. Unfortunately, clinicopathological information was too limited to perform a reliable correlation analysis between Smad7 expression and metastasis. Therefore, no further conclusions can be drawn if the *in vitro* data can be transferred to the *in vivo* situation.

Taken together, the patient data and the results for the HCC cell lines suggest tumor promoting functions of Smad7 during hepatocarcinogenesis. Whether those are limited to inhibition of cytostatic effects of TGF-β or whether Smad7 exerts additional pro-tumorigenic effects remains to be analyzed.

REFERENCES

1. Heldin CH, Landstrom M, Moustakas A. Mechanism of TGF-beta signaling to growth arrest, apoptosis, and epithelial-mesenchymal transition. *Curr Opin Cell Biol* 2009,**21**:166-76.
2. Yan X, Chen YG. Smad7: not only a regulator, but also a cross-talk mediator of TGF-beta signalling. *Biochem J* 2011,**434**:1-10.
3. ten Dijke P, Arthur HM. Extracellular control of TGFbeta signalling in vascular development and disease. *Nat Rev Mol Cell Biol* 2007,**8**:857-69.
4. Derynck R, Jarrett JA, Chen EY*, et al.* Human transforming growth factor-beta complementary DNA sequence and expression in normal and transformed cells. *Nature* 1985,**316**:701-5.
5. Gentry LE, Lioubin MN, Purchio AF, Marquardt H. Molecular events in the processing of recombinant type 1 pre-pro-transforming growth factor beta to the mature polypeptide. *Mol Cell Biol* 1988,**8**:4162-8.
6. Miyazono K, Hellman U, Wernstedt C, Heldin CH. Latent high molecular weight complex of transforming growth factor beta 1. Purification from human platelets and structural characterization. *J Biol Chem* 1988,**263**:6407-15.
7. Wakefield LM, Smith DM, Flanders KC, Sporn MB. Latent transforming growth factor-beta from human platelets. A high molecular weight complex containing precursor sequences. *J Biol Chem* 1988,**263**:7646-54.
8. Saharinen J, Taipale J, Keski-Oja J. Association of the small latent transforming growth factor-beta with an eight cysteine repeat of its binding protein LTBP-1. *EMBO J* 1996,**15**:245-53.
9. Miyazono K, Olofsson A, Colosetti P, Heldin CH. A role of the latent TGF-beta 1-binding protein in the assembly and secretion of TGF-beta 1. *EMBO J* 1991,**10**:1091-101.
10. Sato Y, Rifkin DB. Inhibition of endothelial cell movement by pericytes and smooth muscle cells: activation of a latent transforming growth factor-beta 1-like molecule by plasmin during co-culture. *J Cell Biol* 1989,**109**:309-15.
11. Schultz-Cherry S, Murphy-Ullrich JE. Thrombospondin causes activation of latent transforming growth factor-beta secreted by endothelial cells by a novel mechanism. *J Cell Biol* 1993,**122**:923-32.
12. Munger JS, Huang X, Kawakatsu H*, et al.* The integrin alpha v beta 6 binds and activates latent TGF beta 1: a mechanism for regulating pulmonary inflammation and fibrosis. *Cell* 1999,**96**:319-28.
13. Mu D, Cambier S, Fjellbirkeland L*, et al.* The integrin alpha(v)beta8 mediates epithelial homeostasis through MT1-MMP-dependent activation of TGF-beta1. *J Cell Biol* 2002,**157**:493-507.
14. Lawrence DA, Pircher R, Kryceve-Martinerie C, Jullien P. Normal embryo fibroblasts release transforming growth factors in a latent form. *J Cell Physiol* 1984,**121**:184-8.
15. Groppe J, Hinck CS, Samavarchi-Tehrani P*, et al.* Cooperative assembly of TGF-beta superfamily signaling complexes is mediated by two disparate mechanisms and distinct modes of receptor binding. *Mol Cell* 2008,**29**:157-68.
16. Wrana JL, Attisano L, Carcamo J*, et al.* TGF beta signals through a heteromeric protein kinase receptor complex. *Cell* 1992,**71**:1003-14.
17. Wrana JL, Attisano L, Wieser R*, et al.* Mechanism of activation of the TGF-beta receptor. *Nature* 1994,**370**:341-7.
18. Feng XH, Derynck R. Specificity and versatility in tgf-beta signaling through Smads. *Annu Rev Cell Dev Biol* 2005,**21**:659-93.

19. Shi Y, Massague J. Mechanisms of TGF-beta signaling from cell membrane to the nucleus. *Cell* 2003,**113**:685-700.
20. ten Dijke P, Yamashita H, Ichijo H*, et al.* Characterization of type I receptors for transforming growth factor-beta and activin. *Science* 1994,**264**:101-4.
21. Goumans MJ, Valdimarsdottir G, Itoh S*, et al.* Balancing the activation state of the endothelium via two distinct TGF-beta type I receptors. *EMBO J* 2002,**21**:1743-53.
22. Oh SP, Seki T, Goss KA*, et al.* Activin receptor-like kinase 1 modulates transforming growth factor-beta 1 signaling in the regulation of angiogenesis. *Proc Natl Acad Sci U S A* 2000,**97**:2626-31.
23. Daly AC, Randall RA, Hill CS. Transforming growth factor beta-induced Smad1/5 phosphorylation in epithelial cells is mediated by novel receptor complexes and is essential for anchorage-independent growth. *Mol Cell Biol* 2008,**28**:6889-902.
24. Goumans MJ, Valdimarsdottir G, Itoh S*, et al.* Activin receptor-like kinase (ALK)1 is an antagonistic mediator of lateral TGFbeta/ALK5 signaling. *Mol Cell* 2003,**12**:817-28.
25. Heldin CH, Moustakas A. Role of Smads in TGFbeta signaling. *Cell Tissue Res* 2012,**347**:21-36.
26. Wrana JL, Attisano L. MAD-related proteins in TGF-beta signalling. *Trends Genet* 1996,**12**:493-6.
27. Shi Y, Wang YF, Jayaraman L*, et al.* Crystal structure of a Smad MH1 domain bound to DNA: insights on DNA binding in TGF-beta signaling. *Cell* 1998,**94**:585-94.
28. Macias-Silva M, Abdollah S, Hoodless PA*, et al.* MADR2 is a substrate of the TGFbeta receptor and its phosphorylation is required for nuclear accumulation and signaling. *Cell* 1996,**87**:1215-24.
29. Chacko BM, Qin BY, Tiwari A*, et al.* Structural basis of heteromeric smad protein assembly in TGF-beta signaling. *Mol Cell* 2004,**15**:813-23.
30. Akhurst RJ, Hata A. Targeting the TGFbeta signalling pathway in disease. *Nat Rev Drug Discov* 2012,**11**:790-811.
31. Dennler S, Itoh S, Vivien D*, et al.* Direct binding of Smad3 and Smad4 to critical TGF beta-inducible elements in the promoter of human plasminogen activator inhibitor-type 1 gene. *EMBO J* 1998,**17**:3091-100.
32. Zawel L, Dai JL, Buckhaults P*, et al.* Human Smad3 and Smad4 are sequence-specific transcription activators. *Mol Cell* 1998,**1**:611-7.
33. Chen X, Weisberg E, Fridmacher V*, et al.* Smad4 and FAST-1 in the assembly of activin-responsive factor. *Nature* 1997,**389**:85-9.
34. Seoane J, Le HV, Shen L*, et al.* Integration of Smad and forkhead pathways in the control of neuroepithelial and glioblastoma cell proliferation. *Cell* 2004,**117**:211-23.
35. Feng XH, Lin X, Derynck R. Smad2, Smad3 and Smad4 cooperate with Sp1 to induce p15(Ink4B) transcription in response to TGF-beta. *EMBO J* 2000,**19**:5178-93.
36. Pardali K, Kurisaki A, Moren A*, et al.* Role of Smad proteins and transcription factor Sp1 in p21(Waf1/Cip1) regulation by transforming growth factor-beta. *J Biol Chem* 2000,**275**:29244-56.
37. Stopa M, Anhuf D, Terstegen L*, et al.* Participation of Smad2, Smad3, and Smad4 in transforming growth factor beta (TGF-beta)-induced activation of Smad7. THE TGF-beta response element of the promoter requires functional Smad binding element and E-box sequences for transcriptional regulation. *J Biol Chem* 2000,**275**:29308-17.
38. Higashi K, Inagaki Y, Fujimori K*, et al.* Interferon-gamma interferes with transforming growth factor-beta signaling through direct interaction of YB-1 with Smad3. *J Biol Chem* 2003,**278**:43470-9.
39. Massague J, Seoane J, Wotton D. Smad transcription factors. *Genes Dev* 2005,**19**:2783-810.

40. Chen CR, Kang Y, Siegel PM, Massague J. E2F4/5 and p107 as Smad cofactors linking the TGFbeta receptor to c-myc repression. *Cell* 2002,**110**:19-32.

41. Frederick JP, Liberati NT, Waddell DS*, et al.* Transforming growth factor beta-mediated transcriptional repression of c-myc is dependent on direct binding of Smad3 to a novel repressive Smad binding element. *Mol Cell Biol* 2004,**24**:2546-59.

42. de Caestecker MP, Yahata T, Wang D*, et al.* The Smad4 activation domain (SAD) is a proline-rich, p300-dependent transcriptional activation domain. *J Biol Chem* 2000,**275**:2115-22.

43. Feng XH, Zhang Y, Wu RY, Derynck R. The tumor suppressor Smad4/DPC4 and transcriptional adaptor CBP/p300 are coactivators for smad3 in TGF-beta-induced transcriptional activation. *Genes Dev* 1998,**12**:2153-63.

44. Feng XH, Liang YY, Liang M*, et al.* Direct interaction of c-Myc with Smad2 and Smad3 to inhibit TGF-beta-mediated induction of the CDK inhibitor p15(Ink4B). *Mol Cell* 2002,**9**:133-43.

45. Derynck R, Zhang YE. Smad-dependent and Smad-independent pathways in TGF-beta family signalling. *Nature* 2003,**425**:577-84.

46. Hayashi H, Abdollah S, Qiu Y*, et al.* The MAD-related protein Smad7 associates with the TGFbeta receptor and functions as an antagonist of TGFbeta signaling. *Cell* 1997,**89**:1165-73.

47. Imamura T, Takase M, Nishihara A*, et al.* Smad6 inhibits signalling by the TGF-beta superfamily. *Nature* 1997,**389**:622-6.

48. Nakao A, Afrakhte M, Moren A*, et al.* Identification of Smad7, a TGFbeta-inducible antagonist of TGF-beta signalling. *Nature* 1997,**389**:631-5.

49. Hata A, Lagna G, Massague J, Hemmati-Brivanlou A. Smad6 inhibits BMP/Smad1 signaling by specifically competing with the Smad4 tumor suppressor. *Genes Dev* 1998,**12**:186-97.

50. Topper JN, Cai J, Qiu Y*, et al.* Vascular MADs: two novel MAD-related genes selectively inducible by flow in human vascular endothelium. *Proc Natl Acad Sci U S A* 1997,**94**:9314-9.

51. Afrakhte M, Moren A, Jossan S*, et al.* Induction of inhibitory Smad6 and Smad7 mRNA by TGF-beta family members. *Biochem Biophys Res Commun* 1998,**249**:505-11.

52. Ishisaki A, Yamato K, Nakao A*, et al.* Smad7 is an activin-inducible inhibitor of activin-induced growth arrest and apoptosis in mouse B cells. *J Biol Chem* 1998,**273**:24293-6.

53. Takase M, Imamura T, Sampath TK*, et al.* Induction of Smad6 mRNA by bone morphogenetic proteins. *Biochem Biophys Res Commun* 1998,**244**:26-9.

54. Ishisaki A, Yamato K, Hashimoto S*, et al.* Differential inhibition of Smad6 and Smad7 on bone morphogenetic protein- and activin-mediated growth arrest and apoptosis in B cells. *J Biol Chem* 1999,**274**:13637-42.

55. Itoh S, Landstrom M, Hermansson A*, et al.* Transforming growth factor beta1 induces nuclear export of inhibitory Smad7. *J Biol Chem* 1998,**273**:29195-201.

56. Akiyoshi S, Inoue H, Hanai J*, et al.* c-Ski acts as a transcriptional co-repressor in transforming growth factor-beta signaling through interaction with smads. *J Biol Chem* 1999,**274**:35269-77.

57. Stroschein SL, Wang W, Zhou S*, et al.* Negative feedback regulation of TGF-beta signaling by the SnoN oncoprotein. *Science* 1999,**286**:771-4.

58. Lin X, Duan X, Liang YY*, et al.* PPM1A functions as a Smad phosphatase to terminate TGFbeta signaling. *Cell* 2006,**125**:915-28.

59. Lee MK, Pardoux C, Hall MC*, et al.* TGF-beta activates Erk MAP kinase signalling through direct phosphorylation of ShcA. *EMBO J* 2007,**26**:3957-67.

60. Hartsough MT, Mulder KM. Transforming growth factor beta activation of p44mapk in proliferating cultures of epithelial cells. *J Biol Chem* 1995,**270**:7117-24.

61. Mucsi I, Skorecki KL, Goldberg HJ. Extracellular signal-regulated kinase and the small GTP-binding protein, Rac, contribute to the effects of transforming growth factor-beta1 on gene expression. *J Biol Chem* 1996,**271**:16567-72.

62. Ellenrieder V, Hendler SF, Boeck W*, et al.* Transforming growth factor beta1 treatment leads to an epithelial-mesenchymal transdifferentiation of pancreatic cancer cells requiring extracellular signal-regulated kinase 2 activation. *Cancer Res* 2001,**61**:4222-8.

63. Xie L, Law BK, Chytil AM*, et al.* Activation of the Erk pathway is required for TGF-beta1-induced EMT in vitro. *Neoplasia* 2004,**6**:603-10.

64. Engel ME, McDonnell MA, Law BK, Moses HL. Interdependent SMAD and JNK signaling in transforming growth factor-beta-mediated transcription. *J Biol Chem* 1999,**274**:37413-20.

65. Hocevar BA, Brown TL, Howe PH. TGF-beta induces fibronectin synthesis through a c-Jun N-terminal kinase-dependent, Smad4-independent pathway. *EMBO J* 1999,**18**:1345-56.

66. Hanafusa H, Ninomiya-Tsuji J, Masuyama N*, et al.* Involvement of the p38 mitogen-activated protein kinase pathway in transforming growth factor-beta-induced gene expression. *J Biol Chem* 1999,**274**:27161-7.

67. Yamashita M, Fatyol K, Jin C*, et al.* TRAF6 mediates Smad-independent activation of JNK and p38 by TGF-beta. *Mol Cell* 2008,**31**:918-24.

68. Edlund S, Bu S, Schuster N*, et al.* Transforming growth factor-beta1 (TGF-beta)-induced apoptosis of prostate cancer cells involves Smad7-dependent activation of p38 by TGF-beta-activated kinase 1 and mitogen-activated protein kinase kinase 3. *Mol Biol Cell* 2003,**14**:529-44.

69. Bakin AV, Tomlinson AK, Bhowmick NA*, et al.* Phosphatidylinositol 3-kinase function is required for transforming growth factor beta-mediated epithelial to mesenchymal transition and cell migration. *J Biol Chem* 2000,**275**:36803-10.

70. Shin I, Bakin AV, Rodeck U*, et al.* Transforming growth factor beta enhances epithelial cell survival via Akt-dependent regulation of FKHRL1. *Mol Biol Cell* 2001,**12**:3328-39.

71. Godoy P, Hengstler JG, Ilkavets I*, et al.* Extracellular matrix modulates sensitivity of hepatocytes to fibroblastoid dedifferentiation and transforming growth factor beta-induced apoptosis. *Hepatology* 2009,**49**:2031-43.

72. Wilkes MC, Mitchell H, Penheiter SG*, et al.* Transforming growth factor-beta activation of phosphatidylinositol 3-kinase is independent of Smad2 and Smad3 and regulates fibroblast responses via p21-activated kinase-2. *Cancer Res* 2005,**65**:10431-40.

73. Solovyan VT, Keski-Oja J. Proteolytic activation of latent TGF-beta precedes caspase-3 activation and enhances apoptotic death of lung epithelial cells. *J Cell Physiol* 2006,**207**:445-53.

74. Valderrama-Carvajal H, Cocolakis E, Lacerte A*, et al.* Activin/TGF-beta induce apoptosis through Smad-dependent expression of the lipid phosphatase SHIP. *Nat Cell Biol* 2002,**4**:963-9.

75. Bhowmick NA, Ghiassi M, Bakin A*, et al.* Transforming growth factor-beta1 mediates epithelial to mesenchymal transdifferentiation through a RhoA-dependent mechanism. *Mol Biol Cell* 2001,**12**:27-36.

76. Edlund S, Landstrom M, Heldin CH, Aspenstrom P. Smad7 is required for TGF-beta-induced activation of the small GTPase Cdc42. *J Cell Sci* 2004,**117**:1835-47.

77. Wilkes MC, Murphy SJ, Garamszegi N, Leof EB. Cell-type-specific activation of PAK2

by transforming growth factor beta independent of Smad2 and Smad3. *Mol Cell Biol* 2003,**23**:8878-89.

78. Kretzschmar M, Doody J, Timokhina I, Massague J. A mechanism of repression of TGFbeta/ Smad signaling by oncogenic Ras. *Genes Dev* 1999,**13**:804-16.
79. Matsuura I, Denissova NG, Wang G*, et al.* Cyclin-dependent kinases regulate the antiproliferative function of Smads. *Nature* 2004,**430**:226-31.
80. Wicks SJ, Lui S, Abdel-Wahab N*, et al.* Inactivation of smad-transforming growth factor beta signaling by Ca(2+)-calmodulin-dependent protein kinase II. *Mol Cell Biol* 2000,**20**:8103-11.
81. Matsuzaki K, Murata M, Yoshida K*, et al.* Chronic inflammation associated with hepatitis C virus infection perturbs hepatic transforming growth factor beta signaling, promoting cirrhosis and hepatocellular carcinoma. *Hepatology* 2007,**46**:48-57.
82. Murata M, Matsuzaki K, Yoshida K*, et al.* Hepatitis B virus X protein shifts human hepatic transforming growth factor (TGF)-beta signaling from tumor suppression to oncogenesis in early chronic hepatitis B. *Hepatology* 2009,**49**:1203-17.
83. Hanyu A, Ishidou Y, Ebisawa T*, et al.* The N domain of Smad7 is essential for specific inhibition of transforming growth factor-beta signaling. *J Cell Biol* 2001,**155**:1017-27.
84. Mochizuki T, Miyazaki H, Hara T*, et al.* Roles for the MH2 domain of Smad7 in the specific inhibition of transforming growth factor-beta superfamily signaling. *J Biol Chem* 2004,**279**:31568-74.
85. Ebisawa T, Fukuchi M, Murakami G*, et al.* Smurf1 interacts with transforming growth factor-beta type I receptor through Smad7 and induces receptor degradation. *J Biol Chem* 2001,**276**:12477-80.
86. Kavsak P, Rasmussen RK, Causing CG*, et al.* Smad7 binds to Smurf2 to form an E3 ubiquitin ligase that targets the TGF beta receptor for degradation. *Mol Cell* 2000,**6**:1365-75.
87. Kuratomi G, Komuro A, Goto K*, et al.* NEDD4-2 (neural precursor cell expressed, developmentally down-regulated 4-2) negatively regulates TGF-beta (transforming growth factor-beta) signalling by inducing ubiquitin-mediated degradation of Smad2 and TGF-beta type I receptor. *Biochem J* 2005,**386**:461-70.
88. Seo SR, Lallemand F, Ferrand N*, et al.* The novel E3 ubiquitin ligase Tiul1 associates with TGIF to target Smad2 for degradation. *EMBO J* 2004,**23**:3780-92.
89. Suzuki C, Murakami G, Fukuchi M*, et al.* Smurf1 regulates the inhibitory activity of Smad7 by targeting Smad7 to the plasma membrane. *J Biol Chem* 2002,**277**:39919-25.
90. Shi W, Sun C, He B*, et al.* GADD34-PP1c recruited by Smad7 dephosphorylates TGFbeta type I receptor. *J Cell Biol* 2004,**164**:291-300.
91. Valdimarsdottir G, Goumans MJ, Itoh F*, et al.* Smad7 and protein phosphatase 1alpha are critical determinants in the duration of TGF-beta/ALK1 signaling in endothelial cells. *BMC Cell Biol* 2006,**7**:16.
92. Datta PK, Moses HL. STRAP and Smad7 synergize in the inhibition of transforming growth factor beta signaling. *Mol Cell Biol* 2000,**20**:3157-67.
93. Kowanetz M, Lonn P, Vanlandewijck M*, et al.* TGFbeta induces SIK to negatively regulate type I receptor kinase signaling. *J Cell Biol* 2008,**182**:655-62.
94. Zhang S, Fei T, Zhang L*, et al.* Smad7 antagonizes transforming growth factor beta signaling in the nucleus by interfering with functional Smad-DNA complex formation. *Mol Cell Biol* 2007,**27**:4488-99.
95. Gronroos E, Hellman U, Heldin CH, Ericsson J. Control of Smad7 stability by competition between acetylation and ubiquitination. *Mol Cell* 2002,**10**:483-93.
96. Simonsson M, Heldin CH, Ericsson J, Gronroos E. The balance between acetylation and deacetylation controls Smad7 stability. *J Biol Chem* 2005,**280**:21797-803.

97. Moren A, Imamura T, Miyazono K*, et al.* Degradation of the tumor suppressor Smad4 by WW and HECT domain ubiquitin ligases. *J Biol Chem* 2005,**280**:22115-23.

98. Brodin G, Ahgren A, ten Dijke P*, et al.* Efficient TGF-beta induction of the Smad7 gene requires cooperation between AP-1, Sp1, and Smad proteins on the mouse Smad7 promoter. *J Biol Chem* 2000,**275**:29023-30.

99. Nagarajan RP, Zhang J, Li W, Chen Y. Regulation of Smad7 promoter by direct association with Smad3 and Smad4. *J Biol Chem* 1999,**274**:33412-8.

100. Stopa M, Benes V, Ansorge W*, et al.* Genomic locus and promoter region of rat Smad7, an important antagonist of TGFbeta signaling. *Mamm Genome* 2000,**11**:169-76.

101. Jungert K, Buck A, Buchholz M*, et al.* Smad-Sp1 complexes mediate TGFbeta-induced early transcription of oncogenic Smad7 in pancreatic cancer cells. *Carcinogenesis* 2006,**27**:2392-401.

102. Kim BC, Lee HJ, Park SH*, et al.* Jab1/CSN5, a component of the COP9 signalosome, regulates transforming growth factor beta signaling by binding to Smad7 and promoting its degradation. *Mol Cell Biol* 2004,**24**:2251-62.

103. Koinuma D, Shinozaki M, Komuro A*, et al.* Arkadia amplifies TGF-beta superfamily signalling through degradation of Smad7. *EMBO J* 2003,**22**:6458-70.

104. Li MO, Wan YY, Sanjabi S*, et al.* Transforming growth factor-beta regulation of immune responses. *Annu Rev Immunol* 2006,**24**:99-146.

105. Geissmann F, Revy P, Regnault A*, et al.* TGF-beta 1 prevents the noncognate maturation of human dendritic Langerhans cells. *J Immunol* 1999,**162**:4567-75.

106. Dooley S, Said HM, Gressner AM*, et al.* Y-box protein-1 is the crucial mediator of antifibrotic interferon-gamma effects. *J Biol Chem* 2006,**281**:1784-95.

107. Ulloa L, Doody J, Massague J. Inhibition of transforming growth factor-beta/SMAD signalling by the interferon-gamma/STAT pathway. *Nature* 1999,**397**:710-3.

108. Bitzer M, von Gersdorff G, Liang D*, et al.* A mechanism of suppression of TGF-beta/SMAD signaling by NF-kappa B/RelA. *Genes Dev* 2000,**14**:187-97.

109. Dowdy SC, Mariani A, Janknecht R. HER2/Neu- and TAK1-mediated up-regulation of the transforming growth factor beta inhibitor Smad7 via the ETS protein ER81. *J Biol Chem* 2003,**278**:44377-84.

110. Quan T, He T, Voorhees JJ, Fisher GJ. Ultraviolet irradiation blocks cellular responses to transforming growth factor-beta by down-regulating its type-II receptor and inducing Smad7. *J Biol Chem* 2001,**276**:26349-56.

111. Sorrentino A, Thakur N, Grimsby S*, et al.* The type I TGF-beta receptor engages TRAF6 to activate TAK1 in a receptor kinase-independent manner. *Nat Cell Biol* 2008,**10**:1199-207.

112. Lallemand F, Mazars A, Prunier C*, et al.* Smad7 inhibits the survival nuclear factor kappaB and potentiates apoptosis in epithelial cells. *Oncogene* 2001,**20**:879-84.

113. Landstrom M, Heldin NE, Bu S*, et al.* Smad7 mediates apoptosis induced by transforming growth factor beta in prostatic carcinoma cells. *Curr Biol* 2000,**10**:535-8.

114. Mazars A, Lallemand F, Prunier C*, et al.* Evidence for a role of the JNK cascade in Smad7-mediated apoptosis. *J Biol Chem* 2001,**276**:36797-803.

115. Ohgushi M, Kuroki S, Fukamachi H*, et al.* Transforming growth factor beta-dependent sequential activation of Smad, Bim, and caspase-9 mediates physiological apoptosis in gastric epithelial cells. *Mol Cell Biol* 2005,**25**:10017-28.

116. Yamamura Y, Hua X, Bergelson S, Lodish HF. Critical role of Smads and AP-1 complex in transforming growth factor-beta -dependent apoptosis. *J Biol Chem* 2000,**275**:36295-302.

117. Huo YY, Hu YC, He XR*, et al.* Activation of extracellular signal-regulated kinase by TGF-beta1 via TbetaRII and Smad7 dependent mechanisms in human bronchial

epithelial BEP2D cells. *Cell Biol Toxicol* 2007,**23**:113-28.

118. Akel S, Bertolette D, Petrow-Sadowski C, Ruscetti FW. Levels of Smad7 regulate Smad and mitogen activated kinases (MAPKs) signaling and controls erythroid and megakaryocytic differentiation of erythroleukemia cells. *Platelets* 2007,**18**:566-78.
119. Edlund S, Lee SY, Grimsby S*, et al.* Interaction between Smad7 and beta-catenin: importance for transforming growth factor beta-induced apoptosis. *Mol Cell Biol* 2005,**25**:1475-88.
120. Azuma H, Ehata S, Miyazaki H*, et al.* Effect of Smad7 expression on metastasis of mouse mammary carcinoma JygMC(A) cells. *J Natl Cancer Inst* 2005,**97**:1734-46.
121. Zulehner G, Mikula M, Schneller D*, et al.* Nuclear beta-catenin induces an early liver progenitor phenotype in hepatocellular carcinoma and promotes tumor recurrence. *Am J Pathol* 2010,**176**:472-81.
122. DiVito KA, Trabosh VA, Chen YS*, et al.* Smad7 restricts melanoma invasion by restoring N-cadherin expression and establishing heterotypic cell-cell interactions in vivo. *Pigment Cell Melanoma Res* 2010,**23**:795-808.
123. Schuster N, Krieglstein K. Mechanisms of TGF-beta-mediated apoptosis. *Cell Tissue Res* 2002,**307**:1-14.
124. Oberhammer FA, Pavelka M, Sharma S*, et al.* Induction of apoptosis in cultured hepatocytes and in regressing liver by transforming growth factor beta 1. *Proc Natl Acad Sci U S A* 1992,**89**:5408-12.
125. Perlman R, Schiemann WP, Brooks MW*, et al.* TGF-beta-induced apoptosis is mediated by the adapter protein Daxx that facilitates JNK activation. *Nat Cell Biol* 2001,**3**:708-14.
126. Herzer K, Ganten TM, Schulze-Bergkamen H*, et al.* Transforming growth factor beta can mediate apoptosis via the expression of TRAIL in human hepatoma cells. *Hepatology* 2005,**42**:183-92.
127. Herzer K, Grosse-Wilde A, Krammer PH*, et al.* Transforming growth factor-beta-mediated tumor necrosis factor-related apoptosis-inducing ligand expression and apoptosis in hepatoma cells requires functional cooperation between Smad proteins and activator protein-1. *Mol Cancer Res* 2008,**6**:1169-77.
128. Ju W, Ogawa A, Heyer J*, et al.* Deletion of Smad2 in mouse liver reveals novel functions in hepatocyte growth and differentiation. *Mol Cell Biol* 2006,**26**:654-67.
129. Yang YA, Zhang GM, Feigenbaum L, Zhang YE. Smad3 reduces susceptibility to hepatocarcinoma by sensitizing hepatocytes to apoptosis through downregulation of Bcl-2. *Cancer Cell* 2006,**9**:445-57.
130. Herrera B, Alvarez AM, Sanchez A*, et al.* Reactive oxygen species (ROS) mediates the mitochondrial-dependent apoptosis induced by transforming growth factor (beta) in fetal hepatocytes. *FASEB J* 2001,**15**:741-51.
131. Carmona-Cuenca I, Roncero C, Sancho P*, et al.* Upregulation of the NADPH oxidase NOX4 by TGF-beta in hepatocytes is required for its pro-apoptotic activity. *J Hepatol* 2008,**49**:965-76.
132. Ichikawa T, Zhang YQ, Kogure K*, et al.* Transforming growth factor beta and activin tonically inhibit DNA synthesis in the rat liver. *Hepatology* 2001,**34**:918-25.
133. Lee KY, Bae SC. TGF-beta-dependent cell growth arrest and apoptosis. *J Biochem Mol Biol* 2002,**35**:47-53.
134. Hannon GJ, Beach D. p15INK4B is a potential effector of TGF-beta-induced cell cycle arrest. *Nature* 1994,**371**:257-61.
135. Datto MB, Li Y, Panus JF*, et al.* Transforming growth factor beta induces the cyclin-dependent kinase inhibitor p21 through a p53-independent mechanism. *Proc Natl Acad Sci U S A* 1995,**92**:5545-9.
136. Ewen ME, Oliver CJ, Sluss HK*, et al.* p53-dependent repression of CDK4 translation

in TGF-beta-induced G1 cell-cycle arrest. *Genes Dev* 1995,**9**:204-17.

137. Warner BJ, Blain SW, Seoane J, Massague J. Myc downregulation by transforming growth factor beta required for activation of the p15(Ink4b) G(1) arrest pathway. *Mol Cell Biol* 1999,**19**:5913-22.
138. Claassen GF, Hann SR. A role for transcriptional repression of p21CIP1 by c-Myc in overcoming transforming growth factor beta -induced cell-cycle arrest. *Proc Natl Acad Sci U S A* 2000,**97**:9498-503.
139. Dooley S, Hamzavi J, Ciuclan L*, et al.* Hepatocyte-specific Smad7 expression attenuates TGF-beta-mediated fibrogenesis and protects against liver damage. *Gastroenterology* 2008,**135**:642-59.
140. van Zijl F, Zulehner G, Petz M*, et al.* Epithelial-mesenchymal transition in hepatocellular carcinoma. *Future Oncol* 2009,**5**:1169-79.
141. GLOBOCAN 2008 v2.0, Cancer Incidence and Mortality Worldwide: IARC CancerBase No. 10 [Internet]. Lyon, France: International Agency for Research on Cancer; 2010. Available from: http://globocan.iarc.fr, accessed on 11/08/2011.
142. Ferlay J PD, Curado MP, Bray F, Edwards B, Shin HR and Forman D. Cancer Incidence in Five Continents, Volumes I to IX: IARC CancerBase No. 9 [Internet]. Lyon, France: International Agency for Research on Cancer; 2010. Available from: http://ci5.iarc.fr, accessed on 13/11/2012.
143. World Health Organization (WHO) Databank. International Statistical Classification of Diseases and Related Health Problems 10th Revision (ICD-10), Version from 2010 [Internet]. Available at http://apps.who.int/classifications/icd10/browse/2010/en, accessed on 13/11/2012.
144. Feitelson MA, Sun B, Satiroglu Tufan NL*, et al.* Genetic mechanisms of hepatocarcinogenesis. *Oncogene* 2002,**21**:2593-604.
145. Llovet JM, Burroughs A, Bruix J. Hepatocellular carcinoma. *Lancet* 2003,**362**:1907-17.
146. Bruix J, Sherman M. Management of hepatocellular carcinoma. *Hepatology* 2005,**42**:1208-36.
147. Cervello M, McCubrey JA, Cusimano A*, et al.* Targeted therapy for hepatocellular carcinoma: novel agents on the horizon. *Oncotarget* 2012,**3**:236-60.
148. Xie B, Wang DH, Spechler SJ. Sorafenib for treatment of hepatocellular carcinoma: a systematic review. *Dig Dis Sci* 2012,**57**:1122-9.
149. Massague J. TGFbeta in Cancer. *Cell* 2008,**134**:215-30.
150. Tang B, Bottinger EP, Jakowlew SB*, et al.* Transforming growth factor-beta1 is a new form of tumor suppressor with true haploid insufficiency. *Nat Med* 1998,**4**:802-7.
151. Ingber DE. Cancer as a disease of epithelial-mesenchymal interactions and extracellular matrix regulation. *Differentiation* 2002,**70**:547-60.
152. Vecchione L. Underwriting implications of premalignant disease. *J Insur Med* 1998,**30**:169-74.
153. Niitsu Y, Urushizaki Y, Koshida Y*, et al.* Expression of TGF-beta gene in adult T cell leukemia. *Blood* 1988,**71**:263-6.
154. Gomella LG, Sargent ER, Wade TP*, et al.* Expression of transforming growth factor alpha in normal human adult kidney and enhanced expression of transforming growth factors alpha and beta 1 in renal cell carcinoma. *Cancer Res* 1989,**49**:6972-5.
155. Travers MT, Barrett-Lee PJ, Berger U*, et al.* Growth factor expression in normal, benign, and malignant breast tissue. *Br Med J (Clin Res Ed)* 1988,**296**:1621-4.
156. Gulubova M, Manolova I, Ananiev J*, et al.* Role of TGF-beta1, its receptor TGFbetaRII, and Smad proteins in the progression of colorectal cancer. *Int J Colorectal Dis* 2010,**25**:591-9.

157. Walker RA, Dearing SJ. Transforming growth factor beta 1 in ductal carcinoma in situ and invasive carcinomas of the breast. *Eur J Cancer* 1992,**28**:641-4.

158. Bedossa P, Peltier E, Terris B*, et al.* Transforming growth factor-beta 1 (TGF-beta 1) and TGF-beta 1 receptors in normal, cirrhotic, and neoplastic human livers. *Hepatology* 1995,**21**:760-6.

159. Ji GZ, Wang XH, Miao L*, et al.* Role of transforming growth factor-beta1-smad signal transduction pathway in patients with hepatocellular carcinoma. *World J Gastroenterol* 2006,**12**:644-8.

160. Cui W, Fowlis DJ, Bryson S*, et al.* TGFbeta1 inhibits the formation of benign skin tumors, but enhances progression to invasive spindle carcinomas in transgenic mice. *Cell* 1996,**86**:531-42.

161. Zhu Q, Krakowski AR, Dunham EE*, et al.* Dual role of SnoN in mammalian tumorigenesis. *Mol Cell Biol* 2007,**27**:324-39.

162. Blobe GC, Schiemann WP, Lodish HF. Role of transforming growth factor beta in human disease. *N Engl J Med* 2000,**342**:1350-8.

163. Akhurst RJ, Derynck R. TGF-beta signaling in cancer--a double-edged sword. *Trends Cell Biol* 2001,**11**:S44-51.

164. Derynck R, Akhurst RJ, Balmain A. TGF-beta signaling in tumor suppression and cancer progression. *Nat Genet* 2001,**29**:117-29.

165. Hanahan D, Weinberg RA. The hallmarks of cancer. *Cell* 2000,**100**:57-70.

166. Hanahan D, Weinberg RA. Hallmarks of cancer: the next generation. *Cell* 2011,**144**:646-74.

167. Elliott RL, Blobe GC. Role of transforming growth factor Beta in human cancer. *J Clin Oncol* 2005,**23**:2078-93.

168. Kaklamani VG, Hou N, Bian Y*, et al.* TGFBR1*6A and cancer risk: a meta-analysis of seven case-control studies. *J Clin Oncol* 2003,**21**:3236-43.

169. Sjoblom T, Jones S, Wood LD*, et al.* The consensus coding sequences of human breast and colorectal cancers. *Science* 2006,**314**:268-74.

170. Jaffee EM, Hruban RH, Canto M, Kern SE. Focus on pancreas cancer. *Cancer Cell* 2002,**2**:25-8.

171. Sun Y, Liu X, Eaton EN*, et al.* Interaction of the Ski oncoprotein with Smad3 regulates TGF-beta signaling. *Mol Cell* 1999,**4**:499-509.

172. Alexandrow MG, Kawabata M, Aakre M, Moses HL. Overexpression of the c-Myc oncoprotein blocks the growth-inhibitory response but is required for the mitogenic effects of transforming growth factor beta 1. *Proc Natl Acad Sci U S A* 1995,**92**:3239-43.

173. Longerich T, Breuhahn K, Odenthal M*, et al.* Factors of transforming growth factor beta signalling are co-regulated in human hepatocellular carcinoma. *Virchows Arch* 2004,**445**:589-96.

174. Mamiya T, Yamazaki K, Masugi Y*, et al.* Reduced transforming growth factor-beta receptor II expression in hepatocellular carcinoma correlates with intrahepatic metastasis. *Lab Invest* 2010,**90**:1339-45.

175. Ozturk M. Genetic aspects of hepatocellular carcinogenesis. *Semin Liver Dis* 1999,**19**:235-42.

176. Chen RH, Su YH, Chuang RL, Chang TY. Suppression of transforming growth factor-beta-induced apoptosis through a phosphatidylinositol 3-kinase/Akt-dependent pathway. *Oncogene* 1998,**17**:1959-68.

177. Remy I, Montmarquette A, Michnick SW. PKB/Akt modulates TGF-beta signalling through a direct interaction with Smad3. *Nat Cell Biol* 2004,**6**:358-65.

178. Conery AR, Cao Y, Thompson EA*, et al.* Akt interacts directly with Smad3 to regulate

the sensitivity to TGF-beta induced apoptosis. *Nat Cell Biol* 2004,**6**:366-72.

179. Zekri AR, Bahnassy AA, Abdel-Wahab SA*, et al.* Expression of pro- and anti-inflammatory cytokines in relation to apoptotic genes in Egyptian liver disease patients associated with HCV-genotype-4. *J Gastroenterol Hepatol* 2009,**24**:416-28.
180. Schmitz KJ, Wohlschlaeger J, Lang H*, et al.* Activation of the ERK and AKT signalling pathway predicts poor prognosis in hepatocellular carcinoma and ERK activation in cancer tissue is associated with hepatitis C virus infection. *J Hepatol* 2008,**48**:83-90.
181. Park YN, Chae KJ, Oh BK*, et al.* Expression of Smad7 in hepatocellular carcinoma and dysplastic nodules: resistance mechanism to transforming growth factor-beta. *Hepatogastroenterology* 2004,**51**:396-400.
182. Tang Y, Katuri V, Dillner A*, et al.* Disruption of transforming growth factor-beta signaling in ELF beta-spectrin-deficient mice. *Science* 2003,**299**:574-7.
183. Saha T, Vardhini D, Tang Y*, et al.* RING finger-dependent ubiquitination by PRAJA is dependent on TGF-beta and potentially defines the functional status of the tumor suppressor ELF. *Oncogene* 2006,**25**:693-705.
184. Kitisin K, Ganesan N, Tang Y*, et al.* Disruption of transforming growth factor-beta signaling through beta-spectrin ELF leads to hepatocellular cancer through cyclin D1 activation. *Oncogene* 2007,**26**:7103-10.
185. Frolik CA, Dart LL, Meyers CA*, et al.* Purification and initial characterization of a type beta transforming growth factor from human placenta. *Proc Natl Acad Sci U S A* 1983,**80**:3676-80.
186. Park BJ, Park JI, Byun DS*, et al.* Mitogenic conversion of transforming growth factor-beta1 effect by oncogenic Ha-Ras-induced activation of the mitogen-activated protein kinase signaling pathway in human prostate cancer. *Cancer Res* 2000,**60**:3031-8.
187. Matsuzaki K, Date M, Furukawa F*, et al.* Regulatory mechanisms for transforming growth factor beta as an autocrine inhibitor in human hepatocellular carcinoma: implications for roles of smads in its growth. *Hepatology* 2000,**32**:218-27.
188. Ishikawa O, LeRoy EC, Trojanowska M. Mitogenic effect of transforming growth factor beta 1 on human fibroblasts involves the induction of platelet-derived growth factor alpha receptors. *J Cell Physiol* 1990,**145**:181-6.
189. Strutz F, Zeisberg M, Renziehausen A*, et al.* TGF-beta 1 induces proliferation in human renal fibroblasts via induction of basic fibroblast growth factor (FGF-2). *Kidney Int* 2001,**59**:579-92.
190. Chapnick DA, Warner L, Bernet J*, et al.* Partners in crime: the TGFbeta and MAPK pathways in cancer progression. *Cell Biosci* 2011,**1**:42.
191. Fransvea E, Angelotti U, Antonaci S, Giannelli G. Blocking transforming growth factor-beta up-regulates E-cadherin and reduces migration and invasion of hepatocellular carcinoma cells. *Hepatology* 2008,**47**:1557-66.
192. Giannelli G, Fransvea E, Marinosci F*, et al.* Transforming growth factor-beta1 triggers hepatocellular carcinoma invasiveness via alpha3beta1 integrin. *Am J Pathol* 2002,**161**:183-93.
193. Desruisseau S, Ghazarossian-Ragni E, Chinot O, Martin PM. Divergent effect of TGFbeta1 on growth and proteolytic modulation of human prostatic-cancer cell lines. *Int J Cancer* 1996,**66**:796-801.
194. Dickson MC, Martin JS, Cousins FM*, et al.* Defective haematopoiesis and vasculogenesis in transforming growth factor-beta 1 knock out mice. *Development* 1995,**121**:1845-54.
195. Larsson J, Goumans MJ, Sjostrand LJ*, et al.* Abnormal angiogenesis but intact hematopoietic potential in TGF-beta type I receptor-deficient mice. *EMBO J* 2001,**20**:1663-73.
196. McAllister KA, Grogg KM, Johnson DW*, et al.* Endoglin, a TGF-beta binding protein of

endothelial cells, is the gene for hereditary haemorrhagic telangiectasia type 1. *Nat Genet* 1994,**8**:345-51.

197. Ito N, Kawata S, Tamura S*, et al.* Positive correlation of plasma transforming growth factor-beta 1 levels with tumor vascularity in hepatocellular carcinoma. *Cancer Lett* 1995,**89**:45-8.
198. Kim NW, Piatyszek MA, Prowse KR*, et al.* Specific association of human telomerase activity with immortal cells and cancer. *Science* 1994,**266**:2011-5.
199. Chang JT, Chen YL, Yang HT*, et al.* Differential regulation of telomerase activity by six telomerase subunits. *Eur J Biochem* 2002,**269**:3442-50.
200. Nakayama J, Tahara H, Tahara E*, et al.* Telomerase activation by hTRT in human normal fibroblasts and hepatocellular carcinomas. *Nat Genet* 1998,**18**:65-8.
201. Li H, Xu D, Li J*, et al.* Transforming growth factor beta suppresses human telomerase reverse transcriptase (hTERT) by Smad3 interactions with c-Myc and the hTERT gene. *J Biol Chem* 2006,**281**:25588-600.
202. Shull MM, Ormsby I, Kier AB*, et al.* Targeted disruption of the mouse transforming growth factor-beta 1 gene results in multifocal inflammatory disease. *Nature* 1992,**359**:693-9.
203. Derynck R, Goeddel DV, Ullrich A*, et al.* Synthesis of messenger RNAs for transforming growth factors alpha and beta and the epidermal growth factor receptor by human tumors. *Cancer Res* 1987,**47**:707-12.
204. Ewan KB, Henshall-Powell RL, Ravani SA*, et al.* Transforming growth factor-beta1 mediates cellular response to DNA damage in situ. *Cancer Res* 2002,**62**:5627-31.
205. Kanamoto T, Hellman U, Heldin CH, Souchelnytskyi S. Functional proteomics of transforming growth factor-beta1-stimulated Mv1Lu epithelial cells: Rad51 as a target of TGFbeta1-dependent regulation of DNA repair. *EMBO J* 2002,**21**:1219-30.
206. Rizzo A, Waldner MJ, Stolfi C*, et al.* Smad7 expression in T cells prevents colitis-associated cancer. *Cancer Res* 2011,**71**:7423-32.
207. Osawa H, Nakajima M, Kato H*, et al.* Prognostic value of the expression of Smad6 and Smad7, as inhibitory Smads of the TGF-beta superfamily, in esophageal squamous cell carcinoma. *Anticancer Res* 2004,**24**:3703-9.
208. Boulay JL, Mild G, Lowy A*, et al.* SMAD7 is a prognostic marker in patients with colorectal cancer. *Int J Cancer* 2003,**104**:446-9.
209. Halder SK, Rachakonda G, Deane NG, Datta PK. Smad7 induces hepatic metastasis in colorectal cancer. *Br J Cancer* 2008,**99**:957-65.
210. Dowdy SC, Mariani A, Reinholz MM*, et al.* Overexpression of the TGF-beta antagonist Smad7 in endometrial cancer. *Gynecol Oncol* 2005,**96**:368-73.
211. Kim YH, Lee HS, Lee HJ*, et al.* Prognostic significance of the expression of Smad4 and Smad7 in human gastric carcinomas. *Ann Oncol* 2004,**15**:574-80.
212. Chen YK, Huang AH, Cheng PH*, et al.* Overexpression of Smad proteins, especially Smad7, in oral epithelial dysplasias. *Clin Oral Investig* 2012
213. Theohari I, Giannopoulou I, Magkou C*, et al.* Differential effect of the expression of TGF-beta pathway inhibitors, Smad-7 and Ski, on invasive breast carcinomas: relation to biologic behavior. *APMIS* 2012,**120**:92-100.
214. Reinholz MM, An MW, Johnsen SA*, et al.* Differential gene expression of TGF beta inducible early gene (TIEG), Smad7, Smad2 and Bard1 in normal and malignant breast tissue. *Breast Cancer Res Treat* 2004,**86**:75-88.
215. Matsuo SE, Fiore AP, Siguematu SM*, et al.* Expression of SMAD proteins, TGF-beta/activin signaling mediators, in human thyroid tissues. *Arq Bras Endocrinol Metabol* 2010,**54**:406-12.
216. Luo X, Ding Q, Wang M*, et al.* In vivo disruption of TGF-beta signaling by Smad7 in airway epithelium alleviates allergic asthma but aggravates lung carcinogenesis in

mouse. *PLoS One* 2010,**5**:e10149.

217. Wang P, Fan J, Chen Z*, et al.* Low-level expression of Smad7 correlates with lymph node metastasis and poor prognosis in patients with pancreatic cancer. *Ann Surg Oncol* 2009,**16**:826-35.
218. Kleeff J, Ishiwata T, Maruyama H*, et al.* The TGF-beta signaling inhibitor Smad7 enhances tumorigenicity in pancreatic cancer. *Oncogene* 1999,**18**:5363-72.
219. Bornstein S, Hoot K, Han GW*, et al.* Distinct roles of individual Smads in skin carcinogenesis. *Mol Carcinog* 2007,**46**:660-4.
220. Liu X, Lee J, Cooley M*, et al.* Smad7 but not Smad6 cooperates with oncogenic ras to cause malignant conversion in a mouse model for squamous cell carcinoma. *Cancer Res* 2003,**63**:7760-8.
221. Watanabe T, Morizane T, Tsuchimoto K*, et al.* Establishment of a cell line (HCC-M) from a human hepatocellular carcinoma. *Int J Cancer* 1983,**32**:141-6.
222. Saito H, Morizane T, Watanabe T*, et al.* Establishment of a human cell line (HCC-T) from a patient with hepatoma bearing no evidence of hepatitis B or A virus infection. *Cancer* 1989,**64**:1054-60.
223. Aden DP, Fogel A, Plotkin S*, et al.* Controlled synthesis of HBsAg in a differentiated human liver carcinoma-derived cell line. *Nature* 1979,**282**:615-6.
224. Knowles BB, Howe CC, Aden DP. Human hepatocellular carcinoma cell lines secrete the major plasma proteins and hepatitis B surface antigen. *Science* 1980,**209**:497-9.
225. Doi I. Establishment of a cell line and its clonal sublines from a patient with hepatoblastoma. *Gann* 1976,**67**:1-10.
226. Nakabayashi H, Taketa K, Miyano K*, et al.* Growth of human hepatoma cells lines with differentiated functions in chemically defined medium. *Cancer Res* 1982,**42**:3858-63.
227. Alexander JJ, Bey EM, Geddes EW, Lecatsas G. Establishment of a continuously growing cell line from primary carcinoma of the liver. *S Afr Med J* 1976,**50**:2124-8.
228. Laurent T, Murase D, Tsukioka S*, et al.* A novel human hepatoma cell line, FLC-4, exhibits highly enhanced liver differentiation functions through the three-dimensional cell shape. *J Cell Physiol* 2012,**227**:2898-906.
229. Hasumura S, Sujino H, Nagamori S, Kameda H. [Establishment and characterization of a human hepatocellular carcinoma cell line JHH-4]. *Hum Cell* 1988,**1**:98-100.
230. Doi I, Namba M, Sato J. Establishment and some biological characteristics of human hepatoma cell lines. *Gann* 1975,**66**:385-92.
231. Tesseur I, Zou K, Berber E*, et al.* Highly sensitive and specific bioassay for measuring bioactive TGF-beta. *BMC Cell Biol* 2006,**7**:15.
232. Itoh S, Thorikay M, Kowanetz M*, et al.* Elucidation of Smad requirement in transforming growth factor-beta type I receptor-induced responses. *J Biol Chem* 2003,**278**:3751-61.
233. Fujii M, Takeda K, Imamura T*, et al.* Roles of bone morphogenetic protein type I receptors and Smad proteins in osteoblast and chondroblast differentiation. *Mol Biol Cell* 1999,**10**:3801-13.
234. Ramesh S, Qi XJ, Wildey GM*, et al.* TGF beta-mediated BIM expression and apoptosis are regulated through SMAD3-dependent expression of the MAPK phosphatase MKP2. *EMBO Rep* 2008,**9**:990-7.
235. Halder SK, Beauchamp RD, Datta PK. Smad7 induces tumorigenicity by blocking TGF-beta-induced growth inhibition and apoptosis. *Exp Cell Res* 2005,**307**:231-46.
236. Yuen MF, Norris S, Evans LW*, et al.* Transforming growth factor-beta 1, activin and follistatin in patients with hepatocellular carcinoma and patients with alcoholic cirrhosis. *Scand J Gastroenterol* 2002,**37**:233-8.

237. Song BC, Chung YH, Kim JA*, et al.* Transforming growth factor-beta1 as a useful serologic marker of small hepatocellular carcinoma. *Cancer* 2002,**94**:175-80.

238. Kumar M, Zhao X, Wang XW. Molecular carcinogenesis of hepatocellular carcinoma and intrahepatic cholangiocarcinoma: one step closer to personalized medicine? *Cell Biosci* 2011,**1**:5.

239. Matsuzaki K, Date M, Furukawa F*, et al.* Autocrine stimulatory mechanism by transforming growth factor beta in human hepatocellular carcinoma. *Cancer Res* 2000,**60**:1394-402.

240. Zhang H, Ozaki I, Mizuta T*, et al.* Transforming growth factor-beta 1-induced apoptosis is blocked by beta 1-integrin-mediated mitogen-activated protein kinase activation in human hepatoma cells. *Cancer Sci* 2004,**95**:878-86.

241. Zhang H, Ozaki I, Mizuta T*, et al.* Involvement of programmed cell death 4 in transforming growth factor-beta1-induced apoptosis in human hepatocellular carcinoma. *Oncogene* 2006,**25**:6101-12.

242. Damdinsuren B, Nagano H, Kondo M*, et al.* TGF-beta1-induced cell growth arrest and partial differentiation is related to the suppression of Id1 in human hepatoma cells. *Oncol Rep* 2006,**15**:401-8.

243. Musch A, Rabe C, Paik MD*, et al.* Altered expression of TGF-beta receptors in hepatocellular carcinoma--effects of a constitutively active TGF-beta type I receptor mutant. *Digestion* 2005,**71**:78-91.

244. Inagaki M, Moustakas A, Lin HY*, et al.* Growth inhibition by transforming growth factor beta (TGF-beta) type I is restored in TGF-beta-resistant hepatoma cells after expression of TGF-beta receptor type II cDNA. *Proc Natl Acad Sci U S A* 1993,**90**:5359-63.

245. Im YH, Kim HT, Kim IY*, et al.* Heterozygous mice for the transforming growth factor-beta type II receptor gene have increased susceptibility to hepatocellular carcinogenesis. *Cancer Res* 2001,**61**:6665-8.

246. Nishikawa Y, Wang M, Carr BI. Changes in TGF-beta receptors of rat hepatocytes during primary culture and liver regeneration: increased expression of TGF-beta receptors associated with increased sensitivity to TGF-beta-mediated growth inhibition. *J Cell Physiol* 1998,**176**:612-23.

247. Sue SR, Chari RS, Kong FM*, et al.* Transforming growth factor-beta receptors and mannose 6-phosphate/insulin-like growth factor-II receptor expression in human hepatocellular carcinoma. *Ann Surg* 1995,**222**:171-8.

248. Lee D, Chung YH, Kim JA*, et al.* Transforming growth factor beta 1 overexpression is closely related to invasiveness of hepatocellular carcinoma. *Oncology* 2012,**82**:11-8.

249. Zhang B, Halder SK, Zhang S, Datta PK. Targeting transforming growth factor-beta signaling in liver metastasis of colon cancer. *Cancer Lett* 2009,**277**:114-20.

250. Fransvea E, Mazzocca A, Santamato A*, et al.* Kinase activation profile associated with TGF-beta-dependent migration of HCC cells: a preclinical study. *Cancer Chemother Pharmacol* 2011,**68**:79-86.

251. Imamichi Y, Waidmann O, Hein R*, et al.* TGF beta-induced focal complex formation in epithelial cells is mediated by activated ERK and JNK MAP kinases and is independent of Smad4. *Biol Chem* 2005,**386**:225-36.

252. Feng DY, Zheng H, Tan Y, Cheng RX. Effect of phosphorylation of MAPK and Stat3 and expression of c-fos and c-jun proteins on hepatocarcinogenesis and their clinical significance. *World J Gastroenterol* 2001,**7**:33-6.

253. Zheng Q, Tang ZY, Xue Q*, et al.* Invasion and metastasis of hepatocellular carcinoma in relation to urokinase-type plasminogen activator, its receptor and inhibitor. *J Cancer Res Clin Oncol* 2000,**126**:641-6.

254. Breuhahn K, Longerich T, Schirmacher P. Dysregulation of growth factor signaling in

human hepatocellular carcinoma. *Oncogene* 2006,**25**:3787-800.

255. Yakicier MC, Irmak MB, Romano A*, et al.* Smad2 and Smad4 gene mutations in hepatocellular carcinoma. *Oncogene* 1999,**18**:4879-83.
256. Tian F, DaCosta Byfield S, Parks WT*, et al.* Reduction in Smad2/3 signaling enhances tumorigenesis but suppresses metastasis of breast cancer cell lines. *Cancer Res* 2003,**63**:8284-92.
257. Do TV, Kubba LA, Du H*, et al.* Transforming growth factor-beta1, transforming growth factor-beta2, and transforming growth factor-beta3 enhance ovarian cancer metastatic potential by inducing a Smad3-dependent epithelial-to-mesenchymal transition. *Mol Cancer Res* 2008,**6**:695-705.
258. Millet C, Zhang YE. Roles of Smad3 in TGF-beta signaling during carcinogenesis. *Crit Rev Eukaryot Gene Expr* 2007,**17**:281-93.
259. Nicolas FJ, Hill CS. Attenuation of the TGF-beta-Smad signaling pathway in pancreatic tumor cells confers resistance to TGF-beta-induced growth arrest. *Oncogene* 2003,**22**:3698-711.
260. Seton-Rogers SE, Lu Y, Hines LM*, et al.* Cooperation of the ErbB2 receptor and transforming growth factor beta in induction of migration and invasion in mammary epithelial cells. *Proc Natl Acad Sci U S A* 2004,**101**:1257-62.
261. Huynh H, Nguyen TT, Chow KH*, et al.* Over-expression of the mitogen-activated protein kinase (MAPK) kinase (MEK)-MAPK in hepatocellular carcinoma: its role in tumor progression and apoptosis. *BMC Gastroenterol* 2003,**3**:19.
262. Tsuboi Y, Ichida T, Sugitani S*, et al.* Overexpression of extracellular signal-regulated protein kinase and its correlation with proliferation in human hepatocellular carcinoma. *Liver Int* 2004,**24**:432-6.
263. Fischer AN, Herrera B, Mikula M*, et al.* Integration of Ras subeffector signaling in TGF-beta mediated late stage hepatocarcinogenesis. *Carcinogenesis* 2005,**26**:931-42.
264. Hsu C, Huang CL, Hsu HC*, et al.* HER-2/neu overexpression is rare in hepatocellular carcinoma and not predictive of anti-HER-2/neu regulation of cell growth and chemosensitivity. *Cancer* 2002,**94**:415-20.
265. Xian ZH, Zhang SH, Cong WM*, et al.* Overexpression/amplification of HER-2/neu is uncommon in hepatocellular carcinoma. *J Clin Pathol* 2005,**58**:500-3.
266. Ito Y, Sasaki Y, Horimoto M*, et al.* Activation of mitogen-activated protein kinases/extracellular signal-regulated kinases in human hepatocellular carcinoma. *Hepatology* 1998,**27**:951-8.
267. Chen L, Shi Y, Jiang CY*, et al.* Expression and prognostic role of pan-Ras, Raf-1, pMEK1 and pERK1/2 in patients with hepatocellular carcinoma. *Eur J Surg Oncol* 2011,**37**:513-20.
268. Behrens A, Sibilia M, David JP*, et al.* Impaired postnatal hepatocyte proliferation and liver regeneration in mice lacking c-jun in the liver. *EMBO J* 2002,**21**:1782-90.
269. Wang Z, Song Y, Tu W*, et al.* beta-2 spectrin is involved in hepatocyte proliferation through the interaction of TGFbeta/Smad and PI3K/AKT signalling. *Liver Int* 2012,**32**:1103-11.
270. Coulouarn C, Factor VM, Thorgeirsson SS. Transforming growth factor-beta gene expression signature in mouse hepatocytes predicts clinical outcome in human cancer. *Hepatology* 2008,**47**:2059-67.

LIST OF FIGURES

LIST OF TABLES

DECLARATION

I hereby declare that this dissertation is, to the best of my knowledge and belief, a presentation of my own work, except where otherwise acknowledged.

Johanna Dzieran

ACKNOWLEDGEMENT

I would not have been able to write this thesis without the guidance, help and support of many kind people.

First and foremost I wish to thank Professor Dr. Steven Dooley (Molecular Hepatology - Alcohol Associated Diseases, II. Medical Clinic, Medical Faculty of Mannheim, University of Heidelberg) for his guidance and for giving me the opportunity to work on such an interesting research topic. I would also like to thank my advisor Dr. Nadja Meindl-Beinker. Thank you for your support and patience, and for the good advices and vivid discussions.

Work is much more enjoyable in a helpful, pleasant and creative environment. Thank you to my colleagues from the research group Molecular Hepatology, who helped to create such an atmosphere. Special thanks to Jasmin, Alex, Yan and, in particular Chris, for your support and many joyful professional, and personal conversations during and outside working hours. Thank you, Tessi. You made my start at a new work and in a foreign city easy and became a good friend.

I would like to thank my friends for their patience and encouragement. Spending time with you always gave me new energy and motivation. My appreciation goes to my flat mates Juliane and Renske, for creating a home and for many entertaining hours.

Last but not least, my deepest gratitude goes to my family. Thank you Mama and Papa, for your unconditional love, for your support and encouragement, and for providing me a home during writing this thesis. Omi, Opa und Oma, ich denke an euch - in tiefster Dankbarkeit für eure Liebe und Lebensweisheit, und für euer Interesse an einem euch fremdem Thema - und werde euch immer in meinem Herzen tragen.